Metal Labeling for Low Affinity Binding Biomolecules

Oleksandra Kuzmich, M.Sc. Chemie

D i s s e r t a t i o n
zur Erlangung des akademischen Grades
d o c t o r r e r u m n a t u r a l i u m
(Dr. rer. nat.)
im Fach Chemie
eingereicht an der
Mathematisch-Naturwissenschaftliche Fakultät
der Humboldt-Universität zu Berlin
von

Oleksandra Kuzmich, M.Sc. Chemie

Präsidentin der Humboldt-Universität zu Berlin
Prof. Dr.-Ing. Dr. Sabine Kunst

Dekan der Mathematisch-Naturwissenschaftlichen Fakultät
Prof. Dr. Elmar Kulke

Gutachter/in: 1. Prof. Dr. Michael W. Linscheid
2. Prof. Dr. Hubert Köster
3. PD. Dr. Michael Weller

Tag der mündlichen Prüfung: 19. Dezember 2017

Eidesstattliche Erklärung

Hiermit erkläre ich an Eides statt, dass die vorliegende Arbeit selbstständig und nur unter Nutzung der angegebenen Hilfsmittel angefertigt wurde.

Berlin, den 1.09.2017 Oleksandra Kuzmich

Acknowledgement

This thesis would not have been possible unless my supervisor Prof. Dr. Michael W. Linscheid gave me the chance to perform my doctoral studies in his research group. I would like to express my sincere gratitude for his encouragement, valuable guidance and continuous support.

I owe my deepest gratitude to Prof. Dr. Hubert Köster who provided me with the opportunity to perform my research in collaboration with caprotec bioanalytics. I am very grateful for his exceptional foresight and expert suggestions.

I would like to acknowledge Dr. Petra Esperling for her friendly assistance and help with numerous organizational issues.

I am heartily thankful to Dr. Mathias Dreger for his patience, guidance, wise and competent advices that helped me to overcome the difficulties throughout my PhD, and for his expert suggestions during the revision of my thesis.

I would like to express my deep gratitude to Dr. Sebastian Beck for his valuable help and useful advices. I am very grateful to Dr. Diego Esteban-Fernández for productive discussion that helped me to overcome difficulties in this work. Many thanks to Dr. Ahmed Hussein El- Khatib and Dr. Yide David He for their professional discussion and assistance in the lab. Also I would like to express my appreciations to Dr. Violette Frochaux, Dr. Ulrike Hochkirch, Dr. Kathrin Brückner, Dr. Georg Kubsch, David Benda, Yeliz Akyürek, Dr. Rajko Winkler, Dr. Lena Ruhe, René Becker, Sabrina Trog, Angelika Woyda, Pablo Loreo Lares, Dr. Kathleen Schwarz, Dr. Gunnar Schwarz, and all the whole former and current group members for the helpful assistance and discussions. Special appreciations to Sarah Aboulmagd for her friendly support, extensive discussions and constructive advises.

My sincere gratefulness goes to Thomas Lenz for his expert guidance. I am also very grateful to Simon Michaelis, Matthias Hakelberg, Uschi Gruber, Sylvia Niquet, Oliver Popp and other employees of caprotec for the friendly atmosphere and helpful support in terms of technical and scientific questions.

Special thanks to Natalia Loibl and to the working group of Professor Dr. Oliver Seitz for the help with fluorescence microscopy measurements.

It is a pleasure to thank the School of Analytical Sciences Adlershof (SALSA) and Mobilities for Innovation and Development (MID) consortium for the funding and continuous support.

The last but not the least my heartfelt thanks to my family and close friends, especially to my parents for their continuous care, support and encouragement, what contributed to the great extend to the fulfillment of this thesis.

Summary

The recent outstanding progress in modern proteomics was to a large extent enabled by the introduction of mass spectrometry (MS) based methods. It is known that for the study of genome obtaining the sequence information is of crucial importance; however, to fulfil the sophisticated study of proteome, the mere identification of proteins and peptides is not sufficient. Thus, proteomics includes both qualitative and quantitative paradigms. Proteomics aims to study also the expression level of proteins, posttranslational modifications, protein- protein interactions, etc. This allows to perform protein expression mapping, improve the understanding of cellular machines, to characterize the disease related protein distribution and to find answers for many other questions. Moreover, another ambitious goal connected to proteomics is drug discovery and preclinical drug testing. Nowadays the pharmaceutical industry has a high demand for methods that can reveal potential off-targets of drugs, and as a result can foresee the potential side effect and toxicity of the medicines. Among numerous proteomic tools developed up to date, chemical proteomics is one of the most promising approaches to address the interactions of drug-like small molecules with native proteins in their cellular context at the scale of proteome of cell or tissue.

Among chemical proteomics techniques Capture compound mass spectrometry (CCMS) has the advantage of addressing low abundant target proteins in lysates as well as in living cells. Moreover, by this approach also low affinity interactions can be studied in an efficient way. The CCMS is based on small molecule probes (capture compounds) that consist of three functional constituents: the first one, selectivity function is a small molecule. Quite often this small molecule is a drug, which interacts with the target protein. The second functionality allows covalent attachment of the molecular probe to captured protein under controlled conditions, namely UV irradiation. The third moiety allows detection either via isolation with magnetic beads followed by LC-MS/MS analysis, or via fluorescence readout. So far the detection functionalities utilized for CCMS can offer high sensitivity; however, the challenge of absolute quantification is still a bottleneck of this technique.

The ambition of this project was to develop a quantification approach applicable to CCMS. Nowadays numerous MS-based quantitative strategies are reported, many of them are based on the introduction of a lanthanide containing label.

Recently, a novel approach for absolute quantification of proteins and peptides was developed in our research group. Metal Coded Affinity Tagging (MeCAT) is a quantitative tool based on the chemical labeling with lanthanide containing metal complexes with a chelating agent. For MeCAT labelling the macrocycle 1,4,7,10-tetraazacyclododecane- N,N′,N″,N‴-tetraacetic acid (DOTA) is typically utilized as a chelate. This approach allows obtaining both the structural information with the utilization of organic MS detection (electrospray ionization and matrix assisted laser desorption ionization) and a quantitative information with the utilization of inorganic mass spectrometry detection (inductively coupled plasma mass spectrometry – ICP-MS).

In the frames of this project, MeCAT was utilized as a new detection

functionality of a capture compound. Besides inductively coupled plasma mass spectrometry quantification, the fluorescence based methods, as well as label free MS-based quantification were used as reference techniques.

Metal tags have not been utilized in chemical proteomics studies yet; therefore, the work included proof of concept experiment on a robust system methyltransferase (M.TaqI) and the cofactor product *s*-adenosyl-L-homocycteine (SAH). The proof of concept study was based on the investigations of SAH-based capture compound that carried MeCAT as the detection function. For this part of research project the capture experiment with the following detection was performed on isolated purified enzyme (M.TaqI). With the proof of concept study the successful utilization of MeCAT as a detection function of capture compound was demonstrated. The absolute quantification of the crosslink yield was achieved; moreover, it was proven that the implementation of metal core into the structure of capture compound does not compromise neither the specificity of photo induced crosslink, nor the affinity of molecular probe to the target protein. In addition to this, the sensitivity of inorganic MS based detection approach was compared to the sensitivity of fluorescence based methods.

The next part of the study was performed on living cells. Here, a G-protein coupled receptor and its interaction with an antagonist was investigated. The dopamine D2 receptor was targeted with a sertindole based capture compound functionalized with a lanthanide tag. In this project the system was first characterized with a corresponding capture compound with a fluorescent tag by fluorescence microscopy. With this reference method it was established that the capture compound targeted the receptor on the surface of the cell; moreover, the selectivity and specificity of capturing the target protein with the reference fluorophore functionalized capture compound was established.

The MS based imaging of cells treated with metal functionalized capture compound was performed; however, with the achieved resolution the localization of lanthanide containing probe across single cells was not possible. Nevertheless, the specificity of the crosslink of capture compound with the attached metal tag was proven via the laser ablation inductively coupled plasma mass spectrometry imaging. Moreover, with the absolute quantification of total cell population labelling with ICP-MS the specificity and selectivity of capture experiment was established.

In conclusion, in this work for the first time the successful utilization of chemoproteomic probes functionalized with a metal tag for the detection and absolute quantification of target proteins was established. With the experiments both on isolated enzymes and living cells it was determined that metal tag does not negatively influence other functional parts of chemoproteomics probes; therefore, capture compounds functionalized with lanthanide chelates demonstrate similar affinity to the target as the reference probes. Moreover, metal tags utilized for this type of molecular probes can offer a promising elemental imaging technique. However, to achieve the sufficient resolution multiple metal tags per molecular probe are needed. The striking advantage of the approach of utilization metal functionalized capture compound combined with inorganic mass spectrometry

detection is that it allows absolute quantification of crosslink yield, what cannot be performed with other detection methods applied for this technology.

Zusammenfassung

Unter den Techniken der chemischen Proteomik hat Capture Compound – Massenspektro- metrie (CCMS) den Vorteil, Interaktionen von Molekülen mit geringer Affinität zueinander effektiv untersuchen zu können. CCMS beruht auf kleinen molekularen Sonden (Capture Compounds oder CCs), die aus drei funktionalen Bestandteilen bestehen: der erste, die Selektivitätsfunktion, ist ein kleines Molekül. Oft ist dieses kleine Molekül ein Pharmazeutikum, das mit einem Zielprotein eine schwache Wechselwirkung eingeht. Die zweite Funktionalität erlaubt kovalente Anhaftung der molekularen Sonde an Proteine unter kontrollierten Umständen, namentlich UV-Strahlung. Der dritte Anteil erlaubt Detektion entweder durch Isolation mittels magnetischer Partikel gefolgt von LC-MS/MS-Analyse, oder durch Auslesung von Fluoreszenz. Beides bietet sehr gute Sensitivität; allerdings ist die Quantifizierung weiterhin ein Schwachpunkt dieser Technik.

Ziel dieses Projektes ist, eine in CCMS verwendbare Quantifizierungsmethode zu entwickeln. Heutzutage gibt es zahlreiche MS-basierte Quantifizierungsstrategien; unsere beruht auf der Einführung von Lanthanoid-haltigen Labels. Metal Coded Affinity Tagging (MeCAT) ist ein Quantifizierungswerkzeug chemischen Labeling durch den Lanthanoide enthaltenden Makrocyclus 1,4,7,10-Tetraazacyclododecan-N, N', N", N"'-tetraessigsäure (DOTA) als Chelat. Diese Methode erlaubt, die strukturelle Information mittels Elektrospray- und Matrixunterstützte Laser-Desorptions-Ionisation) und quantitative Information durch Massenspektrometrie mit induktiv gekoppeltem Plasma (ICP-MS) zu erhalten.

Im Rahmen meines Projektes wurde MeCAT als eine neue Detektionsfunktionalität für CCs verwendet und entsprechende Verbindungen wurden synthetisiert. Neben ICP-MS-basierte Quantifizierung wurden Fluoreszenz-basierte Methoden sowie Label-freie MS Quantifizierungen als Referenztechniken verwendet. Metall-Marker fanden in derartigen Studien bisher keine Verwendung; daher schloss unsere Arbeit ein Experiment zum „Proof of Concept“ an einem stabilen und gut studierten System mit ein: Methyltransferase (M.TaqI) und der Cofaktor S-Adenosyl-L-Homocystein (SAH). Die Proof of Concept-Studie basierte auf den Untersuchungen einer SAH-basierten Capture Compound, das MeCAT als Detektionsfunktion trug. Für diesen Teil des Forschungsprojektes wurde ein Experiment mit der folgenden Detektion auf isoliertem, gereinigtem Enzym (M.TaqI) ausgeführt.

Wir haben eine absolute Quantifizierung der Ausbeute der Quervernetzungen (Crosslink) erreicht; überdies wurde bewiesen, dass die Verwendung von Metallen in CC- Strukturen weder die Spezifität der UV-Licht-induzierten Quervernetzungen noch die Affinität molekularer Sonden zum Zielprotein beeinflusst. Zusätzlich wurde die Empfindlichkeit der ICP-MS mit der Fluoreszenz-basierter Methoden verglichen.

Der nächste Teil der Studie wurde an lebenden Zellen durchgeführt. Es wurde ein G-Proteingekoppelter Rezeptor und seine Interaktion mit einem Antagonisten untersucht. Der Dopamin D2- Rezeptor wurde mit einer Sertindol-basierten MeCAT-Capture Compound funktionalisiert. Das System wurde zuerst mittels einer ähnlichen Capture Compound mit fluoreszierendem Marker durch

Fluoreszenz-Mikroskopie charakterisiert. Durch diese Referenzmethode wurde sichergestellt, dass diese CC an den Rezeptor auf der Oberfläche der Zelle binden. Weiterhin wurde die Selektivität und Spezifität des „Einfangens“ des Zielproteins mit der Referenz des CCs etabliert.

Die MS-basierte bildliche Darstellung von Zellen, die mit einer Metall-funktionalisierten Capture Compound behandelt waren, folgte dann; allerdings war mit der erreichten Auflösung die Lokalisation von Lanthanoid enthaltenden Sonden innerhalb einzelner Zellen nicht möglich. Trotzdem konnte die Spezifität der Crosslink-Verbindung des CCs mit dem Metall- Marker mittels ICP-MS mit Laserablation bewiesen werden. Überdies wurden die generelle Selektivität und Spezifität der synthetisierten Verbindungen mit der Absolutquantifizierung durch ICP-MS von kompletten Zellbestände etabliert.

Zusammenfassend wurde in dieser Arbeit erstmalig die erfolgreiche Verwendung mit Metall- Markern funktionalisierter chemoproteomischer Sonden zur Detektion und absoluten Quantifizierung von Zielproteinen mit schwacher Wechselwirkung etabliert. Mit den Experimenten an isolierten Enzymen und an lebenden Zellen wurde nachgewiesen, dass Metall-Marker keinen negativen Einfluss auf andere funktionelle Teile chemoproteomischer Sonden haben. Capture Compounds, die mit Lanthanoid- Chelaten funktionalisiert sind, zeigen ähnliche Affinität zu ihren Zielproteinen wie die Referenz-Sonden. Zudem erlauben Metall-Marker, die für diese Art molekularer Sonden verwendet werden, die Entwicklung einer element-basierten Technik zur Bilderzeugung. Um eine ausreichende Auflösung zu erreichen benötigen wir allerdings mehrere Metall-Marker pro molekularer Sonde. Der herausragende Vorteil der Metall-funktionalisierten CCs kombiniert mit ICP-MS ist, dass diese eine absolute Quantifizierung der Ausbeute der Quervernetzungen ermöglichen. Andere Strategien, zum Beispiel mit Fluoreszenz, erlauben dies nicht.

Index

1. Introduction

1.1. Proteomics

We are living in an era when the paradigm of biosciences changed to systematic and comprehensive principles. Recently developed analytical techniques such as genomics, proteomics, and metabolomics promoted an outstanding progress in the field of life sciences and turned the study of biological objects into interdisciplinary research. [1][2]

Almost a century ago the term genome was generated by H.Winkler with the cited translation: "I propose the expression Genom for the haploid chromosome set, which, together with the pertinent protoplasm, specifies the material foundations of the species ...". [3]

The words genome and genomics have been a catchphrase for many decades. Genomics can be defined as the study of genome, what means the study of the DNA arrays in a different species. One of the recent crucial milestones in this field was the completion of sequencing of the human genome in 2004.While genomics is answering a question about the sequence of DNA, the goal of proteomics is to answer the questions about proteins synthesized from DNA, which are of higher complexity. [2][4]

The definition of proteome is analogous to the one of genome; it is an array of proteins expressed by the genome in a cell, tissue or an organ. The concept of proteome was firstly proposed by Wikins in 1995, to characterize the gene expression based on protein analysis. However, the starting point of proteomics development stands for an earlier turning point, namely the first powerful tool for protein sequencing – Edman degradation. The implementation of 2-dimentional gel electrophoresis (2-DE) as a resolving tool and mass spectrometry (MS) based detection resulted in a dynamic progress in the research field of proteomics. Some important milestones in development of proteomic techniques are summarized in Figure 1.[1] [5] [6]

One of the biggest challenges of proteomics is a high complexity of proteome (Figure 2). The complex nature of proteome can be explained with post-translational modifications, alternative gene splicing, allosteric regulations, protein-protein interactions. In addition to this, some biochemical mechanisms, resulting in dynamic changes of proteome are not connected to the process of synthesis and degradation of proteins. [1][7][8]

As far as the challenge of the detection of the changes at the level of genome and the proteome is concerned, the amount of the required information is drastically different, what is illustrated with the Figure 2. At the level of genome only two characteristics are important: sequence and abundance. However, in case of proteome analysis, numerous parameters should be considered, such as: structure and function, the level of expression, localization of the protein of interest

(cellular and sub-cellular), post-translational modifications, protein activation, interactions of proteins with proteins, lipids and nucleic acids, protein synthesis and turnover rates, co-factors etc. [1][9][10][11]

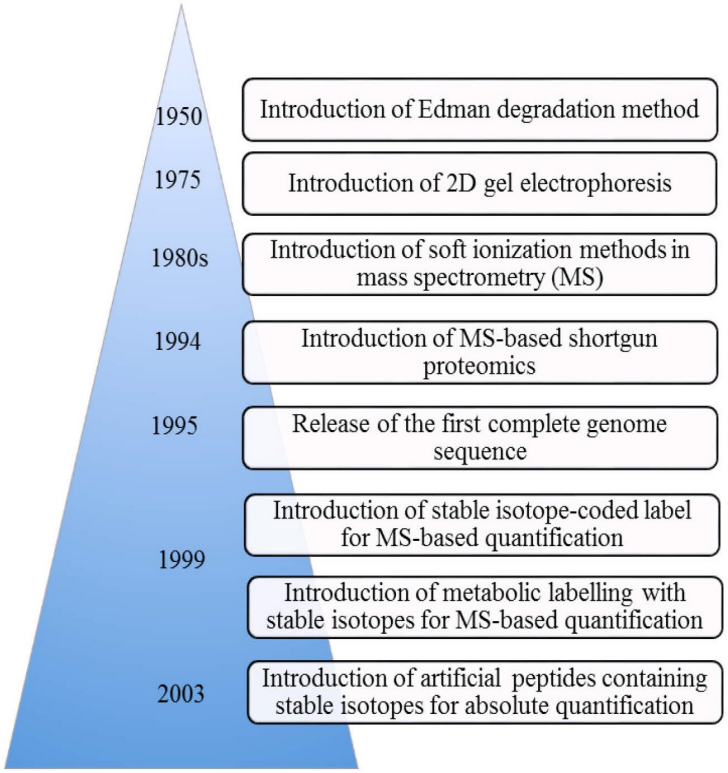

Figure 1. Short overview of milestones in proteomic research. Modified from Becher et.al. [12]

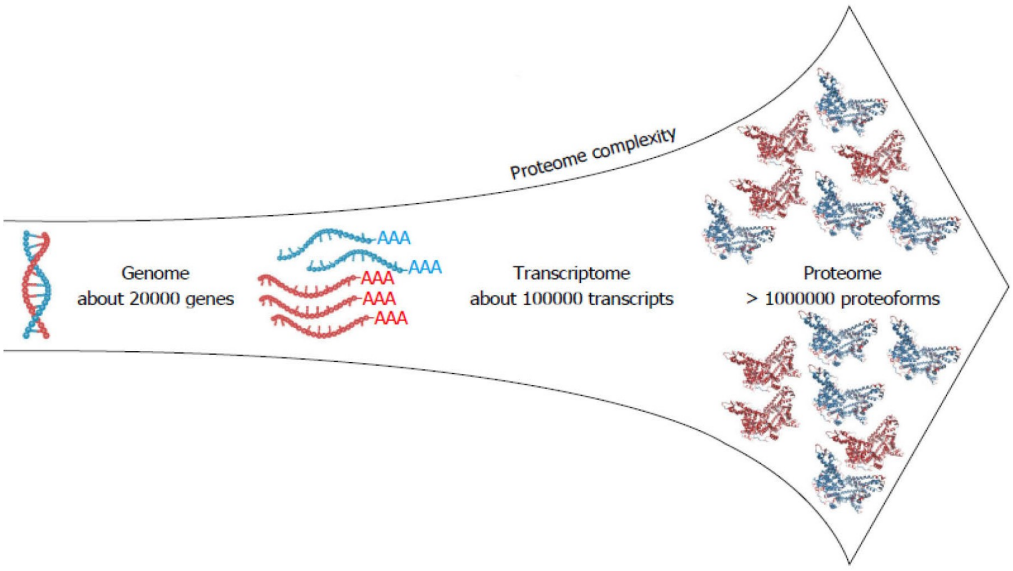

Figure 2. From genome to proteome. Increase of proteome complexity. Contributed from Bennike et al [13]

One of the most promising and vital applications of proteomics is discovering the mechanism of a drug action, revealing the side effects and toxicity and uncovering potential drug targets, what can influence pharmacology to a great extent. Nowadays the dramatic progress in proteomic techniques allows to address up to 10000 proteins; in addition to it, a wide dynamic range of protein abundance can be detected. Among numerous approaches existing nowadays in the rapidly growing field of proteome research, chemical proteomics is one of the most powerful tools. Chemical proteomics is a widely used approach for the preclinical studies of drug molecules that can complement in a great extend to pharmaceutical approach.[14][15][16][17][18][19][20]

1.2. Chemical proteomics

The concept of chemical proteomics encompasses a chemical enrichment or modification of the proteome, to assist the detection of proteins. It is an interdisciplinary unit of proteomic sciences that includes organic chemistry, biochemistry, cell biology and analytical chemistry. Chemical proteomics focuses on study of specific interactions between proteins and small molecules that have bioactive properties, quite frequently these molecular probes represent a drug. This field of study can bring significant input into exploration of unrevealed protein functions, interactions of proteins with drugs and their side effects, what is of crucial importance for the drug development. [21] [22] [23][24]

The graphical comparison of assets and limitation of chemical proteomics is shown in Figure 3. The benefits of chemical proteomics include exploration of proteins functionalities, which were not addressed previously. Moreover, this approach enables the analysis of the entire proteome or subproteome, thus it is feasible to probe proteins in their native state including different level of abundancy, post translational modifications, mutations, protein-protein interactions. In addition to this, with chemical proteomic approach a diversity of samples can be investigated. Several limitations have to be pointed as well: a relatively big amount of sample is needed for the analysis; membrane proteins might be challenging to address due to the solubility reason. Moreover, to avoid incorrect interpretation, the abundance of protein has to be correlated with its affinity, thus additional experiments to evaluate the affinity are needed. [17][25]

In addition to the challenges of synthesis, obtaining information about structure-activity relationship, etc.; chemical proteomics is also concerned with unspecific interactions with the background proteins, the low abundance of target proteins, and the interferences caused by the sample processing. The specificity of interaction between the molecular probe and target protein is influenced by the presence of variety of proteins in a sample, some of these biomolecules might have on the one hand a lower affinity to a molecular probe in comparison with target protein, and on the other hand a higher abundance in comparison with the protein of interest. This can result in generation of a significant background noise and might mislead the data interpretation. Another factor that can increase the intensity of background signal is the co-purification of high abundant proteins via affinity approaches or the off-target high abundant proteins that tend to associate with the protein of interest. Therefore, to distinguish the non-specific interactions, the additional negative

control is needed if available, otherwise the interpretation should be correlated to the evaluated abundance of protein. [17][26]

Another important property of chemical proteomics probes to consider is selectivity, it is defined by the number of proteins that can potentially bind to a probe. Thus, the fewer number of potentially binding proteins correspond to a higher selectivity of a probe. Probe functionalized with maleimide group is an example of non-selective agent, since it reacts with all cysteine groups. As an example of probes with high selectivity those that are utilizing electrophilic groups can be considered. [23][27]

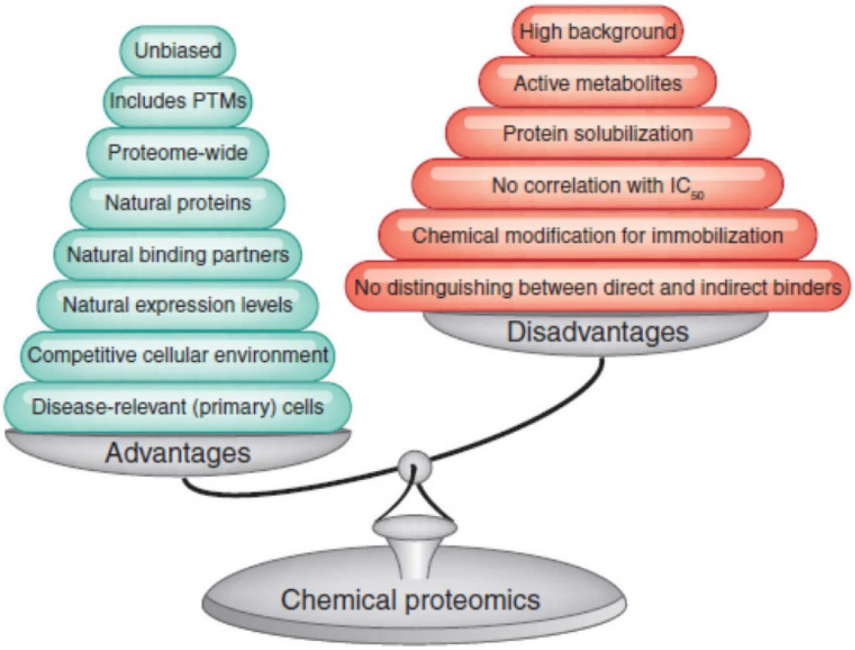

Figure 3. Comparison of advantages and disadvantages of chemical proteomics to conventional methods. Adopted from Rix et.al. [17]

Among the variety of the approaches utilized for chemical proteomic research three main categories can be featured: the global proteomic approach which aim is to identify and quantify all proteins in the sample; the functional approach based on molecular probes to address the certain target, and affinity enrichment approach. The comparison of the most favored workflows for the characterization of drug interaction with the proteome are illustrated with the Figure 4. The global proteomics (Figure 4 A) provides information about protein sequence, expression, abundance, and post-translational modifications based on mass spectrometry detection and comparison of the treated and control samples. The functional approaches are represented with protein profiling based on interaction with small molecular probes (Figure 4 B) and affinity enrichment (Figure 4 C). With affinity chromatography approach the sample undergoes affinity based enrichment via exposition to a solid surface functionalized with small bioactive probes, followed by isolation of subproteome and mass spectrometry based detection (Figure 4 C). The approach based on interactions with small molecular probes is

based on the chemical reaction between target protein and a probe resulting in a formation of a covalent bond. After that sample undergoes isolation and mass spectrometry based analysis (Figure 4 B).[19][14]

Prior to discuss these approaches in more details, a short overview of sample preparation methods utilized for the analysis of proteome, and the ionization methods for mass spectrometry detection will be introduced.

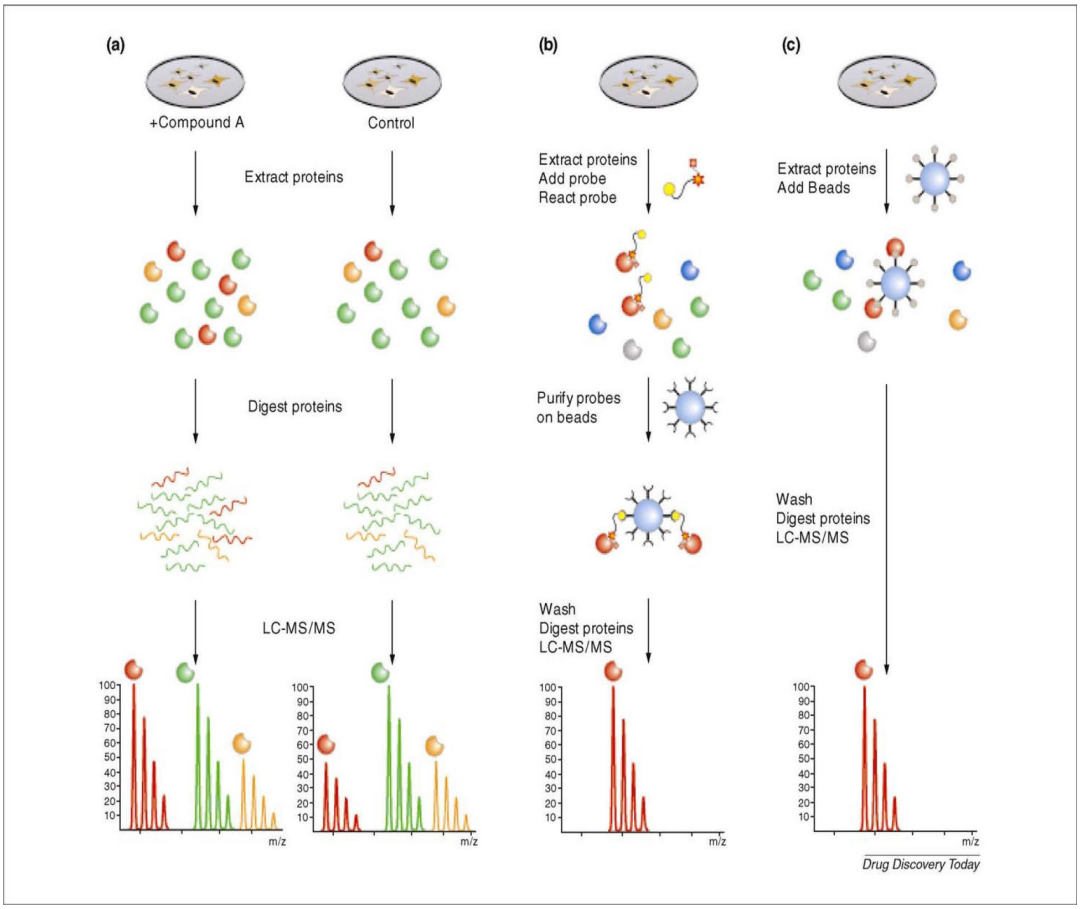

Figure 4. Experimental workflows in chemical proteomics: (a) global proteomic approach; (b) protein profiling based on the interactions with the small molecule; (c) affinity chromatography. Adopted from Bantscheff et al [19].

1.3. General sample preparation strategies for proteomic research

It is known that the sample preparation plays a crucial role for chemical and biochemical analysis. As far as the proteomic research is concerned, the importance of the sample preparation cannot be underestimated due to the complexity of proteome, different abundances and solubility properties of proteins and other factors. The vast number of the possible sources of samples for the proteomic research, for example body fluids, cell cultures, tissues, etc. are causing the diversity of the sample preparation strategies. [28]

The sample preparation for proteome analysis includes homogenization, purification, fractionation, enrichment, etc. First of all, the sample material such as tissue or cell lysate should be homogenized with mechanical, ultrasonic or freeze-thaw methods to increase the reproducibility of detection outcome. The second important factor for the successful analysis is the dissolution of the sample.

The solubilization factor is a typical source of difficulties for the protein analysis, because the proteins in their native state are quite often not soluble; membrane proteins, acidic or basic proteins, and low abundant proteins are especially challenging to address, and usually requiring the sophisticated optimization of the experimental conditions. After the successful solubilization, the exclusion of the possible interferences from such contaminants as salts, detergents, lipids, nucleic acids, and abundant proteins is necessary. One of the most popular methods for protein extraction is protein precipitation with acetone, methanol, and ethanol. Other methods utilized for protein enrichment are: centrifugation, electrophoretic separation (capillary and gel electrophoresis), chromatography, fractionation with size-exclusion filters, and the enrichment on the solid support. The protein enrichment is of the crucial importance for the mass spectrometry based proteomics, since this approach is vulnerable to the signal overlapping, the ionization suppression, and the possible obscure outcome of the MS detection.[20] [28][29]

1.3.1. Gel electrophoresis and Western blot

The protein separation via electrophoretic approach is nowadays one of the trivial sample preparation methods utilized in proteomic research. The main principle of this separation technique is the migration of charged molecules under the application of the electric field. The charged proteins are pushed to move through a gel grid; the migration pattern of is dependent on its charge and size. Among other approaches utilized for electrophoretic separation of biomolecules, the sodium dodecyl sulfate-polyacrylamide electrophoresis (SDS-PAGE) is one of the most frequently used ones due to its convenience. With the addition of sodium dodecyl sulfate (SDS) a formation of complex compound between detergent and biomolecule takes place, this minimizes the impact of the proteins native charges and also causes the unfolding of the proteins into the linear structure, which is negatively charged. [20][28]

The resolving of proteins with electrophoresis was reported for the first time by Hoch [30]; the successful utilization of the electrophoresis in polyacrylamide gels in the presence of sodium dodecyl sulfate for the estimation of molecular weight of protein was described for the first time by Shapiro; in his work the linear relationship between the migration rates and molecular weights of protein was established [31].

The one dimensional separation approach as it is most frequently used nowadays, was suggested by Laemmli [32]. Currently the one dimensional SDS-PAGE is used mostly for the pre-fractionation due to its non-sufficient resolving power for a complex samples.

The approach of the two dimensional gel electrophoresis (2-DE) was firstly introduced by O´Farrell in 1974. [33] This technique allows the separation of proteins based on their isoelectric point, molecular weight, solubility and relative abundance. The two-dimensional gel electrophoresis is one of the core techniques of the modern proteomics with the limit of detection lower than 1 ng of the protein of interest, and the resolving power of more than 5000 proteins at the one run. Currently the 2-DE technology is challenged with separation of hydrophobic and low abundant proteins and the protein quantification based on fluorescence readout. [1][34]

Several general approaches for gel-based protein identification and quantification can be featured: staining with anionic dyes (Coomassie brilliant blue), silver staining, fluorescent staining, etc. The main requirements for staining methods are high sensitivity, low limit of detection and the good reproducibility. The more specific detection approaches for gel-based proteomics are beyond the scope of this work.[1][28]

The method, which allows the correlation between the results of electrophoretic separation and the activity of the resolved proteins was proposed by Towbin [35]. The main idea behind it was the transfer of the resolved proteins from polyacrylamide-urea gel to a nitrocellulose membrane, followed by the immunoassay detection (Figure 5). However, with the application of this approach to SDS-based gels the quantitative transfer was not achieved. Later the successful quantitative electrophoretic transfer of the protein bands from SDS-polyacrylamide gel to the nitrocellulose membrane was reported by Burnette, this method was coined Western blotting [36]. The Western blotting technique is widely applied for the analysis of proteins due to its high sensitivity and simplicity. For many years this method was successfully utilized as a principal tool for detection of specific proteins, for study of the protein relative abundance, relative molecular mass, and posttranslational modifications. Nowadays, the Western blotting is frequently used as reference method for validation of results of mass spectrometry analysis of proteins.[37][38]

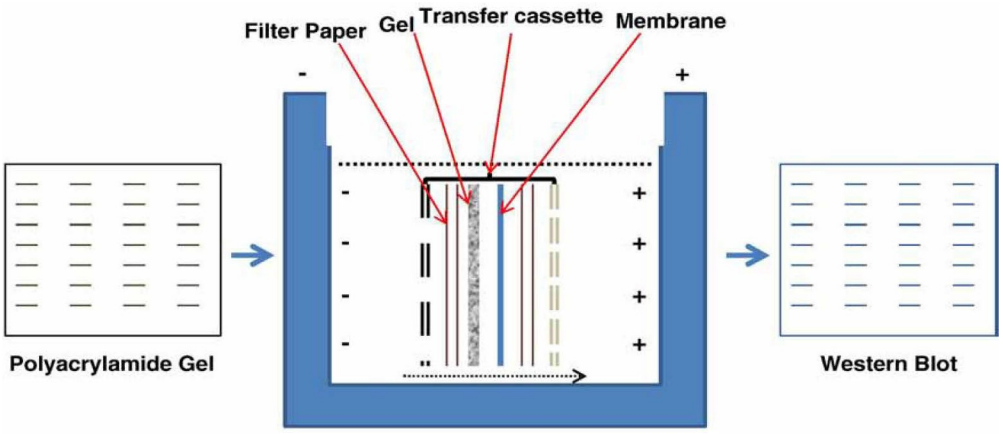

Figure 5. A schematic image of the process of electroblot transfer. Adopted from MacPhee [37].

1.3.2. Liquid chromatography

Liquid chromatography (LC) is one of the key separation techniques in proteomics. The method is based on migration of dissolved sample (mobile phase) through the chromatographic system and its interaction with the stationary phase. These interactions are dependent from different factors: adsorption properties, size, ion charge, etc. The retention time is proportional to the intensity of interactions. The chromatographic system can be characterized with separation power, retention time and loading capacity, etc. [20][39]

The chromatography was discovered by Tswett; however, the method gained popularity only in 1931 after its introduction by Kuhn, Winterstein, and Lederer. The liquid-partition chromatography was reported by Martin and Syne for the first time in 1941. The LC analysis of amino-acids was automated already at 1960s. The broad implementation of high performance liquid chromatography (HPLC) started in 1964. The term "reverse-phase chromatography" was suggested by Howard [40] to describe the technique when the non- polar bonded phases were used with hydro-organic eluents in HPLC separation. Historically in 1970s, the majority of liquid chromatography separations were performed with the utilization of hydrophilic stationary phase with the polar surface. This approach has been known as the "normal-phase chromatography". [41]

HPLC method is based on utilization of small particles as a stationary phase and a high flow pressure in order to obtain higher resolution and to enhance the speed of separation, the RP- HPLC is one of the most frequently utilized separation methods for proteomic research. The commonly used stationary phase for RP-HPLC is organic-silica compounds, functionalized with linear alkyl chains, the commonly used solvents are aqueous solutions of methanol or acetonitrile. [20] [39][42]

One of the main advantages of this technique for analysis of proteins and peptides is that it allows the sample separation directly prior to the MS detection. The main limitation factors for the sample loaded to HPLC column are the solubility, the elution strength of the solvent, and the presence of detergents. [29]

1.4. Ionization sources for mass spectrometry detection

1.4.1. Ionization techniques for mass spectrometry detection

The mass spectrometer consist of three major blocks: ion source, mass analyzer and detector. In the frames of this work, only ion sources will be briefly outlined. The mass analyzers and detectors are discussed in numerous books, for instance Ekman et al. "Mass Spectrometry". [39]

The ion source generates gas phase ions from analyte. Generally the sources can be divided into two categories: soft (molecular) ion sources that can ionize even large molecules without decomposition and the sources that decompose the sample into atoms (atomic sources). Numerous methods of ion generation can be featured: gas discharge, thermal ionization, spark source, glow discharge, inductively coupled plasma, electron ionization, chemical ionization, electrospray ionization, desorption electrospray ionization, laser desorption ionization, matrix assisted laser desorption

ionization, etc. [39]

Among this variety, the most frequently utilized techniques in the field of proteomics are electrospray ionization (ESI) and matrix-assisted laser desorption ionization (MALDI); in addition to it, recently the inductively coupled plasma (ICP) became a popular ionization source to address the quantification challenge. These techniques will be discussed further.[1] [20]

1.4.2. Electrospray ionization

Electrospray ionization was introduced for the first time in 1968 by Dole, this technique was further developed by Yamashita and Fenn [43] resulting in coupling of this ionization source to mass spectrometer. ESI method was promoted with the introduction of a nanospray by Wilm and Mann, this improvement (application of a smaller capillary tip) could significantly decrease the amount of the analyte required for the analysis.[20][39]

The core of electrospray ionization technique is the formation of gas phase ions from molecules in solution via spraying into electric field. The high electric potential induces the formation of a Taylor cone which generates droplets that are highly charged on their surface (Figure 6). The droplets decrease in size due to evaporation, as the result the small charged droplets enter the chamber where they are desolvated with the dry nitrogen, this results in the entering a mass analyzer of a charged molecules of analyte.[20][39][43]

The electrospray ionization is a “soft” ionization method, the striking feature of this technique is that it allows to address large biomolecules avoiding their decomposition, what allows to detect intact post-translational modification, and non-covalently bound complexes. Since with electrospray ionisation of proteins and peptides multiple charged ions are produced, the obtained spectra for such molecules consists of the multiple peaks with the difference of one charge. [1][39][43]

The sample preparation for the ESI-MS analysis is not demanding: it includes the dissolution of a sample in a mixture of water and organic solvent (for instance methanol) with addition of a small amount of organic acid (for example formic acid). The main limitation of this ionization technique is the suppression of the signal from analyte; therefore, such factors as pH, the composition of solvent, concentrations of salts can notably influence the sensitivity of the analysis.[39]

1.4.3 ***Matrix-assisted laser desorption ionization***

Matrix-assisted laser desorption/ionization (MALDI) technique was introduced by Karas et al in 1987. Nowadays, MALDI is a comprehensive tool for analysis of proteins, peptides and other biomolecules.[44][45]

The backbone of MALDI analysis is co-crystallization of analyte with an excess of a matrix. The main requirements for matrix compounds are the low molecular mass and high absorption of light, in many cases weak organic acids are corresponding to these demands. Under the laser radiation the analyte containing matrix is vaporized, what results in a mixture of ionized and not ionized matrix molecules with ionized and not ionized analyte molecules in a gas phase (Figure 7). The matrix can act both like donor and receptor of proton, thus the ions can be both of positive and

negative charge. [39][45]

MALDI is considered to be a very easy technique to learn and use practically; however, the sample preparation for MALDI analysis is not that simple and straightforward in comparison with ESI. First of all the choice of matrix is of crucial importance of the quality of the obtained results; secondly the transfer of the mixture of matrix and analyte to the sample plate and its drying can influence the outcome of analysis. [1][20][39][45]

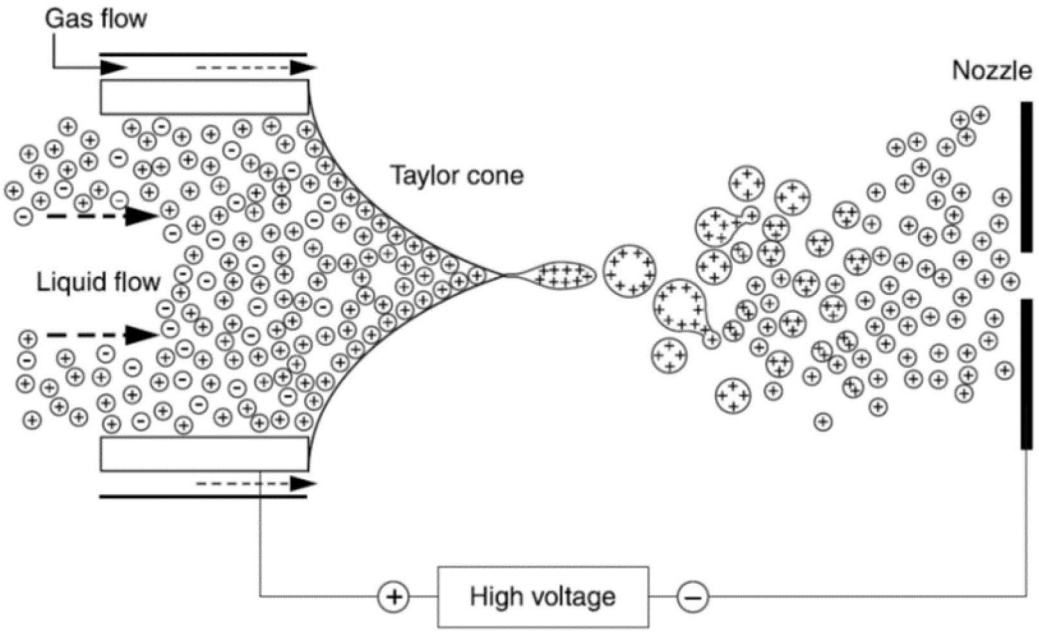

Figure 6. Schematic representation of ESI source. Adopted from Ekman et al. [39]

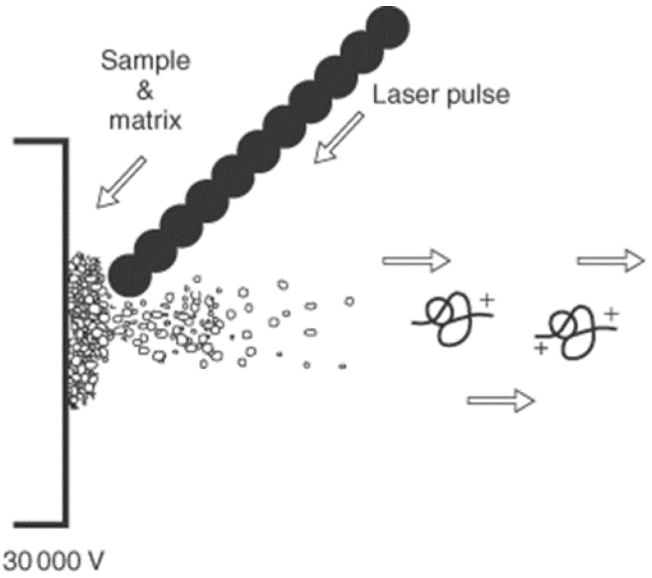

Figure 7. Schematic representation of MALDI source. Adopted from Lewis et al. [45]

Among advantages of this ionization technique are high ionization efficiency, high sensitivity and accuracy. MALDI is one of the most favorable ionization sources

for protein analysis, since it allows to address large, intact proteins and provide the detection on the femtomole level. The main restriction of MALDI is that results can vary based on the utilized matrix; in addition to it, obtaining quantitative information with MALDI based analysis is still challenging. [20][39][45]

MALDI mass spectrometry has a broad application in medical sciences as a diagnostic tool applicable both for fluid samples and tissues. MALDI mass spectrometry imaging is an outstanding technique for pathology-directed research since it allows to detect biomarkers, perform spatial mapping of molecules of interest in biopsy samples; moreover, it is a promising method for cancer diagnostics. [20][46][47]

1.4.4. Inductively coupled plasma

The inductively coupled plasma (ICP) is one of the pioneer ionization techniques utilized in combination with mass spectrometry detection. The application of inductively coupled plasma combined with mass spectrometry detection was reported by Houk in 1978. [39]

This ionization technique is based on the introduction of analyte molecules to a high temperature plasma, where it is desolvated, collapsed into atoms and ionized due to a high- temperature plasma discharge. As it is shown in Figure 8, the ICP source consists of torch and load coil, the radiofrequency is passing through the coil, resulting in formation of a strong magnetic field. The plasma is generated due to the interaction of magnetic field on a flow of gas (in most cases argon) through a concentric tube (torch). The produced ions enter the mass spectrometer through the interface region (cone with orifice).[39][48]

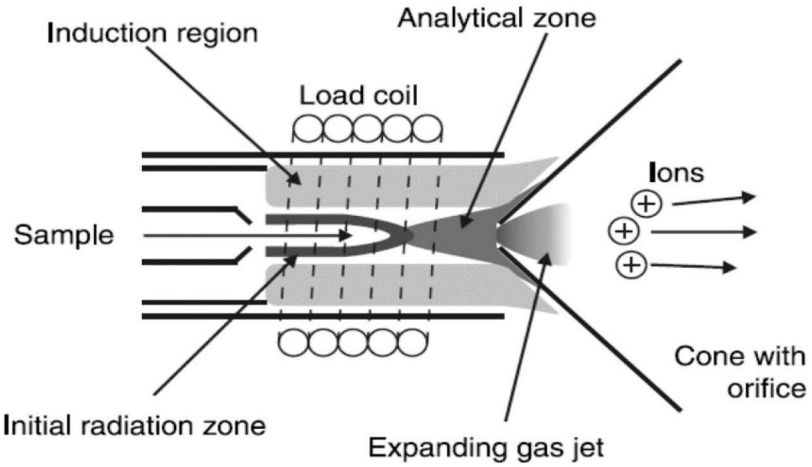

Figure 8. Schematic representation of ICP source. Adopted from Ekman et al. [39]

Nowadays ICP-MS is frequently used for the analysis of inorganic compounds, trace element analysis and isotope ratio measurement. The fields of application of ICP-MS include environmental, geological, nuclear, and biomedical studies. In addition to it, recently it became a tool of choice in the field of proteomics. Moreover, the term metallomics was coined as the study of metals and metalloid compounds, their interaction with biomolecules in biological system, the ICP-MS became one of the

crucial research tools in this field. [2][39][49] [48]

The merits of ICP-MS are high sensitivity, low detection limit (femtogram level), matrix- independent analysis, wide dynamic range (up to 9 orders of magnitude), multielement and multiisotopic analysis, the last but not the least ICP-MS is an excellent quantification tool. The main limitation of this ionization technique are possible spectral interferences occurring in an argon containing plasma. [39] [49] [50]

1.4.5. Laser ablation inductively coupled plasma mass spectrometry

Recently ICP-MS based analysis found a broad application in the field of bioimaging via the utilization of laser ablation inductively coupled plasma mass spectrometry (LA-ICP-MS). This technique is mainly focused on measurement of metals in solid samples. The LA-ICP- MS includes the ablation of the sample by laser beam, the ablated sample is carried to the ICP source with the flow of inert gas (Ar or He) as is shown in Figure 9, after that the atomization and ionization of sample is taking place as was described previously. [2] [51]

The merits of LA-ICP-MS are high sensitivity, high accuracy; in addition to it the results of LA-ICP-MS detection are not dependent from matrix what enables the quantification. Nowadays LA-ICP-MS is one of the most sensitive tools applied for bioimaging. [2][52]

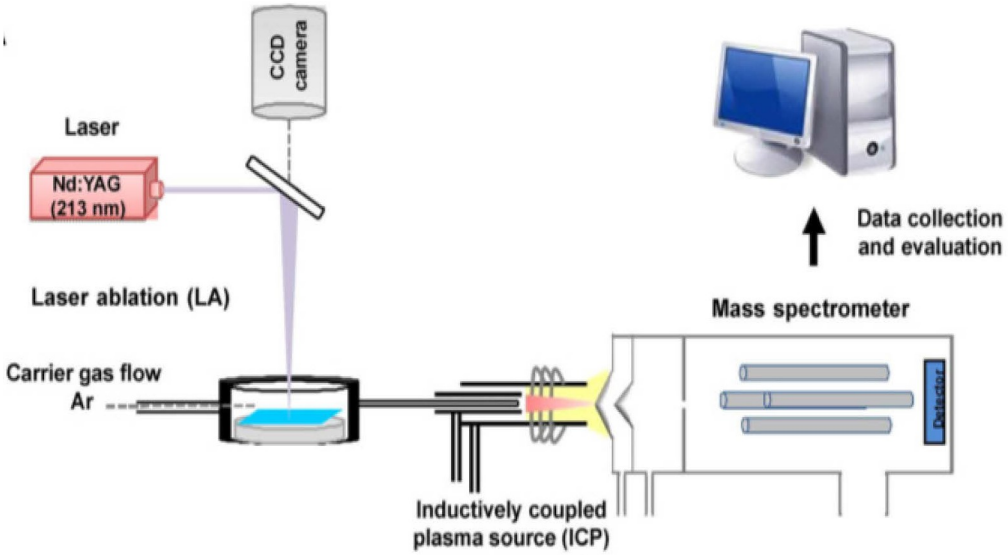

Figure 9. Schematic representation of LA-ICP-MS analysis. Modified from Pornwilard et al. [53]

Among the numerous applications of LA-ICP-MS as a bioimaging tool the investigation of Parkinson´s disease, stroke and aging on brain tissues, metal uptake, cancer studies, etc. Moreover, this technique is involved in drug development and plant sciences. The promising directions of further development of this method include the mapping of 3D distribution of element of interest in organ and the imaging of single cells. [2][51][52]

Since the fluorescent microscopy has been utilized as a reference method in frames of this research project, a brief overview of this technique will be presented.

1.5. Fluorescence microscopy

The challenge of obtaining contrast in order to distinguish and perceive details via microscopy was one of the stumbling blocks of biological investigations for many years. Among such approaches as color staining, phase contrast, differential interference contrast, the fluorescence based technique became the prevalent one. Nowadays, the fluorescence microscopy is an excellent tool for life sciences research, especially for biochemical analysis of living cells. [54] [55]

The fluorescence microscopy is based on illumination of the specimen with one wavelength and filtering the return light, thus the longer wavelength shifted fluorescence is observed against a black background. The schematic image of fluorescent microscope is shown in Figure 10. The source of generates light of a full spectra, the light beam goes through the filter cube, which is cutting the wavelength that excites the targeted fluorophore. A fluorescence light is emitted in all directions; however, only a fraction of obtained fluorescence is collected by objective and directed through the filter cube to the ocular or to the camera. [54][56]

The detection with fluorescence microscopy provides the high contrast, sensitivity on the level of a single molecule, high selectivity and specificity. Among the restrictions of method are a limited time of stability of fluorophores, misinterpretation of small object (smaller than 250nm) and a possible phototoxic effect, which can lead to various alterations of cell functions or even to lethal damages. [54]

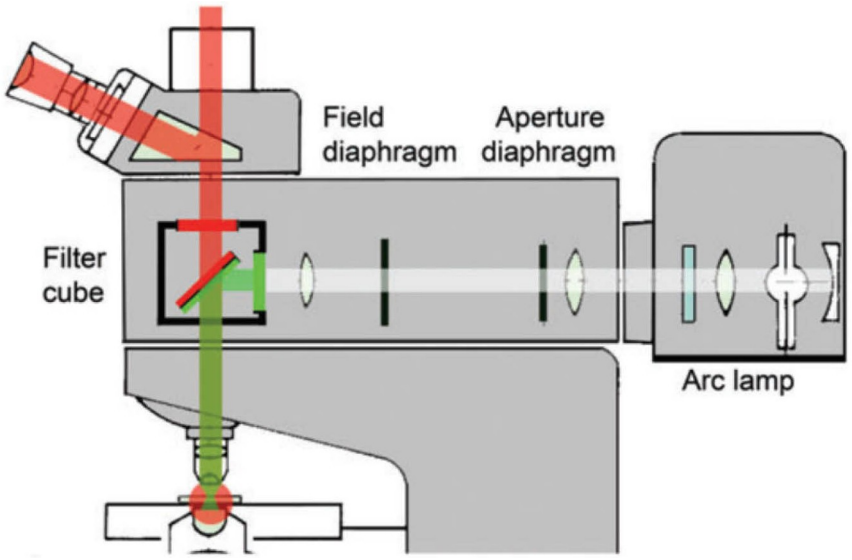

Figure 10. Schematic representation of fluorescence microscope. Contributed from Lichtman et al. [56]

In the field of proteomic research the fluorescence microscopy is utilized for characterization of protein expression, function and activity. This technique is used to address fluorescent proteins, quantum dots and samples tagged with small organic dyes. The proteins are mostly tagged via immunolabeling approaches and genetically encoded modifications. [57]

1.6. Global approach. Mass spectrometry based proteomics

Among various techniques utilized for the studies of proteome, as for instance protein arrays and microarrays based detection, fluorescence, etc., the mass spectrometry-based approach became a mainstream method for the analysis of protein samples. Mass spectrometry based proteomics became one of the leading techniques in the field due to such generalized reasons as: intrinsic specificity, comprehensive workflow, and the potential for high sensitivity. Moreover, with this approach numerous peculiar features of proteome can be addressed such as: sequence information, quantitative data, monitoring of modifications, structural information and the characterization of intramolecular interactions. Nowadays, besides the conventional approaches when proteins are isolated and analyzed based on their structural and functional properties, with the method of choice, the rapid development of computational techniques also contributed to the study of proteome to a big extend. [1][10][11] [16][58]

Historically, the trivial approach for the identification of proteins was de-novo sequencing accomplished by the stepwise chemical degradation, which is known as Edman degradation. This is a powerful and robust technique; however, it is also a time consuming method and with this approach chemically modified proteins cannot be addressed. The acceleration of LC-MS and LC-MS/MS techniques contributed to a great improvement in proteome sequencing especially in terms of dealing with a big number of samples. The approach is based on the correlation of the information obtained from the analysis of proteins with the one from the database. Nowadays, the complete sequence databases, combined with the advanced mass-spectrometry techniques and breakthrough searching algorithms resulted in a robust, rapid and sensitive approach for the identification of proteins and peptides. [39][59]

The identification of proteins is based on peptide mass fingerprinting approach, based on the acquired peptide map that is unique for every protein; more advanced approach is based or the acquired fragmentation spectra of peptides from the digest product.[39]

For the mass spectrometry based analysis of proteins two methods of protein identification can be featured: top-down and bottom-up (shortgun). Their schematic comparison is illustrated with Figure 11. The workflow for the top-down approach starts with sample fractionation and electrophoretical separation, followed by tryptic digestion. The resulting digestion product – mixture of peptides, is analyzed with LC-MS/MS, the obtained information is proceeded with the database searching tool, as the result the corresponding peptide sequence is retrieved from the database library. This approach provides quite straightforward identification of protein. In case of bottom-up method the protein is firstly enzymatically cleaved into peptides then the mixture of peptides undergoes the fractionation,
after that the sample is analyzed by tandem LC-MS(MS/MS) the identification of protein is based on peptide fragmentation readout (MS^2 spectra).[60] [61][62]

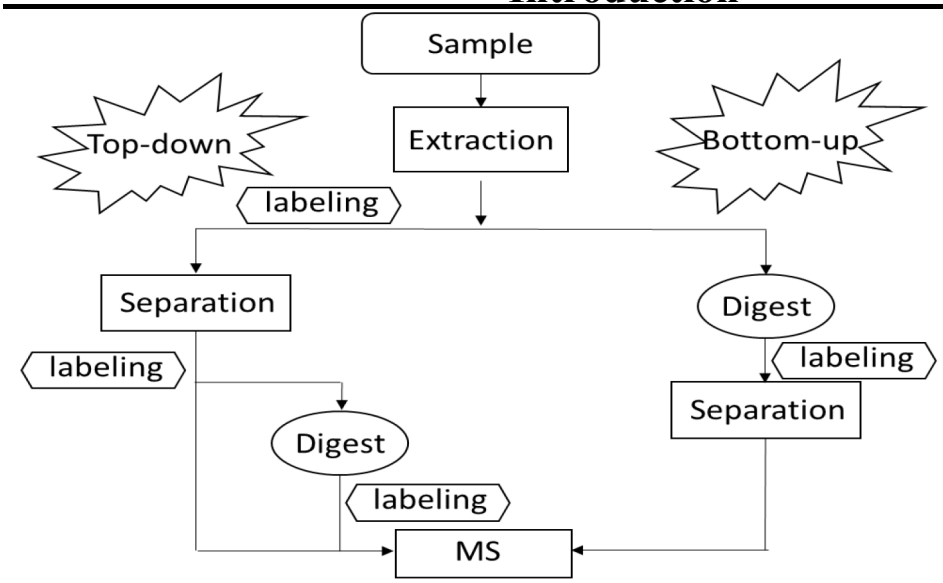

Figure 11. Approaches for mass-spectrometry based proteomics. Modified from Tholey et al[60]

However, the sheer identification cannot address numerous questions regarding the biological relevance, such as the abundance of protein in samples, or how the certain disease or the drug affects the distribution of proteins. To obtain the broader scope of information about the functionality of proteome and to monitor the variety its changes, the quantitative characterization is required.[61][63]

The conventional quantitative approaches in proteomics were based on the on the integration of the signal obtained from the fluorescent tags, dyes, radioactive labels readout or with protein microarrays. The main limitation for these methods was the need to separate proteins with the high resolution; moreover, the information about the assignment of proteins was missing. The quantification based on mass spectrometry technology could overcome many of these constraints. Nevertheless, in spite of the breakthrough in terms of MS technologies, the task of the complete identification and quantification of all the proteins in a biological system is still one of the biggest challenges of the proteomics. The Figure 12 illustrates the drastic difference between the amounts of proteins in the sample, which can be identified and quantified. As is seen from the Figure 12, usually not all the proteins that are present in the sample are annotated; moreover, in most cases only a small fraction of identified proteins can be quantified. [61][64]

This gap between the quantification and identification outcome can be explained with the following reasons: some peptides cannot be analyzed with MS because if the size of molecules is very big or small, its mass to charge ratio is out of the mass area that is usually scanned with MS. In addition to this, the proteins and peptides interactions with the chromatographic column during the separation step can result in significant losses of sample. [61] [64]

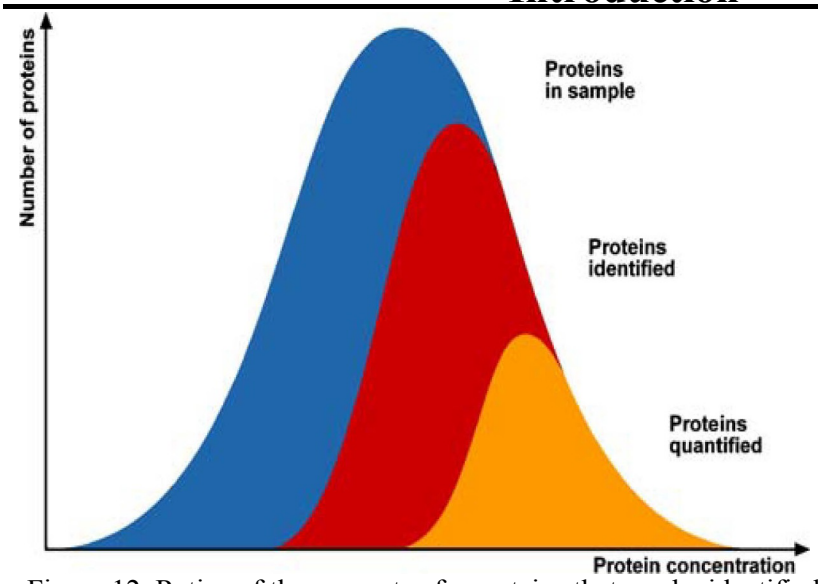

Figure 12. Ratios of the amounts of a proteins that can be identified and quantified by with mass- spectrometry-based approach. Adopted from Bantscheff et al. [64]

Generally the quantification with MS based approach can be performed in two ways: absolute and relative. With the absolute quantification the amount of the protein of interest in a sample is determined in a respect to a quantified amount of a label attached to the target protein. Information obtained with the absolute quantification can be crucial for biomarker screening or for the monitoring of drug influence. Nowadays, numerous labeling approaches for the absolute quantification are developed, some of them will be discussed further. The relative quantification gives information based on the ratios of the amount of protein of interest to another characteristic value, in this way the dynamic changes of protein abundance can be monitored. [61][63]

The conventional proteomic workflows for MS-based quantification are shown in Figure 13. All of them are designed to establish the comparison of the individual peptides between the experiments. Therefore, the main requirements for them can be featured: the sample treatment should be minimized, during labeling all target proteins should be addressed, the labeling reagent should not create interferences during detection, etc. Further the prevalent strategies for quantitative proteomics will be reviewed. [64]

1.7. Quantitative proteomics approaches

1.7.1. Metabolic labeling

Many tagging approaches for mass spectrometry based detection are based on labeling *in vitro* with various agents. Unlike the majority of labeling techniques that will be discussed further in this work, the metabolic tagging is an *in vivo* technique that characterizes relative protein expression. With this approach the stable isotope tag is incorporated during the process of the biosynthesis, thus all the proteins are replaced with isotopically labelled ones. This is achieved with the addition of the isotope label to the cell media. This strategy is applicable only to the samples which demonstrate the metabolic activity. Two most broadly utilized metabolic labeling approaches can be featured: tagging with ^{15}N isotope and stable isotope labeling by amino acids in a cell culture (SILAC). [61] [65] [66]

Among the first tags utilized for metabolic labeling was the isotope of nitrogen – ^{15}N, it was successfully employed to address the changes of protein expression in a quantitative way. The labeling technique is based on growing the cell culture of interest (otherwise bacteria or yeast) in a media that is enriched with ^{15}N isotope. With this approach also the labeling of the whole organism was reported to be possible; however, the remarkable high cost and ethical issues were the restraining factors for the broader implementation of metabolic labeling of the whole organism. The significant drawback of this labeling approach is that it allows the comparison of only two samples per experiment. Generally for ^{15}N tag the highest labeling efficacy was demonstrated when plants or bacteria were targeted.[67][68][63]

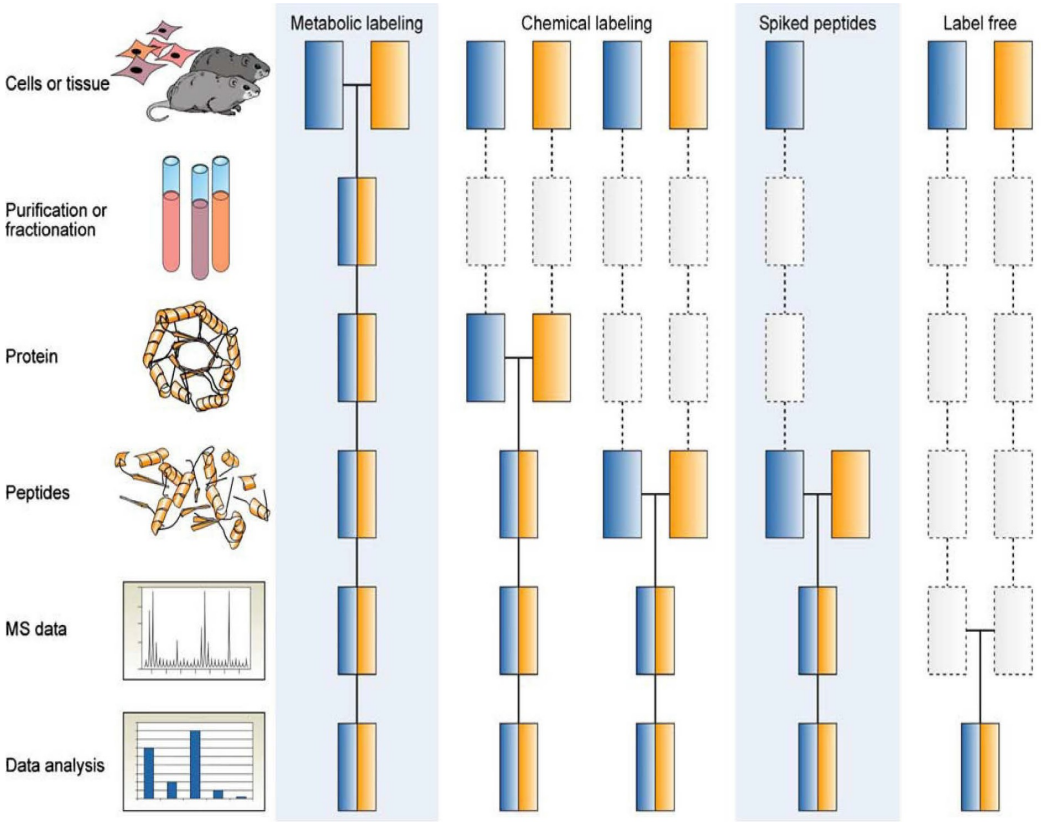

Figure 13. Labeling workflows in MS-based proteomics. Boxes in blue and yellow stand for two different experimental conditions. Horizontal lines point when samples are combined together. Dashed lines indicate when experimental variation and quantification errors can take place. Adapted from Bantscheff et al [64].

Another method for metabolic labeling is stable isotope labeling by amino acids in a cell culture (SILAC). With this approach the label is introduced via isotopically modified amino acids added to the cell media. Among the variety of amino acids, lysine and arginine are the most frequently used for the SILAC technology. Unlike the ^{15}N isotope tagging, this method is more suitable for mammalian cells, since they are not synthesizing certain amino acids. In addition to it, SILAC labeling approach enables the comparison of several samples per experiment. [65][63]

The numerous advantages of metabolic labeling such as simple labeling procedure, obtaining the complete set of information on the protein level including the

post-translational modifications and protein turnover could make this approach an ideal coding system; however, there are several limitations. The metabolic labeling cannot be applied to all the cell types as was mentioned already, another restriction is the different transportation efficacy of the label inside the cell what can lead to variations of tagging capability. In addition to this, the interpretation of results can be challenging due to the fact that the number of isotope tags introduced to the protein will vary based on the composition of amino acids and molecular weight.[61][65][63][69][66]

1.7.2. Enzymatic labeling

The stable isotopes can be introduced into peptides via the process of enzymatic digestion. With the enzymatic labeling approach ^{18}O isotope is incorporated to the sample during the proteolytic digestion in $H_2{}^{18}O$ solvent. The control sample is hydrolyzed in H_2O solvent. As the result, the peptide are coded with different isotopes of oxygen. The reaction scheme is illustrated with Figure 14. Since this labeling approach does not have multiple steps, the impact of technical variations is decreased. [65][69][70]

The ^{18}O isotope labeling approach was utilized for the studies of protein expression, post- translational modifications, protein-protein interactions and for the identification of disulfide linkages. In addition to it, with this technique various protein samples can be addressed (for instance tissues). The main limitations of enzymatic labeling is the high cost of water labelled with ^{18}O; moreover, the small mass shift can result in overlapping of analyzed isotopic patterns. In addition to this, the complete labeling of the target groups is hard to achieve due to the lack of lysine or arginine at C-terminal; another problem is the limited time of stability of the pooled samples. [63] [69][70] [71]

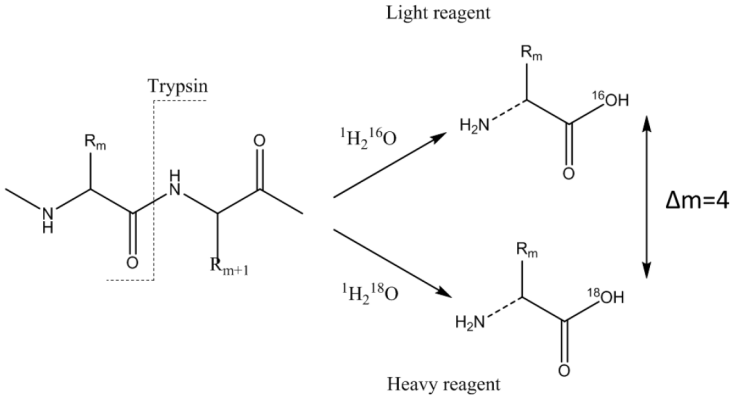

Figure 14. Reaction scheme of ^{18}O water labeling approach. Modified from Prange et al. [65]

1.7.3. Chemical labeling

The chemical labeling approach is based on the attachment of the label to one of the functional groups of amino acids via the chemical reaction, in this way both proteins and peptides can be addressed. The Figure 15 illustrates the functional groups of amino acids that can covalently attach to the label, among most outstanding reactive functionalities are lysine and cysteine. These groups can be targeted with N-acyloxysuccinimide esters of acids, aldehydes, maleimide based

reagents and iodoacetamide. Generally, with the tagging strategy based on the chemical modifications, the accuracy of the quantitative outcome can suffer from the influence of side reactions and the non-sufficient labeling efficacy. The prevalent approaches for chemical labeling will be discussed further. [61] [64][65]

1.7.3.1. Isotope coded affinity tag

Isotope coded affinity tag (ICAT) was one of the pioneering labeling agents, utilized for the MS-based quantification. The core of this approach is the detection of the mass shift of the reference and isotopically modified probes. The sample is tagged with the two probes, the reference one ("light") and the one modified with isotopes ("heavy"). The workflow includes digestion, purification and analysis with LC-MS/MS followed by identification and quantification of protein of interest. The first generation of ICAT probes was designed as a molecule that carries iodoacetamide function, which addresses thiol groups; several atoms of deuterium, which are providing the mass shift during the detection, and biotin group, which enables isolation (Figure 16). One of disadvantages of this tag was the differential elution of "light" and "heavy" labeled proteins due to isotope effect; therefore, the reagent was further
optimized with the utilization of ^{13}C isotopes instead of deuterium, and the cleavable biotin
functionality. The functionalization of the probe with ^{13}C isotope allowed co-elution of the peptides labelled both with the heavy and light forms. One of the main limitations of ICAT approach was that the proteins, which do not contain cysteine residues could not be addressed; thus the proteome coverage for this method was not very high. A notable advantage of this pioneer tag was the reduction of proteome complexity. This method was utilized for the characterization of protein complexes, post-translational protein modifications, applications of this approach for the analysis of extracellular proteome samples were also reported. [61] [63] [71] [72]

1.7.3.2. Isotope coded protein label

Isotope coded protein label (IPCL) approach is based on tagging of free amino groups in proteins, to address these groups N-Hydroxysuccinimide (NHS) functionality is utilized. The structure of IPCL probe that consists of Nicotinyl-N-Hydroxysuccinimide in which ^{2}H isotopes are incorporated is shown in Figure 17. The ^{13}C isotopes are also frequently utilized for this kind of probes. The labeling workflow is based on differential tagging of proteins with heavy and light ICPL moieties, afterwards they are combined, fractionized and analyzed with LC-MS/MS. Based on the results of MS detection both the identification and quantification are possible. One of the main advantages of IPCL technology is that it can be applied to all
the kinds of protein samples and can be combined with all the separation methods utilized for the proteomics. With this approach the detection of the sample with low concentrations is feasible, the low abundant proteins can be addressed; moreover, it enables the high throughput of analysis. This method is also applicable for the characterization of post-translational modifications and isoforms of proteins. [65][73]

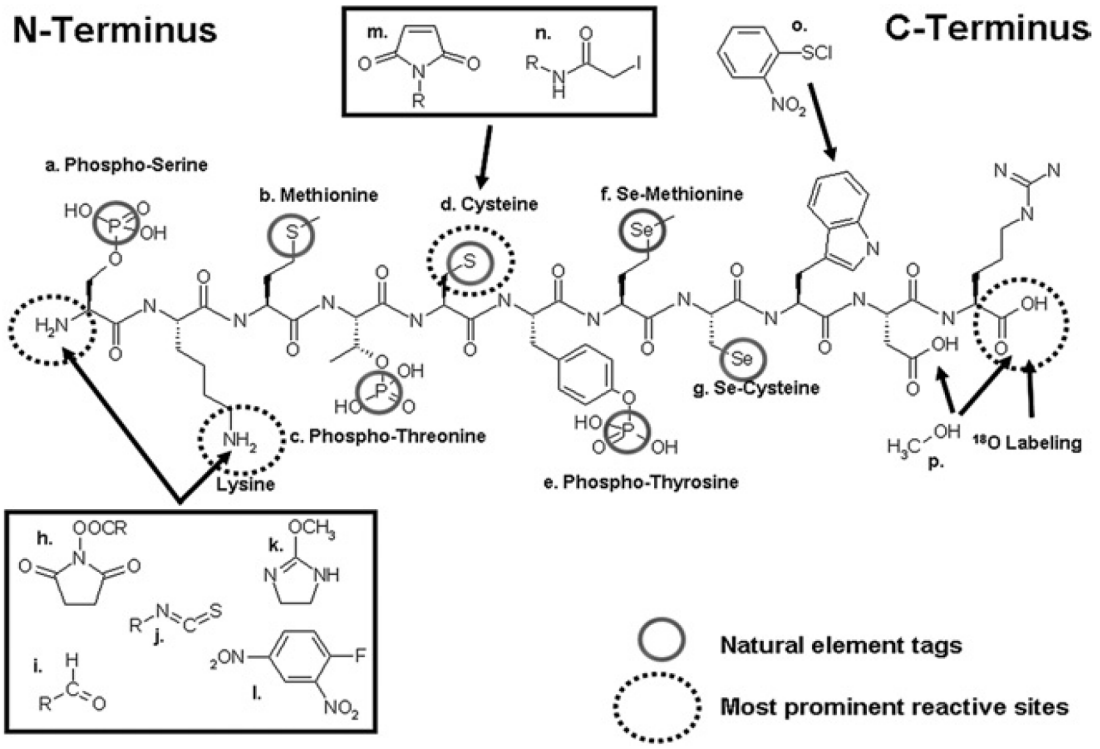

Figure 15. Functional groups of amino acids suitable for chemical labeling and the chemical groups utilized for addressing these groups. (a) phosphor serin; (b) metionin; (c) phosphor threonine; (d) cysteine; (e) phosphor thyrosin; (f) Se methionine; (g) Se cysteine, amine reactive groups; (h) N- acyloxysuccinimide esters of acids; (i) aldehydes; (j) isothiocyanates; (k) imidazole based reagents; (l) 2,4 dinitro-1-fluorbenzene, cysteine reactive groups; (m) maleimide based reagents; (n) iodoacetamide; (o) 2-nitrobenzenessulfenyl chloride; (p) esterification. Adapted from Prange et al. [65]

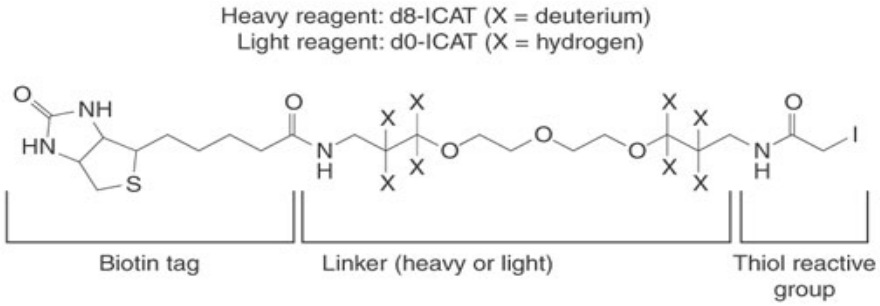

Figure 16. Structure of ICAT probe. Adopted from Shiio et al [72]

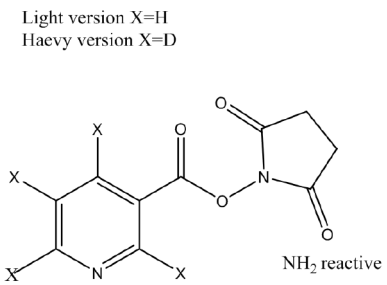

Figure 17. Structure of IPCL probe. Adopted from Schmidt et al [73]

1.7.3.3. Isobaric tag for relative and absolute quantification

Another approach for relative quantification – isobaric tag for relative and absolute quantification (iTRAQ) addresses the primary amino groups with NHS functionality, similar to IPCL technology. The iTRAQ label consists of NHS-ester derivative, a carbonyl and a reporter groups. This labeling approach is based on tagging proteins and peptides after their derivation and enzymatic digestion. The quantification is based on the readouts of a low mass molecular reporter signal intensities which are generated within MS/MS fragmentation. The utilization of iTRAQ method allows the multiple peptide detection per sample; therefore, the confidence of protein identification is enhanced. The main limitations of this method are possible alterations of labeling efficacy and laborious multi-stages sample preparation procedures. [63] [70]

1.7.4. Utilization of lanthanide chelates as chemical labels for quantitative proteomics

The tagging strategies discussed previously, were based on the introduction of stable isotopes such as ^{2}D, ^{13}C, ^{15}N and ^{18}O to obtain a mass shift between light and heavy variants of the label; however, the relative high price and complicated synthesis inspired the development of different tags. Some of these labels utilized rare earth metals bound to the chelating agent. As a tag applied for protein targeting, lanthanides can offer certain advantages. First of all since lanthanides are heavy elements, the provided mass shift is of exact value. Secondly many rare earth metals are monoisotopic, what simplifies mass tag preparation. Moreover, because lanthanides have similar chemical properties multiplex labeling is possible. [65][74][75]

Initially the approach of peptide, protein or antibody labeling with chelated radioactive nuclides was utilized in the field of radiopharmacology. Out of numerous chelates those that were based on DOTA and DTPA found a broad application as a bi-functional chelating agents for targeting functional groups of amino acids due to stability of their complex compounds with lanthanides. [60][65]

1.7.4.1. Element coded affinity tag

Element coded affinity tag (ECAT) was reported for the first time by Whetstone et al. [75] The novelty of this approach was based on the utilization of DOTA (1,4,7,10- tetraazacyclododecane-1,4,7,10-tetraacetic acid) rare earth chelates for the labeling of proteins and peptides. The structure of ECAT functionalized with bromoacetamido reactive group to target cysteine groups is shown in Figure 18. The ECAT label addressing primary amines was reported as well. [75][76]

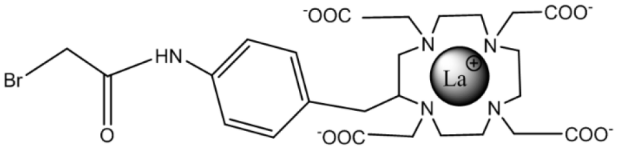

Figure 18. Structure of ECAT probe. Modified from Whetstone et al [75]

Similarly to ICAT approach, the relative quantification was based on calculation of the ratio between heavy and light label. However, within ECAT approach the shift from the heavy label was induced by the introduction of a lanthanide containing label. The utilization of chelated lanthanides as affinity tags was considered to

avoid unspecific binding during the affinity purification step and to increase selectivity, since chelated lanthanides do not have analogues in nature; moreover, many of them are monoisotopic and the provided mass shift is of the certain value. [75]

1.7.4.2. Metal element chelate tag

Metal element chelate tag (MECT) labeling approach was introduced by Liu et.al. [74] The method is also based on introduction of metal chelates containing labels into the protein sample. However, differently from ECAT approach, MECT was targeting the primary amine groups in peptides. The advantages of lanthanide tags for protein labeling was taken by this approach. The chelating agent utilized for this method was the bicyclic anhydride diethylenetriamine-N,N,N`,N``,N``-pentaacetic acid (DTPA). The structure of MECT is shown in Figure 19. [65] [74]

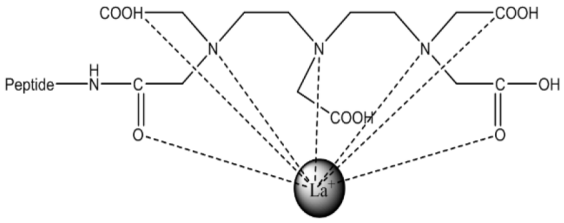

Figure 19. Structure of MECT probe coupled to peptide. Modified from Liu et al [74]

With MECT labeling workflow, samples were at the first stage digested with trypsin, on the second stage – DTPA was attached to primary amino groups, the third stage was the chelation with lanthanides. Afterwards samples were analyzed with LC-MS/MS. The detection with MALDI-MS based on this approach was also reported. [74] [77]

The notable advantages of MECT approach are the low cost of chelating ligand, the quick sample preparation, and the sensitivity of femtomole level. Moreover, this approach can address all primary amino groups and, therefore, can recognize any peptide and provide the better coverage and confidence level for the detection of proteins. [65] [74]

1.7.5. ICP-MS based quantification of proteins

The numerous approaches of protein quantification that were discussed previously in this work are based on molecular mass spectrometry analysis. In spite of the broad development of this area and the recent advances of labeling techniques, the quantification approaches based on inorganic mass spectrometry (ICP-MS) detection and on the combination of organic and inorganic mass spectrometry are nowadays developed by many groups. [65][78] [50]

The main components of proteins: C, H, N and O cannot be addressed by ICP-MS. However, it is known that the majority of proteins naturally contain at least on of elements detectable by inorganic mass spectrometry (P, S, Se, Fe, etc). Besides the utilization of ICP-MS for detection of natural occurring tags, this technique can also address biomolecules tagged with chemical labels. [65][78]

In comparison with the molecular mass spectrometry which is based on “soft”

ionization methods such as electrospray ionization (ESI) and matrix assisted laser desorption ionization (MALDI), the ICP-MS can offer certain advantages. First of all the obtained signal is not dependent from the compound structure, thus a simple straightforward calibration that does not need such standards as synthesized proteins or peptides is possible. Secondly the wide linear dynamic range up to 9 orders of magnitude is achievable with this technique. Moreover, ICP-MS provides multi-element detection capabilities; high sensitivity, specificity and robustness. ICP-MS is very frequently utilized coupled to the liquid chromatography, this allows specific detection and quantification of element of interest which is present in a protein sample. [60] [65][50]

In most cases the data obtained via ICP-MS detection is not sufficient for the characterization of proteins, since the information regarding protein identification is missing, thus this detection method needs to be complemented. The combination of molecular and atomic MS analysis can offer definite benefits. Firstly organic-based MS provides a limited dynamic range, while inorganic MS affords the dynamic range up to 12 orders of magnitude. In addition to this the ICP-MS based analysis can offer simple and straightforward calibration in comparison with MS detection based on "soft" ionization. Furthermore, molecular MS can provide the information necessary for the identification of the analyzed protein, while inorganic MS can target the absolute quantification of heteroatom incorporated to the sample of interest. [60][79]

1.7.6. ICP-MS based quantification of naturally containing tags

1.7.6.1. Sulphur

One of the elements that is naturally incorporated into the amino acids and is detectable by ICP-MS is sulphur. This element is a constituent of two amino acids: cysteine and methionine, which are of abundance around 5% of all the amino acids in eukaryotic cells; therefore, sulphur should occur in all proteins that consist of more than 25 residues. Due to this reason, the majority of proteins can be addressed by the detection of the sulfur component. Moreover, the four stable isotopes (^{32}S, ^{33}S, ^{34}S, ^{36}S) enable the utilization of isotope dilution analysis and the metabolic labeling.[65] [78][50]

Despite the high abundance of sulphur in proteins the total number of reported examples of its inorganic MS based detection is rather limited. The reason for this is the number of difficulties that one has to face while performing ICP-MS readout of sulphur. First of all, sulfur has a high first ionization potential (10,357 eV) and a relatively low ionization efficiency. Secondly, numerous spectral interferences with molecules presented in plasma like $^{16}O_2^+$, $^{15}N^{16}O^1H^+$ or $^{16}O^{18}O$ can affect the detection. Thus, in order to exclude the interferences, the high resolution of mass analyzer or the utilization of collision or reaction cell are required.[65][50]

1.7.6.2. Phosphorus

Phosphorus is present in protein samples as a part of the ribose-deoxyribose phosphorus backbone in RNA or DNA chain, this element is also involved in phosphorylation – an important and quite common post-translational modification

of proteins that is crucial for intracellular regulation and homeostasis. Therefore, the quantitative characterization of the degree of phosphorylation can contribute in a big extend to understanding of signal transduction pathways. [65][69][78][50][80]

It is known that more than 30% of mammalian cells are phosphorylated at any given time. Nevertheless, the suppression of signal generated from phosphorylated peptides in the presence of non-phosphorylated ones was reported. Therefore, a high sensitivity is needed to address this element in protein samples. [50][80]

There are several complications in terms of detection of phosphorus via ICP-MS: similar to sulphur, this element has a high ionization potential (10,484 eV) and a low ionization efficiency in argon plasma. Since for the phosphorus the undesirable spectral interferences are possible, this element can be addressed only with the high resolution instrument or with the utilization of collision or reaction cells. [50][65]

1.7.6.3. Metals (copper, iron, zinc)

Several metals are naturally incorporated in a protein structure, these biomolecules are named metalloproteins and divided into two groups: metal-transport proteins and metalloenzymes. Metals are usually coordinated to histidine, cysteine or carboxyl groups. Numerous scientific works were performed in order to characterize metalloproteins, most of them were utilizing isotope dilution analysis. [65][78][81] [82]

ICP-MS has certain advantages for detection of metal containing proteins: sensitivity, wide dynamic range, multi-elemental capability, etc. Moreover, in combination with chromatographic separation techniques such as size exclusion chromatography, anion- exchange chromatography and reversed-phase high performance liquid chromatography (RP- HPLC), the elemental distribution or the dynamic changes of metalloprotein can be monitored. Nevertheless, commonly to address metalloproteins the combination of organic and inorganic MS-based detection is employed. [78][50][81]

1.7.7. ICP-MS based quantification of tagged proteins

1.7.7.1. Ferrocene

The ferrocene tag was initially developed for electrochemical detection combined with liquid chromatography; however, this label was also probed for MS based detection. The notable advantage of ferrocene is the low polarity in comparison with DOTA-based tags, what can improve the RP-HPLC separation of tagged proteins or peptides. [60] [83]

The generalized structure of ferrocene tag is shown in Figure 20. The functional group has reactivity towards either amino or thiol groups. For instance, Bomke et al reported the utilization of succinimidylferrocenyl propionate and Ferrocenecarboxylic acid(2- maleimidoyl)ethylamide to address primary amino groups and thiol groups correspondingly. [60][83]

The limited utilization of this technique can be explained with the following restrictions for ICP-MS readout of iron: isobaric plasma interferences; background signal due to the presence of iron in biological samples.[60][83]

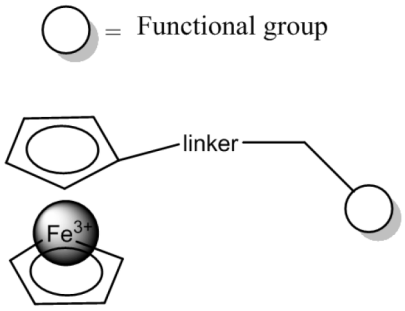

Figure 20. The structure of ferrocene tag. Modified from Tholey et al [60]

1.7.7.2. Metal-coded affinity tag

As was mentioned already, the chelated lanthanides found a broad application in radiopharmacology as contrast agents for magnetic resonance imaging. Lately bi-functional chelating tags that consist of cyclic chelate as DOTA or noncyclic open form as diethylentriaminepenraacetic acid (DPTA) assosiated with rare-earth metals were probed as tags for protein quantification. Among other complexation agents, DOTA gained the highest popularity due to its exceptional high thermodynamic stability. The approaches based on utilization of lanthanide chelates for chemical labeling described above, were based on molecular MS detection; in contrast to them, the strategy of metal-coded affinity tag (MeCAT) based detection included the absolute quantification via ICP-MS and identification via LC-MS/MS. [65][79] [84][85][86]

The application of lanthanides for labeling followed by ICP-MS detection can offer certain advantages. First of all the low ionization energies of rare-earth metals provide high sensitivity. Secondly since lanthanides are not naturally containing in biomolecules the low background signal is commonly obtained. In addition to this, there is a wide choice of isotopic distribution patterns of rare-earth element from mono- to multi-isotopic, what enables different strategies of analysis. [60][79]

Ahrends et al for the first time reported the utilization of MeCAT for quantification of proteins and peptides. [84] The structure of MeCAT label is illustrated with Figure 21. The tag consists of DOTA coordinated to lanthanide, a reactive group that allows covalent attachment to proteins and peptides, and an affinity functionality allowing isolation. [79][84]

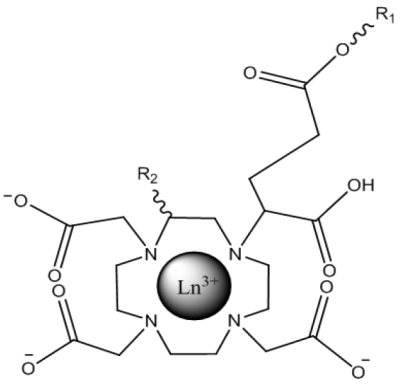

Figure 21. The structure of MeCAT. R_1, R_2 stand for the attachment positions of linkers with reactive groups. Modified from Schwarz et al [79]

The robustness of MeCAT labeling approach and its compatibility with biological systems was demonstrated; moreover, MeCAT was successfully utilized for absolute quantification of proteins [84] [87] [88], quantification of DNA [89], and quantification of proteins via isotope dilution approach [90]. In addition to it, the labeling of antibodies with MeCAT was reported. [91][92]

Schwarz et al established a tagging strategy based on the utilization of iodoacetamide MeCAT to address cysteine residues. With this approach a formation of diastereomers was eliminated, what was one of the main disadvantages of the first generation of MeCAT. Moreover, the consumption of a lanthanide tag for labeling was decreased.[87]

El-Khatib et al reported the application of MeCAT tag for quantification of sulfenic acid in proteins and peptides together with thiol groups; to achieve it, a DOTA based probe functionalized with dimedone was developed.[93]

Lately He et al introduced a MeCAT labeling method with the utilization of click chemistry reaction. [94][95] This approach was developed to decrease possible spatial interferences caused by a relatively big size of DOTA-based tag and to increase the number of protein sites that can be potentially addressed. To achieve this, two step labeling strategy base on copper catalyzed azide-alkyne cycloaddition reaction was proposed. At the first stage a small tag functionalized with alkyne (Figure 22 A) was attached to the thiol group of cysteine. At the second stage MeCAT (Figure 22 B) was conjugated to alkyne containing label via click chemistry reaction. [94]

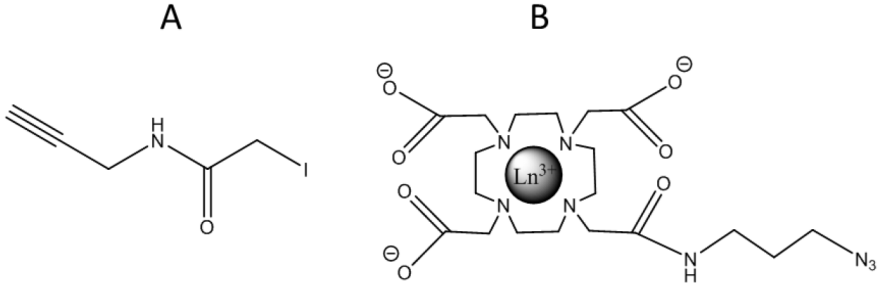

Figure 22. Structure of reagent for labeling via click chemistry approach. (A) Structure of 2-iodo-N- (prop-2-yn-yl)acetamide alkyne. (B) Structure of MeCAT functionalized with azide. Modified from He et al [94]

This labeling approach was successfully tested on standard protein (Bovine serum albumin). Furthermore, the MeCAT tagging strategy based on click chemistry was utilized to characterize the complex biological sample: a response of the proteome of Escherichia coli (E-coli) to the heat shock. With these works, high labeling efficiency of click-MeCAT was confirmed. Moreover, the high potential of this tagging strategy was clearly demonstrated.[94][95]

1.7.7.3. Nanoparticles

The outstanding progress in the development of nanostructures, resulting in an introduction of numerous nanosystems with unique properties, emerged the development of novel approaches in bio analytics. The numerous investigations of nanoparticle influence on living organisms showed that the interaction of

nanosystem with biological objects are based on the biological recognition of the features of nanoparticles. [2][96]

Since the studies of nanosystems is relatively young field of science, there are numerous questions to address in terms of pharmacological applications, nanotoxicology and development analytical methods for nanoparticles detection. [2][97]

The utilization of ICP-MS for the detection of conjugates between nanoparticles and biomolecules via immunoreaction was introduced for the first time by Zhang et al, in this study high potential of tagging with nanoparticles for the analysis of proteins was highlighted [98]. Another approach to target nanoparticles with ICP-MS is to perform bioimaging via laser ablation inductively coupled mass spectrometry (LA-ICP-MS) analysis. Mueller et al reported successful application of combination of LA-ICP-MS detection with Western Blot to target proteins via immunoassay functionalized with metal clusters. [99] Drescher et al utilized LA-ICP-MS to perform high special resolution imaging of the distribution of nanoparticles in a single cell. [97]

The utilization of nanoparticles as tags for ICP-MS detection has definite limitations. First of all, to perform accurate quantification the knowledge about stoichiometry of metal clusters is needed. Secondly, in case of the big size of nanoparticle, the undesired steric hindrance might occur. [60]

1.7.7.4. Polymer-based metal tags

A labeling approach based on the utilization of polymer-based metal tags was introduced by Lou et al. [100] It provides high sensitivity since every tag contains multiple lanthanide atoms, what allows to address low abundant proteins and biomarkers. [100]

The structure of polymer-based label is shown in Figure 23. The tag is attached via maleimide group to the previously reduced antibodies disulfide bridges. So far this labeling technique was utilized exclusively in combination with antibodies. Since the size of label is big, undesired steric hindrances are possible; moreover, the high price of antibodies allowing specific recognition of target proteins is another restricting factor of this approach.[60][100]

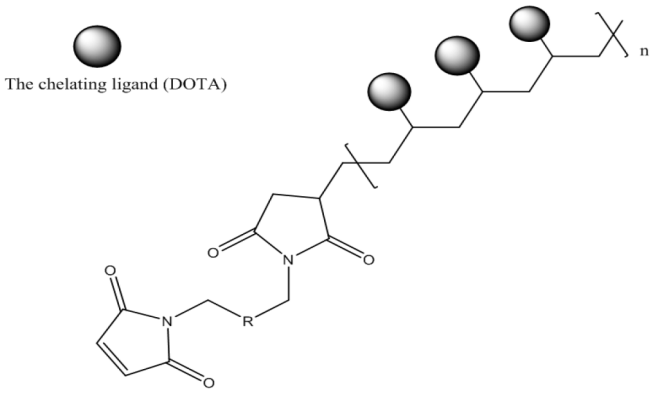

Figure 23. The structure of polymer-based lanthanide containing tag. Modified from Lou et al [100]

1.7.8. Spiked peptides

1.7.8.1. Approach for absolute quantification of proteins (AQUA)

Opposed to the methods mentioned previously, the approach for absolute quantification (AQUA) of proteins is based on the utilization of synthetic peptides, which carry stable isotopes. The artificial peptides can resemble not only natural peptides in their native state but also their modifications such as phosphorylation, methylation etc.[64]

The workflow of AQUA labeling consists of two parts, on the first stage the elaboration, synthesis and validation via the LC-MS/MS readout and analysis of fragmentation patterns of the internal standard are performed. On the second stage the isotope labelled synthesized peptide is introduced to the sample via its addition to the cell lysate, followed by fractionation and SDS-PAGE separation and the tryptic digestion of protein. The final step is Liquid chromatography Selected reaction monitoring Mass Spectrometry (LC-SRM/MS) analysis.

With SRM method, the specific fragment ions which indicate the abundances of product or precursor can be addressed. This allows detection of the amount of proteins or peptides in complex samples. The quantification is based on the ratio of abundances of spiked peptide with a known concentration, to the endogenous one, which concentration is unknown.[101][102]

The main advantage of AQUA method is that it allows not only absolute quantification of the native forms of proteins and peptides but also facilitates the quantification of post- translational modifications. In addition to this, the introduction of the spike before the digestion reduces the impact of sample preparation variabilities. There are two critical limitation factors for this technique, the first one is the demanding synthesis of the standard peptide; the second one is the possible difficulties with the estimation of the amount of spike and in addition to this the costs of such standard is high. [65][101]

1.7.9. ***Label free quantification***

In order to avoid expensive and laborious protein labeling, MS-based quantitative approaches that do not include tagging step were developed. The quantification with the label free approach can be performed with two different strategies (Figure 24). Spectral counting is the first approach, it is based on the idea that the increase in amount of peptide in a sample mixture leads to a rise of the count of tandem mass spectra for this peptide. Thus, with this strategy the number of MS/MS spectra for particular peptide is compared. Spectral counting can provide reproducible and significant quantitative results for the replicate measurements. The second method is named chromatographic. It is based on the integration of chromatographic peak areas. This approach is not that straightforward as the previous one. However, the areas of chromatographic peaks can be correlated to the abundances of many proteins in a linear way, what provides the conditions for the quantification. [63][103]

The utilization of label free quantification technology obviously reduces the

expenses and efforts, which are required for the utilization of any labeling approach. Another benefit of this method is that due to the absence of additional labeling steps, the risk of the sample losses is minimized and the reproducibility is improved. The main disadvantage of label free quantification is the relatively low accuracy of the quantification outcome, which can be upgraded with the reproducibility control and the increase of compared number of experiments. In addition to this, the high resolution separation method as the multidimensional chromatography is of crucial importance to avoid protein interferences and to allow the detection of proteins with the low abundance. The label free approach was successfully utilized for numerous studies of biomarkers and drug targets. [64] [103]

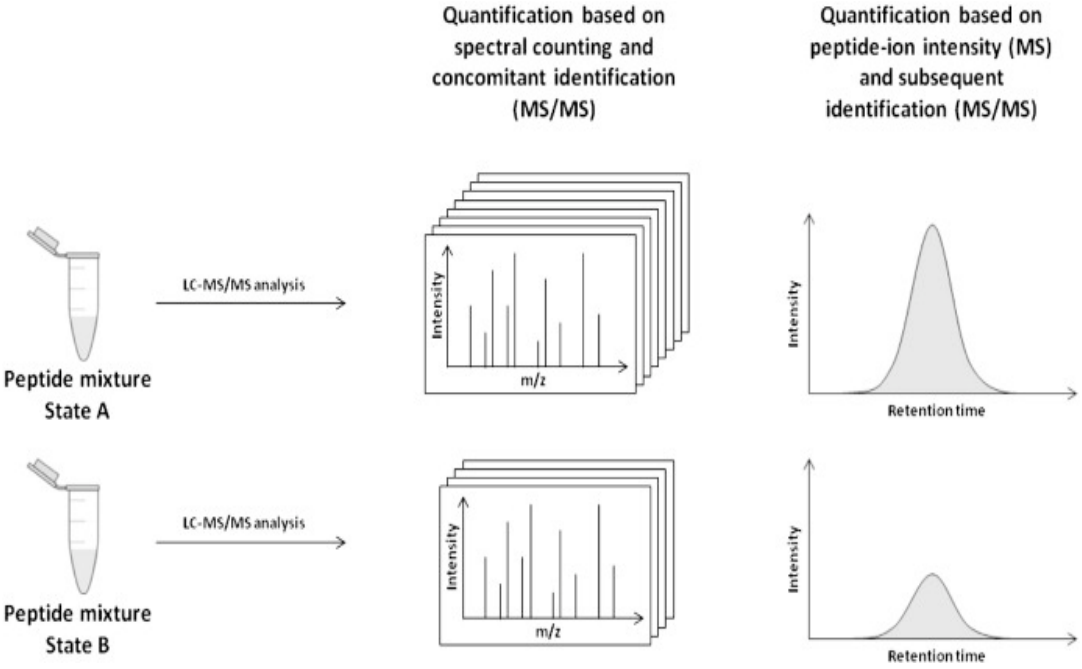

Figure 24. The comparison of two approaches for label free quantification. Adopted from Megger et al [103]

1.8. Functional proteomics. Affinity chromatography and protein profiling based on the interactions with the small molecular probes.

The information about protein abundance and distribution is crucial for proteomic research; nevertheless, the knowledge of biological activity of proteins is even more important. The global proteomics approach discussed previously can give bring an information about protein expression and detect changes in it. However, this approach fails to monitor the changes in activity of proteins caused by different factors and specific interactions with molecules of interest. [9][19][18]

To target the functional state of protein a several approaches based on the interaction of proteins with small molecular probes were developed. Generally several strategies has the potential to target specific functional interactions of proteins: affinity-based chromatography or pull down approach (Figure 25 A), activity-based protein profiling (Figure 25 B) and capture compounds (Figure 25 C).[19][104]

1.8.1. Affinity based chromatography

Affinity based chromatography is one of the most frequently used approaches of chemical proteomics. This method is based on the immobilization of the molecular probes on the solid support, these probe interact with the target protein in a reversible non-covalent way. Pull down approach can be used for the enrichment purpose. Moreover, with affinity based approach followed by mass spectrometry detection the complexity of proteome is reduced, thus the targeting of low-abundant proteins is facilitated. [19] [104][105]

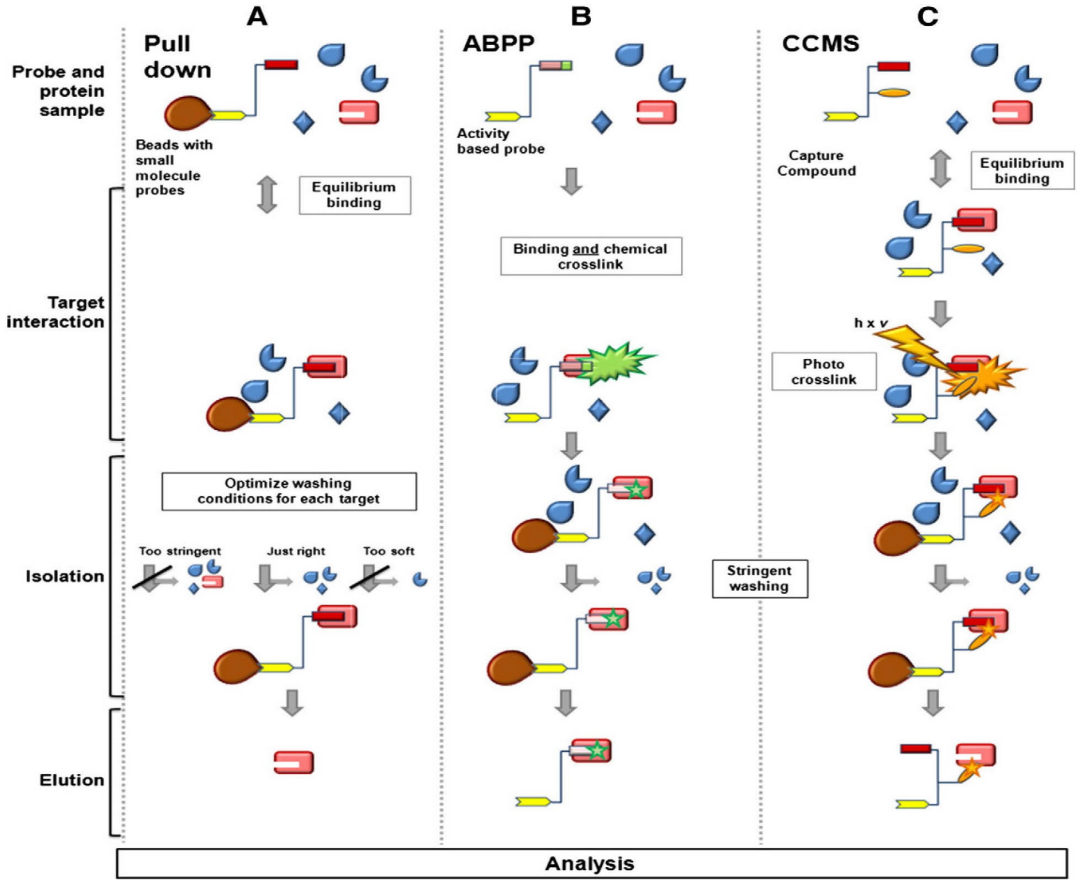

Figure 25. Schematic workflows for affinity pulldown (panel A), activity-based protein profiling (ABPP, panel B), and Capture Compound Mass Spectrometry (CCMS, panel C) experiments. In affinity pulldown experiments (A), probes reversibly interact with target proteins defined by a dynamic equilibrium. Non-binding proteins are washed away, and retained proteins are analyzed after elution using denaturing buffer or an excess of free affinity ligand. The choice of buffer conditions requires a tradeoff: low stringency will lead to high unspecific background binding, while high stringency will lead to loss of weakly, but still specifically interacting proteins. In ABPP experiments (B), the selectivity function of the probe binds to and chemically reacts with the active site of target enzymes. Harsh washing conditions can be applied to remove proteins unspecifically bound to the solid phase. As a limitation, ABPP can only be used with small molecules that chemically react with their targets. In CCMS experiments (C) the Capture Compound selectivity function reversibly interacts with target proteins defined by a dynamic equilibrium, and this equilibrium is fixed through a photo-induced cross-linking of the reactivity function. Harsh washing conditions can be applied to remove unspecific background. Some unspecifically cross-linked proteins are retained as well. Contributed from Lenz et al [104]

The affinity based (pull-down) probe consists of a bioactive molecule (selectivity function) attached to a reporter tag (sorting function) or directly to the solid surface via the linker. The schematic structure of pull down probe is shown in Figure 26. Ordinary drugs or signaling molecules are commonly utilized as selectivity function; however, practically any small molecule can perform as selectivity function. Since not all the bioactive molecules contain functional groups required for the attachment to the solid support, such as amino, hydroxyl or carboxyl groups, an attached linker that carries the appropriate functionality is utilized. However, the impact of the linker on the affinity of molecular probe should be taken into consideration. [19][14][104]

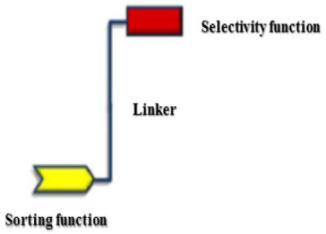

Figure 26. Schematic structure of affinity pulldown probe. Modified from Lenz et al [104]

In conventional affinity chromatography experimental workflow the bioactive molecule is immobilized on a solid support (aragose, sepharose, or magnetic beads), the attached proteins are removed from resins, digested and analyzed with mass spectrometry (Figure 25 A). [21][19][14][106]

Since the selectivity function of a pull down probe attaches to a target in a non-covalent way, the competition with other proteins containing in the sample is possible. Moreover, in most cases the target protein is the one of low abundance but with the high affinity to the probe (nM range); thus, the proteins of higher abundance and of lower affinity (uM range) can be potential competitors. Therefore, as was discussed previously to assure the specificity of the molecular probe towards target protein, additional experiments with competition control are needed. In addition to it, high abundant proteins can attach in non-specific way or with the low affinity to probe creating in this way a background signal. The non-specific binders can be removed via the washing step. However, due to non-covalent attachment of target protein to the probe the washing conditions should be carefully optimized in order to remove the background proteins and to keep the specifically attached proteins.[19][106]

Pull down probes were successfully utilized to address cyclic nucleotide-binding proteins, protein kinases, post-translational modifications (phosphorylation, glycosylation, ubiquitination) and isatin-binding proteins. [105]

The affinity based chromatography approach is a well-established tool for the investigations of drugs especially in terms of detection their potential off-targets. However, the restrictions of this approach such as [19][106]

1.8.2. Activity-based protein profiling

The main focus of activity-based probe profiling (ABPP) is the area of enzymatic activity of protein families. The approach of ABPP is based on utilization of molecules with the high selective affinity to target enzymes in order to generate a subproteome which is analyzed afterwards, thus the complexity of sample can be reduced in a significant way. The high selectivity of probes combined with affinity based enrichment strategies facilitates the detection of such challenging targets to address as low abundant proteins and membrane proteins. [17] [24]

The activity based probe consists of following parts: a recognition unit and a reactive group combined in a one moiety, a linker and a reporter tag that enables isolation or detection (Figure 27). The task of reporter group is to enable either detection high sensitivity or affinity enrichment. Fluorescent tags, radioisotope labels and biotin are most commonly utilized for this purpose. The linker connects reporter tag with recognition unit and reactive group. Moreover, the presence of linker provides the space between the two moieties, which is necessary to avoid steric interferences. The constituents of recognition unit and reactive group can be electrophiles, latent electrophiles and photocrosslinkers. [8][21] [107]

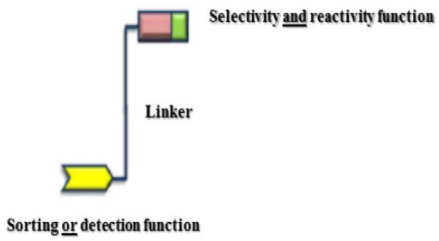

Figure 27. Schematic structure of activity-based probe. Modified from Lenz et al [104]

There are two strategies of utilization of ABPP: it can be either non-directed approach when the compound is screened in a complex samples for protein reactivity, or directed approach, which is utilized to target functional state of specific family of enzymes. The schematic workflow for ABPP is shown in Figure 25 B. The reactive moiety attaches to the reactive sites of enzymes in a covalent way, this reaction is induced by the catalytic properties of enzyme; therefore, binding and covalent cross-link are taking place at the same time. After that the sample can undergo washing and isolation steps. Finally the fluorescent or MS-based readout is performed.[8][104][107]

With ABPP approach numerous families of enzymes were profiled, such as serine and cysteine proteases, serine hydrolases, tyrosine phosphatases, lipolytic enzymes (lipases and esterases), kinases, deubiquitinating enzymes etc. [24][104][107]

One of the biggest challenges in terms of designing the activity-based probes is the duality of the moiety that combines recognition unit and reactive group. It should demonstrate affinity only to specific group of protein, and at the same time stay unreactive towards other components of proteome. [18]

The main disadvantage of ABPP is the applicability of this method to a limited

group of bioactive molecules (inhibitors of enzymes). However, lately due to the introduction of non- directed activity based probes functionalized with alkyl binding groups, protein ligands and a click chemistry approach, the number of potentially addressed targets expanded in a significant way. Since in the core of ABPP is covalent attachment of the probe to the target protein, this approach cannot be applied in many cases for the investigation of drug interaction with proteome.[24][25][107]

1.8.3. Capture compounds

The capture compound (CC) technology is based on combination of affinity interactions and photo cross-linking approach. Capture compounds (CCs) were introduced as a tool for monitoring protein families in biological sample, interactions of drugs with proteins including discovery of potential off targets and related toxicity.[108]

The design of capture compounds probes benefits both from affinity based interactions and covalent binding of molecular probe to the target. The structure of CC is shown in Figure 28. [104]

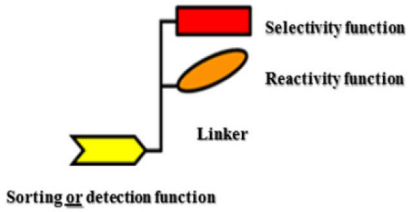

Figure 28. Schematic structure of capture compound. Modified from Lenz et al [104]

The small molecular probe consist of a selectivity function represented with a bioactive molecule which can be a substrate, co-factor, inhibitor of enzyme, a receptor ligand, etc. The attachment of selectivity function to the scaffold plays a crucial role for the interaction of molecular probe with the target biomolecule, thus in many cases several attachment positions of selectivity moiety to the molecular probe should be tested. [104] [109]

The reactivity function is a photoreactive moiety that attaches to the protein only under the UV irradiation conditions. The design of reactivity functionality is challenging since it should be on the one hand stable under reaction conditions, on the other hand it should be activated under such irradiation conditions that are not harmful for the proteins (long wavelength). Among other photoreactive compounds trifluoromethylaryldiazirine suits to all the requirements listed above. This compound under irradiation conditions forms a reactive carbene, which reacts with proteins without the induction of intramolecular rearrangements.

Other reported photoreactive groups were also based on azide and benzophenone molecules. [21][104] [108][109]

Similar to other molecular probes, the role of linker is to join the moieties together, providing the distance between functionalities to avoid spatial hindrances. Moreover, in case of CCs linker allows the reactivity function to crosslink to

surface located functional groups of proteins, while at the same time selectivity function binds to the binding pocket. The reporter tag (sorting or detection function) is usually represented with biotin that allows isolation or with a fluorophore that enables the fluorescence readout. [104][109][108]

Conventional workflow for CCMS consist of several steps (Figure 25 C). On the first stage the affinity-based reaction between selectivity function of capture compound and protein is taking place under equilibrium conditions. On the second stage under irradiation the reactivity function covalently attaches to the protein attached to selectivity function, thus the protein is "fixed" to molecular probe in an irreversible way. The third stage includes isolation with streptavidin magnetic beads followed by mass spectrometry based detection or fluorescence readout.[104][108]

Capture compounds mass spectrometry was successfully utilized to address following protein families: kinases [110][111], methyltransferases [109][112][113], GPTases [114], cAMP- binding proteins [115] and G-protein coupled receptors [116]. In these works the proteins of interest were isolated and detected from cell lysates or subcellular fractions. In comparison with affinity pulldown probes a higher sensitivity of analysis was reported: with CCs less than a one milligram of protein can be targeted, while in case of affinity chromatography the minimal amount of protein is in the range from ten milligram. [104]

The striking advantage of capture compound based approach is the controlled transformation of affinity based attachment into the covalent bond of the probe to the target protein. This allows on the one hand to address the interactions of bioactive molecules and proteins in the range of relatively law affinity, which is challenging to target with the affinity pulldown probes. On the other hand the covalent attachment allows rigorous washing conditions; therefore, it facilitates the removal of unspecific proteins.[104][109]

Since nowadays the click chemistry found a broad application in the field of biomolecules labeling, the brief introduction of click chemistry will be introduces further.

1.9. Click chemistry and bioortogonal reactions for the labeling of biomolecules

The research of biomolecules under the native conditions are of the great interest for the fields of biology and chemistry. By performing chemical reactions inside cells or living organisms, a labeling of subcellular targets can be done; therefore, an information about cellular processes. The development of the labeling approaches, which will allow the selective modification of biomolecules of interest without interaction with the numerous other components of the living system is of crucial importance for the studies of biological samples, especially if *in vivo* labeling is concerned. [117][118]

The complexity of a cellular system and numerous processes occurring inside the living cell cause several important restrictions for *in vivo* labeling: the reactions sensitive to the presence of water and to redox conditions should be excluded;

moreover, the additional heating, the utilization high pressure and high concentrations should be avoided. For many years proteins have been a favored target for chemical modifications based on conversion of protein residues, enzymatic conversion, etc. More recent methods for protein modification are based on chemoselective approach. However, nowadays click chemistry based approach became a powerful tool for the investigation of biomolecules. [117][118] [119]

It is known that in nature the reactions resulting in formation of carbon-heteroatom bond are quite ubiquitous, the good illustration for this are biomolecules such as proteins or nucleic acids, which consist of the subunits connected together with the carbon-heteroatom bond. The click chemistry approach was developed inspired from this idea, as the synthesis of the new compounds with the heteroatom bridging. The main criteria for the click chemistry reaction were formulated by Kolb: the reaction should be modular, wide in scope with simple conditions, and the high product yield. In addition to this, the resulting product should be easy to isolate and it should be stable under physiological conditions; in case of the presence of side products they should be effortless to remove.[120][121][122]

Out of this broad criteria, a subclass of the reactions, products of which do not demonstrate the toxicity under in vivo conditions, are named bioorthogonal reactions. A schematic illustration of the generalized bioortogonal reaction conditions in living system is shown in Figure 29. [118]

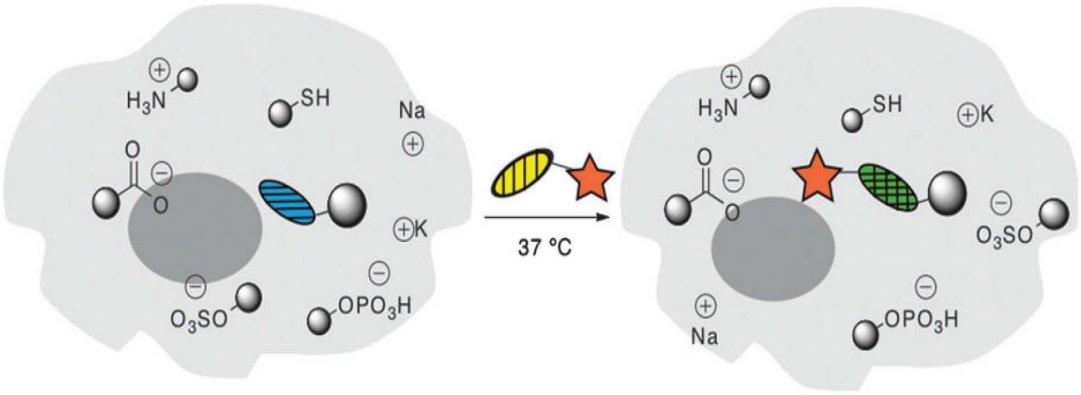

Figure 29. A generalized scheme of bioortogonal reaction. The bioorthogonal functionality, oval with horizontal lines, reacts with its counterpart, oval with vertical lines, to label a biomolecule in live cells or organisms. Contributed from Jewett et al[118]

Among the diversity of bioorthogonal reactions reported in a literature, the selection of the most relevant one to hit the certain target can be a challenging task. Since the estimation of the pros and cons of such reaction is not a straightforward issue. The majority of bioortogonal reactions are having the nitrogen-based functional groups involved. Azide is known to be of the most favored functionalities for the bioorthogonal reactions due to its reactivity towards several bio functional groups and the absence from the biological systems. In addition to this, the small size of this functional group can cause fewer side effects to the modified compound. [117][118][121]

1.9.1. Staudinger ligation

The Staudinger ligation is the modified form of Staudinger reaction, which refers to the phosphine and azide coupling resulting in aza-yilide, the reaction scheme is shown in Figure 30.

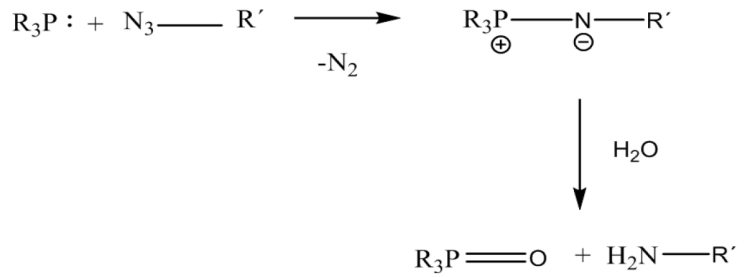

Figure 30. Staudinger reaction scheme. Adopted from Saxon [123]

This reaction product (aza-yilide) is hydrolyzed, producing the primary amine and the phosphine oxide. In spite of many advantages of this reaction in terms of its bio labeling properties, the non-stability of the intermediate product (aza-yilide) in water was a crucial limitation factor. In order to overcome it, Saxon suggested the improvement which allowed the rearrangement of the unstable intermediate product into the stable covalent adduct. This was achieved with the introduction of the different phosphine structure, which was containing electrophilic trap. This modification of the Staudinger reaction was named Staudinger ligation. The reaction scheme of Staudinger ligation is shown in Figure 31. [121][123]

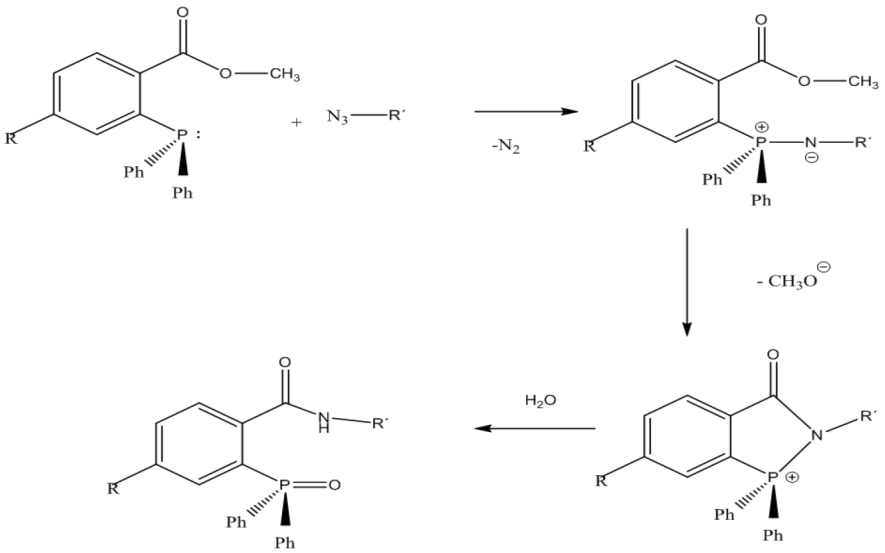

Figure 31. Staudinger ligation reaction scheme. Adopted from Saxon [123]

The Staudinger ligation was successfully applied for biomolecules labeling in a cellular environments and living organisms. However, the slow kinetic of this reaction remains a significant drawback in comparison with the other click chemistry reaction where the azide group is also involved – 1,3-dipolar [3+2] cycloaddition of azides and alkynes. [117][121]

1.9.2. [3+2] cycloaddition (CuAAC) of azides and alkynes catalyzed with copper (I)

The mechanism of the reaction, based on the azide-alkyne cycloaddition was introduced by Huisgen for the first time. [124] However, this reaction was not applicable to the bio-systems due to the conditions required for the conversion with the high yield: high temperature and high pressure. In spite of this, the potential benefits of these two reactive groups (azide and alkyne) as their small size, which would not affect the properties of the modified compounds and their stability was making them very promising agents for the labeling of biomolecules. [117][121]

Later, several groups reported the successful utilization of copper (I) for the catalysis of this reaction. The application of this catalyst has led to the acceleration of the azide-alkyne cycloaddition with the high rate. This breakthrough made the copper-catalyzed azide-alkyne 1,3-dipolar cycloaddition one of the most popular click chemistry reactions nowadays; it is widely utilized in the fields of organic synthesis, material chemistry, chemical biology etc.. The scheme of the copper-catalyzed azide-alkyne 1,3-dipolar cycloaddition is shown in Figure 32. [117] [121][125] [126] [127]

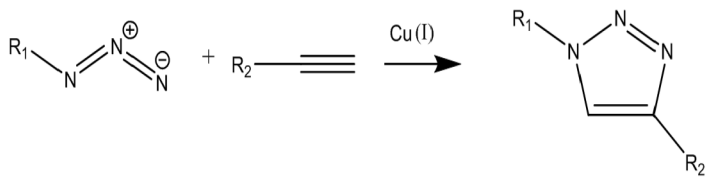

Figure 32. Copper-catalyzed azide-alkyne 1,3-dipolar cycloaddition reaction scheme. Contributed from Best [121]

The mechanism of the catalysis was initially proposed by Rostovtsev et al. [125]. They suggested the formation of copper (I) acetylide followed with the stepwise ligation, the mechanism is shown in Figure 33. In the same work the in situ utilization of the reducing agent – ascorbic acid or sodium ascorbate was introduced. The application of this compound was especially attractive due to the simplification of reaction conditions: no addition of the organic solvent was needed, the reaction was taking place in an aqueous environment. [125]

The most recent mechanism of the catalysis of the reaction with two copper atoms involved was suggested by Worrel [128], the proposed model is shown in Figure 34.

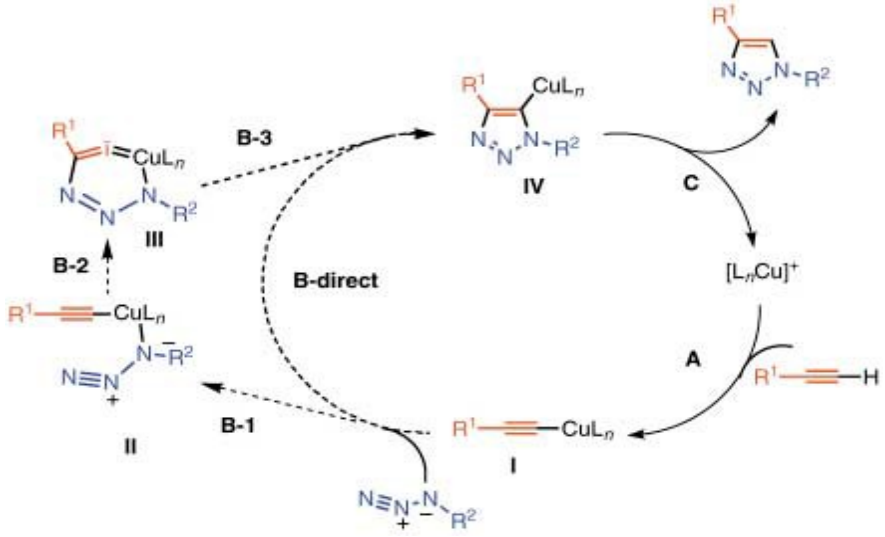

Figure 33. Catalytic model for the CuAAC, contributed from Rostovtsev et al [125]

The presence of copper (I) influences the mechanism and the product outcome of [3+2] cycloaddition reaction in a drastic way. Nevertheless, in many cases the reaction rate was not as high as required for sufficient labeling. It can be explained with the low concentration of chemicals, which is a common case for the targeting of biomolecules. To accelerate the reaction, the utilization of polytriazolylamines as copper (I) stabilizing ligands was introduced by Chan et al [129]. The successful usage of tris-(benzyltriazolylmethyl)amine (TBTA) (structure of which is demonstrated in Figure 35 A) was confirmed with the obtained high reaction yield. This can be explained with the ability of the ligand to bind to the center in a way that no free potential binding sites were left. [121]

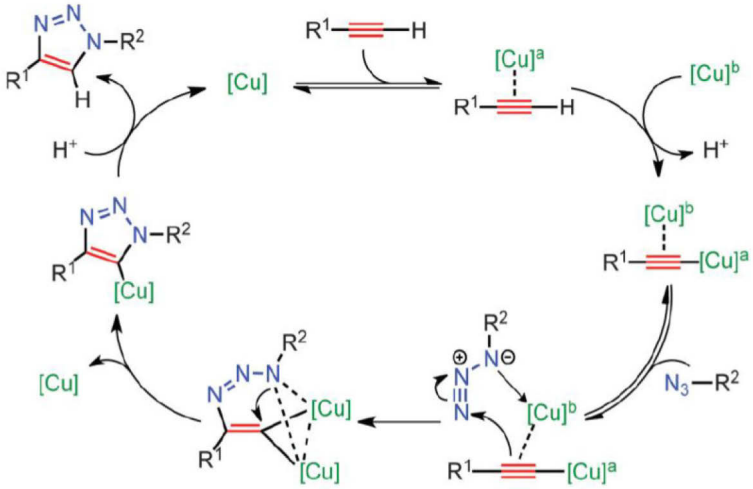

Figure 34. Catalytic model for the CuAAC, contributed from Worrel et al [128]

Another problem to address in the case of the biological system labeling is the toxicity of the copper (I), it is a limitation factor towards its application for *in-vivo* systems. As was reported by Hong et al, the toxic impact of copper was mainly caused by the production of the oxygen copper species. This negative impact can be reduced with the addition of a ligand, which would play a role of a reductant for the oxidative species. However, the utilization of such ligand as TBTA, which was mentioned

previously, could not exclude the toxic effect. [130]

In order to solve this problem, Soriano del Amo et al [131] proposed a ligand that combines tert-butyl groups with a sulfate functionality, this provides a good balance between reactivity and solubility properties of the ligand. Moreover, the sulfate group is minimizing the penetration of copper to the cell membrane. The structure of a bis(tert-butyltrazoly) ligand (BTTES) is shown in Figure 35 B.

Another copper chelating ligand, which was reported as the one that eliminates the toxicity, was introduced by Hong et al [130]. Tris(hydroxypropyltriazolyl)methylamine (THPTA), the structure of which is shown in Figure 35 C, was proven to accelerate the reaction and to protect cells from the damage.

A different approach of the introduction of the chelating agent was suggested by Bevilacqua et al [132], the idea behind it was to include the copper chelating ligand into the structure of the azide. The functionalization of the azide with the copper-chelating moiety led to the unprecedented reactivity and efficient ligation even under diluted conditions.

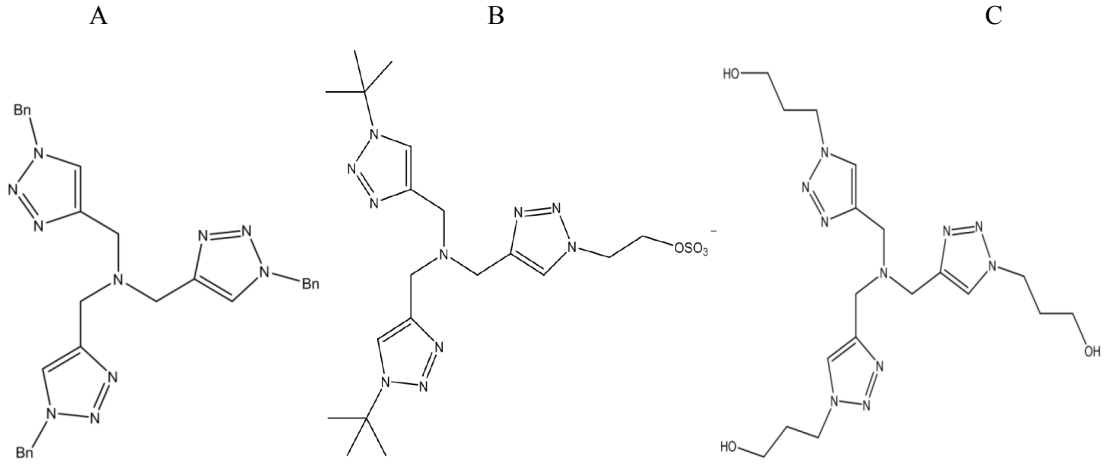

Figure 35. (A) Structure of copper (I) chelating ligand, TBTA, contributed from Chan et al [129]; (B) Structure of copper (I) chelating ligand, BTTES, contributed from Soriano et al [131]; (C) Structure of copper (I) chelating ligand, THPTA, contributed from Hong et al [130]

1.9.3. Copper-free [3+2] cycloaddition (CuAAC) of azides and alkynes

As was discussed previously, in spite of all the advantages of the Huisgen reaction, the toxicity of copper and the need to accelerate the reaction was remaining a significant limitation factor. This has inspired numerous studies aimed to further optimize the reaction for both in-vitro and in-vivo conditions.[117][118][121]

Bertozzi et al proposed the utilization of the strained alkynes to increase the reaction rate, avoiding the addition of copper at the same time. This approach was based on the studies of Wittig and Krebs done in 1961, where the reaction between cyclooctyne and phenylazide resulted in the formation of triazole. [133] The reaction scheme of Copper –free [3+2] cycloaddition is shown in Figure 36.[117][118]

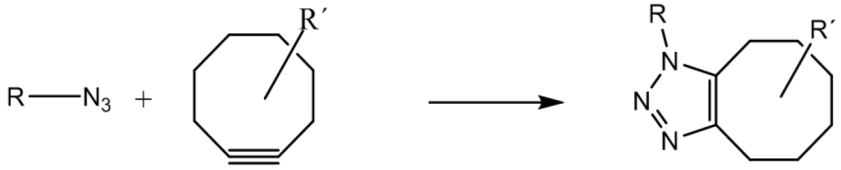

Figure 36. Copper –free [3+2] cycloaddition, contributed from Agard et al [133]

The strain-promoted azide-alkyne cycloaddition was successfully tested for the labeling of biomolecules and cells, however, with the first generation of utilized cyclooctynes, the reaction rate was not sufficiently high. [117] Due to this reason, the fluorine functionalized cyclooctynes were probed: the cyclooctyne, which bears two fluorine groups –DIFO (the structure is shown in Figure 37) was demonstrating the significant enhancement of the reaction kinetics. [117] [118][121]

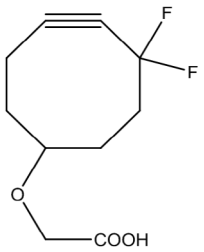

Figure 37. Difluorinated cyclooctyne (DIFO) contributed from Sletten et al [117]

In terms of the application of this reaction approach, the main limitation factors so far are the need of utilization of organic solvents and the further acceleration of the reaction rate. The Copper-catalyzed azide-alkyne 1,3-dipolar cycloaddition currently remains more accessible for the application in the field of labeling of biomolecules and living cells.[117][118]

1.9.4. Tetrazine ligation

Among bioortogonal reactions, the one with the unprecedented fast reaction rate, the tetrazine ligation, was reported by Blackman et al. [134] Moreover, the reaction did not demonstrate a toxic impact on the biological samples and did not have solvent restrictions. The inverse electron demand Diels-Alder reaction was taking place between tetrazine and trans- cyclooctene (TCO), the trans-isomer of this compound was reported to have the higher reaction activity (7 orders of magnitude) in comparison with the cis-isomer.[134] It is important to note that synthesis of reactive components for inverse electron demand Diels- Alder reaction is less challenging in comparison with activated cyclooctynes. The mechanism of the tetrazine ligation is shown in Figure 38. The only side product obtained with this reaction is the nitrogen, the release of which makes the reaction irreversible.[117][118]

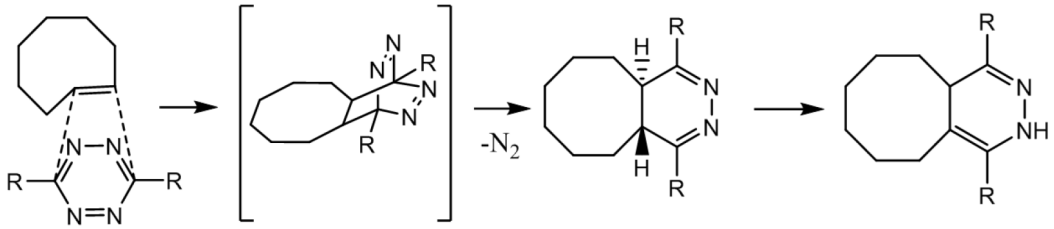

Figure 38. Diels-Alder reaction, contributed from Blackman et al [134]

In spite of such advantages as very high reaction yield, no toxic impact and very fast kinetics, there are several difficulties for the practical application. The first one is the possible conversion of trans-cyclooctene into cis-cyclooctene, what can affect the reaction yield in a drastic way. Another possible difficulty is that the big size of molecule can cause steric hindrances on the compound of interest. [117]

2. Aim and scope of the present work

The isolation of a protein target for a small molecule is a challenging area in current proteomics. There are several approaches with that one can perform this task. Isolation can be based on physical (fractionation) or chemical properties (functional enrichment). Functional enrichment strategies include affinity pulldown, activity based protein profiling (ABPP), capture compound mass spectrometry (CCMS). Each of them has certain advantages and limitations due to their design. ABPP is a quite straightforward for the characterization of enzymatic activity, while it is not applicable for the case of non-covalent interactions between small molecules and protein. For such interactions affinity pulldown can be a successful solution. However, some target proteins can be profiled only with CCMS, especially for the relatively weak but still specific interaction between molecular probe and target protein, because CCMS provides a covalent cross-link between the small molecule probe and the target protein triggered after establishment of equilibrium binding. Also in comparison to affinity pulldown and ABPP the advantage of CCMS is that it allows stringent washing conditions and no limitation by a solid support.

In order to enable detection and isolation, Capture compounds (CC) are usually functionalized with fluorophore or with biotin. The first one allows fluorescence readout, the second one – isolation with streptavidin magnetic beads followed by MS analysis. In spite of all the advantages allowed by this method, there are restrictions in terms of absolute quantification of the captured proteins. Inductively coupled plasma mass spectrometry (ICP-MS) stands out as a promising method to achieve this goal. However, since the common constituent elements of protein (such as C, N, O) cannot be detected with ICP-MS, a specific type of labeling is required. In order to improve sensitivity, reduce the background interferences, the approach of using lanthanide-containing probes is implemented for the further ICP-MS detection. Hence concerning utilization of an absolute quantification for CCMS, the attachment of a lanthanide tag (MeCAT) followed by ICP-MS quantification can be the approach of choice.

The aim of this work is to probe the utilization of a MeCAT label as a detection function of CC with the intention to find out it´s applicability for the absolute quantification purpose as well as for imaging.

Aiming to proof this concept, capture experiments were performed initially on a single isolated purified protein, the methyltransferase M.TaqI, with CCs that contain either fluorophore or a MeCAT label as detection function. Readout methods were fluorescence detection and ICP-MS. The main goal was to perform specific capture of a target protein and to utilize ICP-MS for the absolute cross-link yield quantification. Another important issue was to compare the reproducibility of the results obtained from several detection methods.

In order to test the utilization of imaging for capture experiments, the dopamine D2 receptor DRD2, a G-protein coupled receptor, on the living cells was addressed. Fluorescent microscopy and LA-ICP-MS were used as an imaging tools. Moreover, a quantification of a total cell population labeling was conducted as well with ICP-

MS. As a reference for fluorescence microscopy detection, Western blotting and nano-LC-MS/MS analysis were used. The goal was to detect if the specific capture takes place, to visualize labeling and to see the labeling distribution on the cells. Aiming to control the number of cells per slide and to enable stringent washing conditions, different cell post-treatment workflows were tested.

3. Results and discussion

3.1. Proof of concept. Capture experiment on a single purified protein

3.1.1. The main concept and workflow

As discussed previously in introduction, one of the current challenges in the modern proteomics is the isolation of those proteins, which specifically interact with the small molecules. Numerous experiments proved that a characteristic feature of CCs to crosslink specifically to the target protein to be particularly suited for this purpose [108] [135] [136] and that this also allows both detection with the fluorescence readout as well as the isolation followed with MS detection. However, as yet, for such chemoproteomics probes, the problem of absolute quantification is unaddressed. The ambition of this project is to investigate possible benefits of using inorganic mass spectrometry (ICP-MS) for the absolute crosslink determination.

This proof of concept study aims to examine the hypothesis that metal chelates can be utilized as a detection function of CC followed by ICP-MS detection. Overall, the experiment setup was designed to test the ability of the molecular probe that carries lanthanide tag to crosslink to a target protein in a specific way and also to perform the absolute crosslink yield quantification. During these investigations, capture experiments were performed on an isolated purified enzyme: DNA adenine N6 M.Tase from Thermus aquaticus (M.TaqI). The investigations of photoinduced isolation of methytransferases with cofactor product *s*-adenosyl-L-homocycteine (SAH) based CCs, which carries biotin as the sorting/detection function, have been done in caprotec and were reported already [109] [104] [113]. Moreover, the areas of enzyme where selectivity function of CC binds and reactivity function covalently crosslinks were also indicated during experiments. Figure 39 displays the structure of M.TaqI complex with DNA. To the region of enzyme, coded with the violet color, selectivity function of CC (SAH) binds, while to the region coded with the red color the reactivity function photocrosslinks.

The scheme of the workflow for the experiment setup for the capture assay is shown on Figure
40. During the first stage selectivity function (SAH) is interacting with target protein (M.TaqI) in a reversible way; within this step competition is possible. During the second stage, CC photocrosslinks to target via reactivity function. After SDS-PAGE separation at the third step, the detection via fluorescence and ICP-MS readout is performed.

Since the metal tag was tested the first time for the capture experiment setup, a reference method was needed. Successful utilization of fluorophore as a detection function of CC has been already reported; therefore, fluorescence readout was chosen as a reference method.

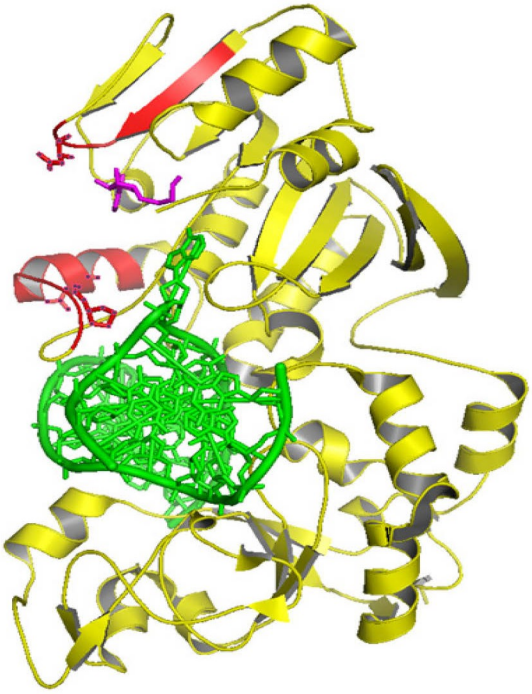

Figure 39. Complex of M.TaqI with DNA. Green color stands for DNA, yellow, red and violet to M.TaqI. Areas of M.TaqI marked with violet correspond to the area where SAH attaches, red to the area where the reactivity function crosslinks.

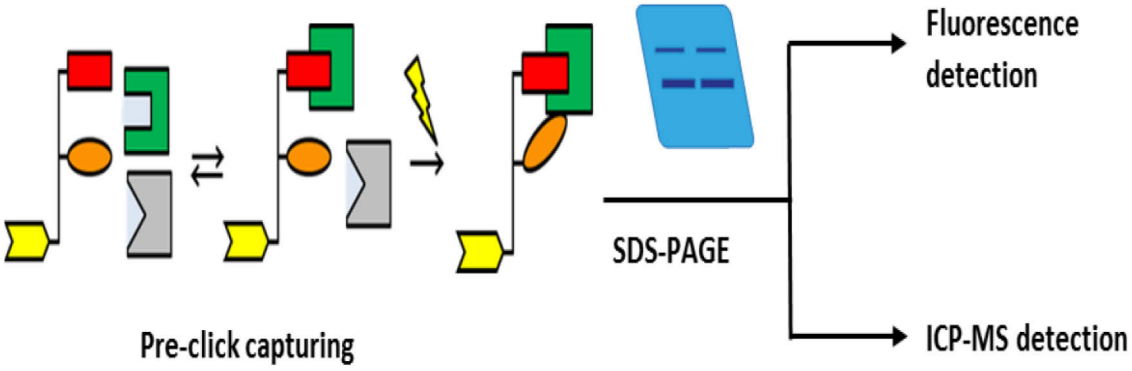

Figure 40. Workflow of capture experiment on a single purified protein (assay). Red figure corresponds to selectivity function, orange to reactivity function, yellow to detection function. Green figure stands for target protein, grey for non-specific protein.

3.1.2. Isolation of M.TaqI with SAH based CC

As was already mentioned, CCs that carry SAH as a selectivity function have been successfully investigated in caprotec. Therefore, for the testing of MeCAT as a detection function of CC the system SAH-M.TaqI was chosen as a well-studied and a robust test system. An approach of the isolation of enzymes, which have affinity to SAH, from E-coli lysate, followed by ICP-MS detection was also considered, since this system was addressed already with the biotin functionalized CC, as was established previously. In E-coli lysate the amount of proteins, which can be targeted by SAH based CC, is close to 2 percent. However, for this experimental setup an antibody against DOTA would be needed, to enable a successful pull-out experiment. Without the isolation of the covalently attached protein, the specificity of the photocrosslink is hard to establish. Because out of the 2 percent of protein from E-coli lysate, only from 5 to 10 percent are supposed to covalently crosslink to CC. It was considered, that such a small amount will be suppressed with the background of the rest of proteins. Since the required antibody was not available, this idea could not be developed further.

3.1.3. Detection tags, synthesis and functionalization of CC

Of crucial importance for the proof of concept experiments was the comparison between the two detection functionalities of CC: the lanthanide tag studied here for the first time, and the fluorescent tag that had been established in caprotec in the meantime [112]. To enable the comparison, two different detection functions (fluorophore and MeCAT) were attached to the SAH based CC. Because of such advantages as a high reaction yield and biocompatibility, a click chemistry approach was chosen. Among the variety of bio-orthogonal click chemistry reactions reported in the literature [118], for the proof of concept experiments the tetrazine ligation was chosen, since the functionalized ligands were accessible, and because it was convenient for this particular experimental setup with low working concentrations.

3.1.3.1. *Fluorophore functionalized tag*

The structure of clickable detection function that carries fluorophore (TAMRA) and functionalized with trans cyclooctene (TCO) - CPT 533 is displayed in Figure 41.

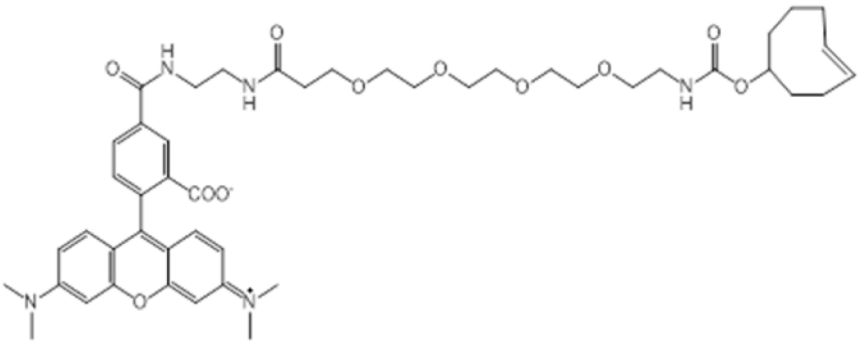

Figure 41. Structural formula of fluorophore detection function (TAMRA-TCO) CPT533

This detection function was already synthesized in caprotec, neither synthesis optimization nor additional purification was done in the frames of this research project.

3.1.3.2. *Lanthanide functionalized tag*

The detection function that carries metal tag – MeCAT (TCO-DOTA-Tb) shown in Figure 4 was synthesized under optimized conditions. The following reaction parameters were improved: solvent composition for the reaction of TCO-DOTA coupling, reaction time, and concentration of added organic base (TEA).

The synthesis of the compound shown in the Figure 42 was performed in the chemistry department in caprotec.

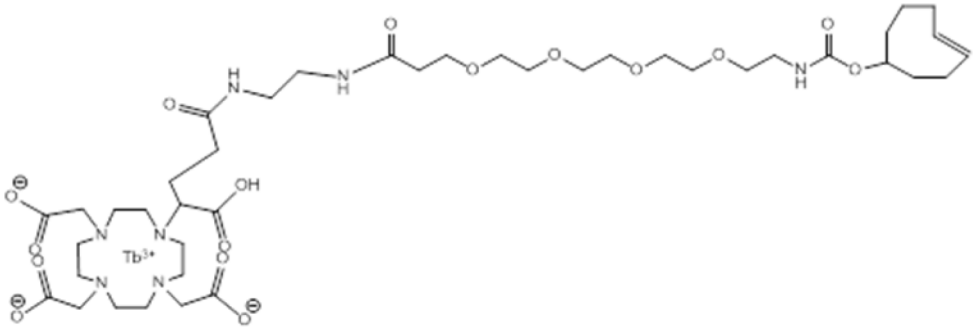

Figure 42. Structural formula of MeCAT (DOTA-TCO-Tb)

3.1.3.3. *Optimization of synthesis of clickable MeCAT and purification*

It is known that the coupling reaction of the primary amine to N-Hydroxysuccinimide esther (NHS ester) can compete with the hydrolysis of ester. To promote higher reaction yield and to eliminate the presence of unwilling side products of hydrolysis, the amount of water in the reaction mixture should be minimized. However, DOTA-GA-NH_2 is a hydrophilic compound, and it is not soluble in most of organic solvents recommended for these type of reactions in literature: DMF, DMSO, etc. Because of it, the solvent content for the coupling reaction had to comprise water. The solvent composition for DOTA needed additional optimization: water, DMF, methanol, the mixture of DMF with water (90% DMF) and the mixture of methanol with water (90% methanol) were tried. For all the tested solvents, additional stirring and sonication was utilized. The summary of the trials is represented in a Table 1. The good solubility was obtained only in water and in the mixture of water and methanol (90% methanol).

	water	DMF/water	DMF	methanol/water	methanol
DOTA-GA-NH_2	sol	n/sol	n/sol	sol	n/sol
TCO-NHS ester	n/sol	sol	sol	sol	sol

Table 1. Optimization of a solvent composition for the coupling reaction

Another important factor, is the time of conversion; the results of optimization of reaction time is shown in Figure 43. For the optimization of this reaction conditions one of the main goal was to decrease the amount of TCO functionality unattached to DOTA chelate in a reaction mixture. As is displayed on the bar chart, the total conversion of TCO containing moiety takes place during one hour; the further incubation does not influence the ratio of TCO to the reaction product.

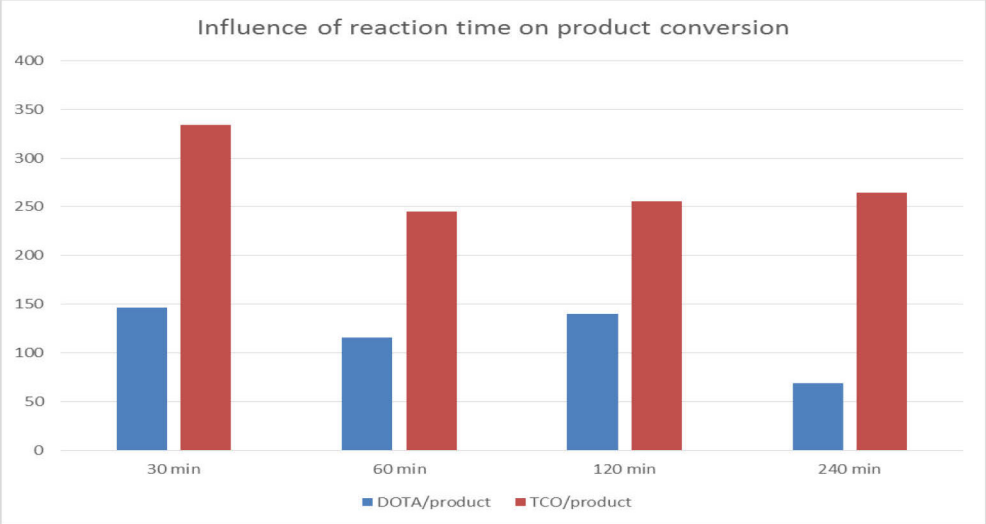

Figure 43. Influence of reaction time on TCO-DOTA conversion, the reaction was quenched with liquid nitrogen after 30 minutes, 60 minutes, 120 minutes and 240 minutes. The blue bars stand for the ratio of the amount of unattached DOTA chelate to the reaction product, red bars for the ratio of the amount of unattached TCO to the reaction product.

In order to catalyze the coupling reaction, the proton acceptor – trimethylamine (TEA) was added.

The influence of this compound in excess to amine functionalized DOTA is shown in Figure 6. For the first trials, TEA dissolved in water was added; it is worth noting that the conversion yield for coupling reaction where water was used as a solvent for TEA was not as high as expected. Moreover, the addition of water enhanced the presence of hydrolysis side products, which is illustrated by the data displayed in Figure 44.

Since the presence of water provided certain limitations, DMF was used as a solvent for the organic base in order to decrease the presence of unwilling side products of hydrolysis. Also higher concentrations of organic base were tested; the results are demonstrated in Figure 7. In these trials the observed conversion efficiency was significantly higher. As is displayed on the bar chart from Figure 45 the 80 fold excess is the suitable amount, since the further enhancements of TEA concentration did not influence the conversion efficiency.

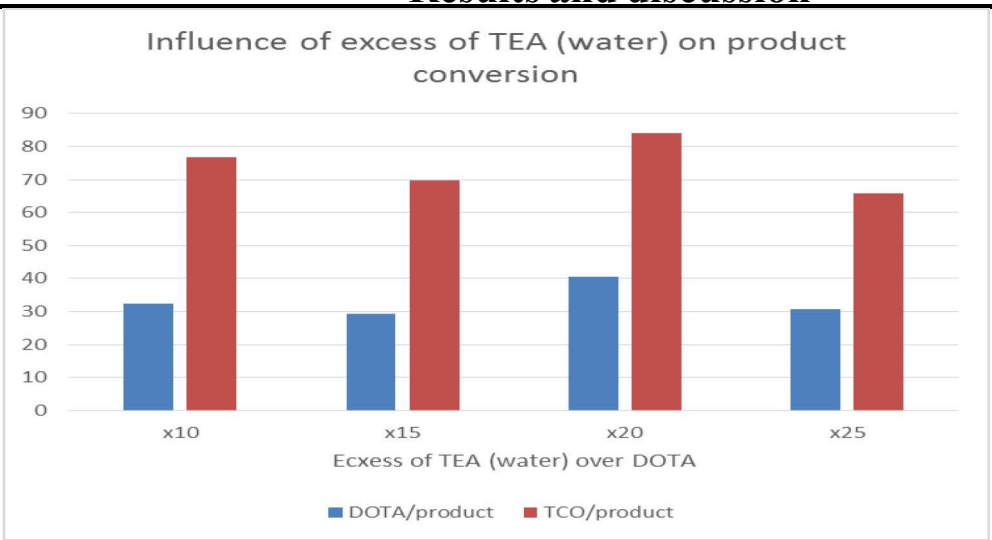

Figure 44. Influence of the TEA excess (solvent is water) on reaction yield

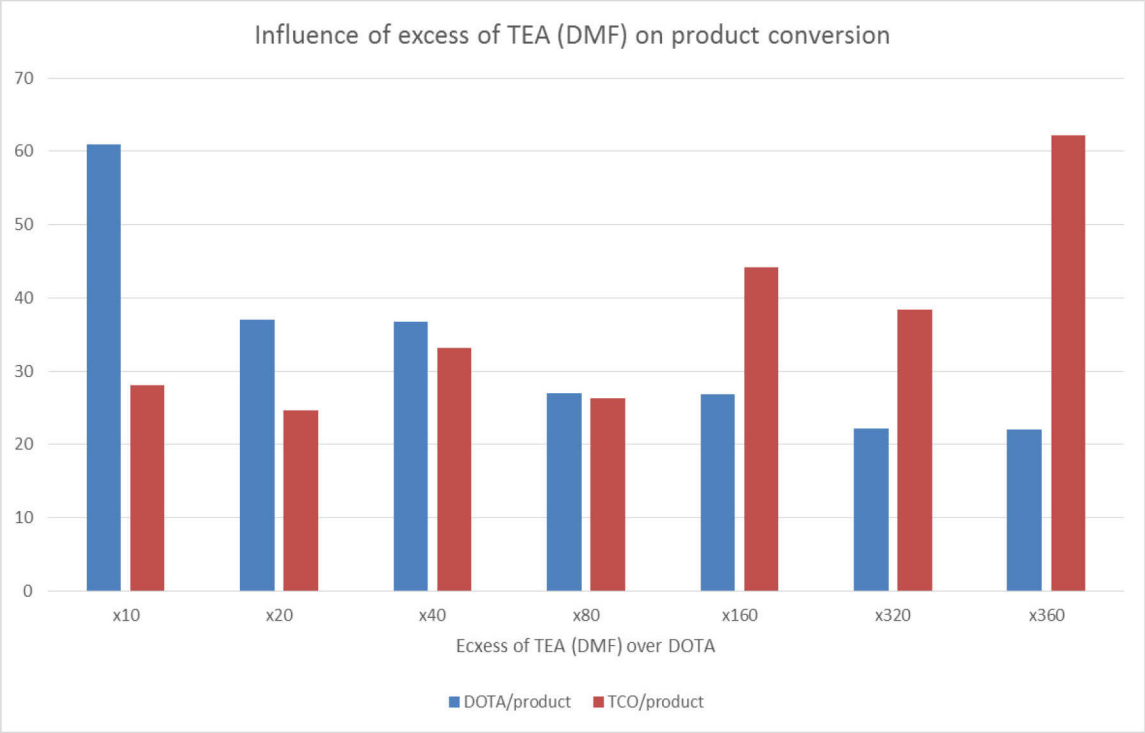

Figure 45. Influence of the TEA excess (solvent is DMF) on reaction yield

After the coupling reaction of primary amine to NHS ester, the lanthanide was introduced inside the DOTA ring. The advantages of the utilization of metals from these group for ICP-MS detection are the low limits of detection and low spectral interferences. Terbium was selected among the other lanthanides since it is monoisotopic element, which simplifies the quantification task. It is also known that such lanthanides as terbium and europium have fluorescent properties.

In such a case the same metal tag could be utilized both for fluorescence and ICP-MS readout. However, the primary fluorescent measurements of the complex compound, which consists of DOTA-GA-NH2 with terbium inside the cage, did now show any favorable outcome. It can be explained via the structure of the complex compound DOTA-Tb. The scheme of complex formation of lanthanide

with the DOTA chelate is displayed on Figure 46 [137]. It is known that the fluorescence signal of lanthanide can be quenched by water molecules [138]. Based on the structure of the complex compound, it can be suggested that the Tb-O(H_2) bond is the reason of the quenching.

The metalation of TCO-DOTA was done following by a standard protocol, developed in a working group of Prof. Linscheid and did not require any additional optimization. Synthesized MeCAT was purified with preparative liquid chromatography; mass-triggered fractionation was used for detection since no UV-activity from the obtained compound was observed. The product of metalation appeared to be ionized efficiently only in the negative mode. As is shown in Figure 47, the batch with 95% purity was obtained. Because of the mentioned properties of synthesized MeCAT, only the negative mode of ESI-MS spectrum is demonstrated in Figure 47 to illustrate the purity of obtained product. The concentration calculations for the purified MeCAT were based on the weight of the obtained purified compound.

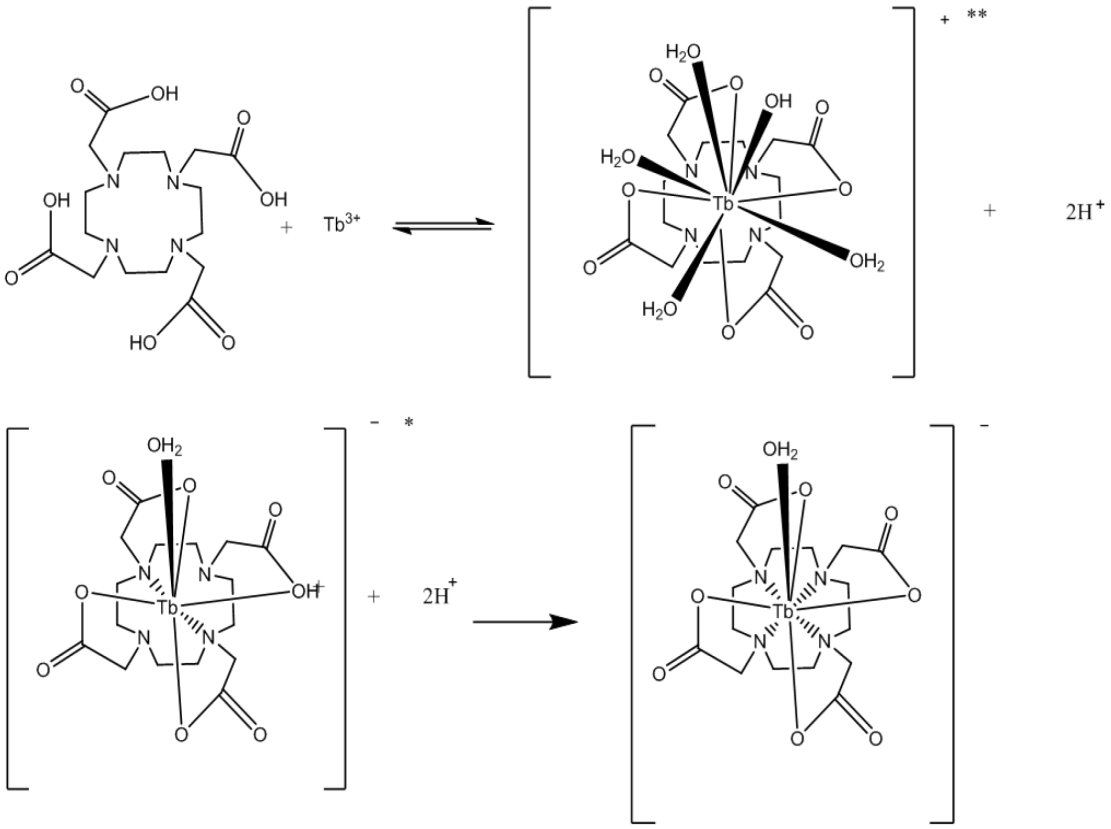

Figure 46. The formation of complex between DOTA and lanthanide. The first and the third steps. Modified from [137]

3.1.3.4. *Optimization of tetrazine ligation conditions for clickable MeCAT*

After the purification, the mass of crystallized compound was determined. Based on the mass, the concentration of MeCAT was calculated. However, in order to establish the actual ("real") concentration of purified compound, an experiment with titration was done. The concentration of DOTA-TCO-Tb was adjusted to the concentration of SAH-based CC functionalized with tetrazine (CPT594). The structure of click reaction product is shown in Figure 48. The results of optimization of reaction conditions (the concentration ratio of tetrazine functionalized CC to TCO functionalized MeCAT) are shown in Figure 49. As is illustrated by Figure 49 the actual concentration of the purified MeCAT was significantly lower than was expected. The initial ratio of compounds taking part in click reaction was supposed to be equal 1 to 1. For subsequent experiments, the adjusted concentration of MeCAT was used.

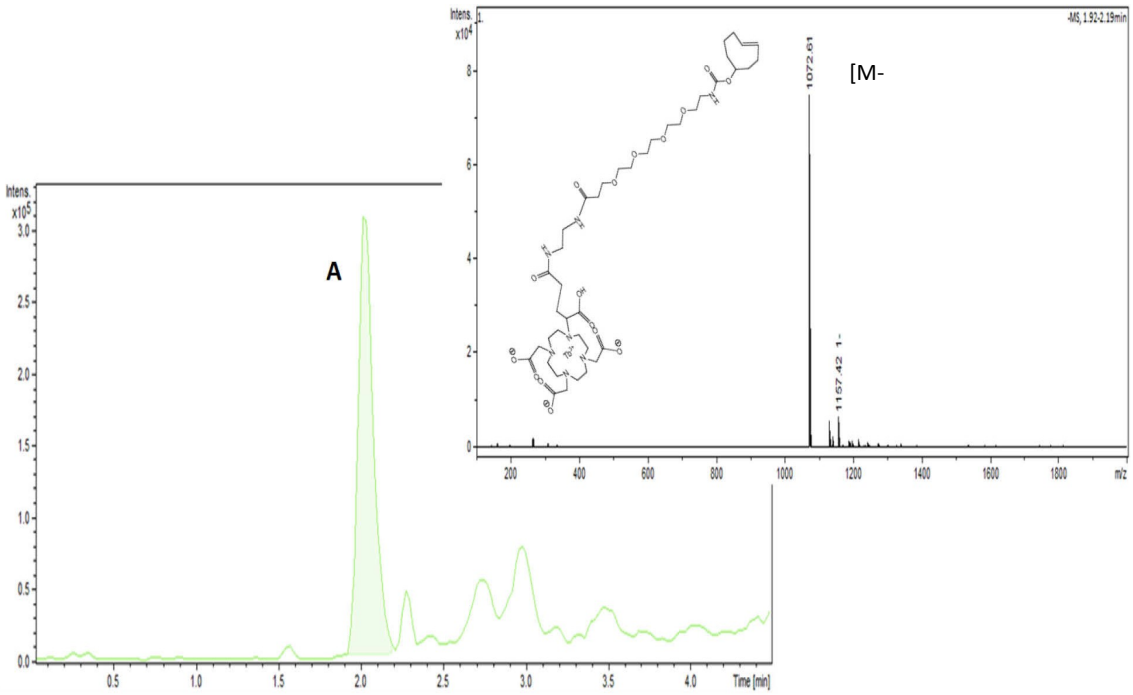

Figure 47. HPLC chromatogram for preparative purification of DOTA-TCO-Tb. Peak A corresponds to the elution of purified compound. On the right side ESI-MS spectrum of the peak A, negative mode.

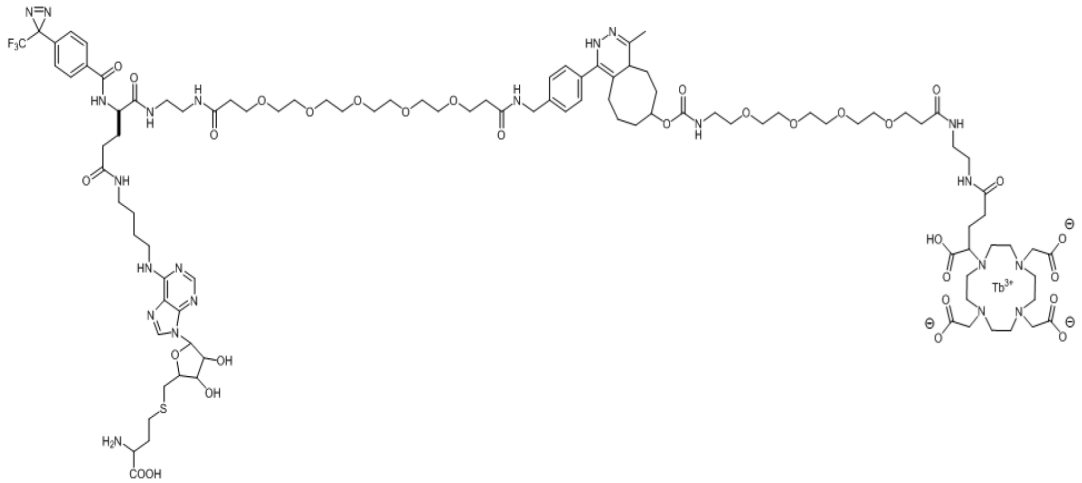

Figure 48. Product of click reaction. SAH based CC functionalized with MeCAT.

The reaction conditions of tetrazine ligation for the attachment of TAMRA to the CC as a detection function were optimized previously in caprotec; no further optimizations were done. The structure of SAH-based CC that carries TAMRA as a detection function is shown on Figure 50.

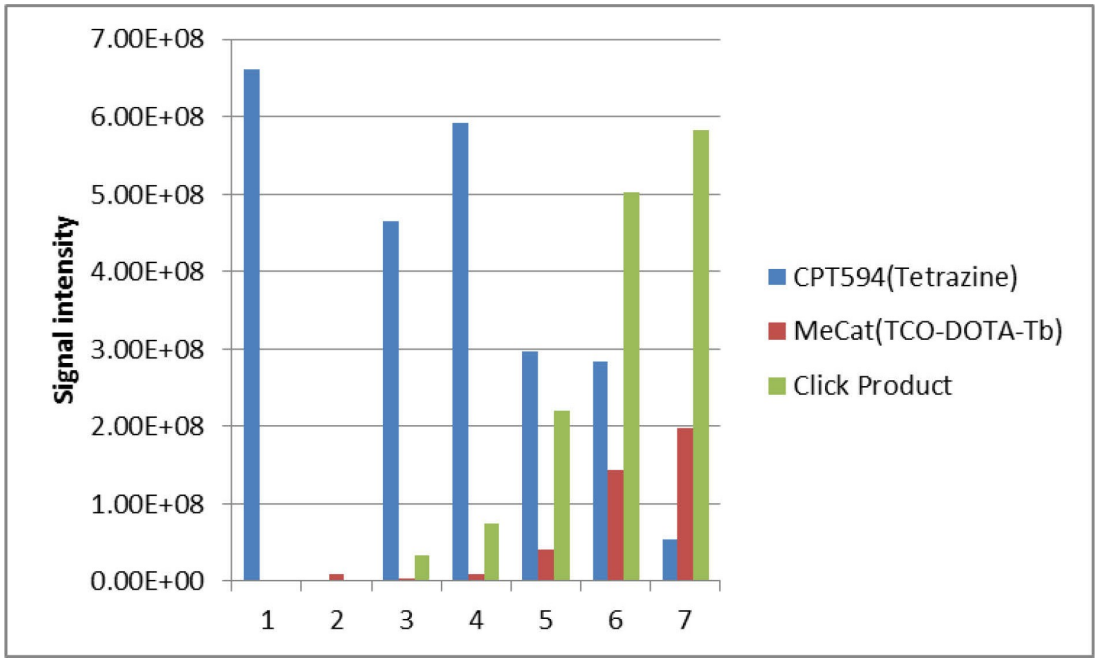

Figure 49. Optimization of reaction conditions (TCO-DOTA-Tb concentration titration). 1 – corresponds to control sample that contains exclusively tetrazine functionalized CC; 2 – control sample that contains exclusively MeCAT; 3 – 1x excess of MeCAT; 4 – 2x excess of MeCAT; 5 – 8x excess of MeCAT; 6 – 16x excess of MeCAT; 7 – 24x excess of MeCAT.

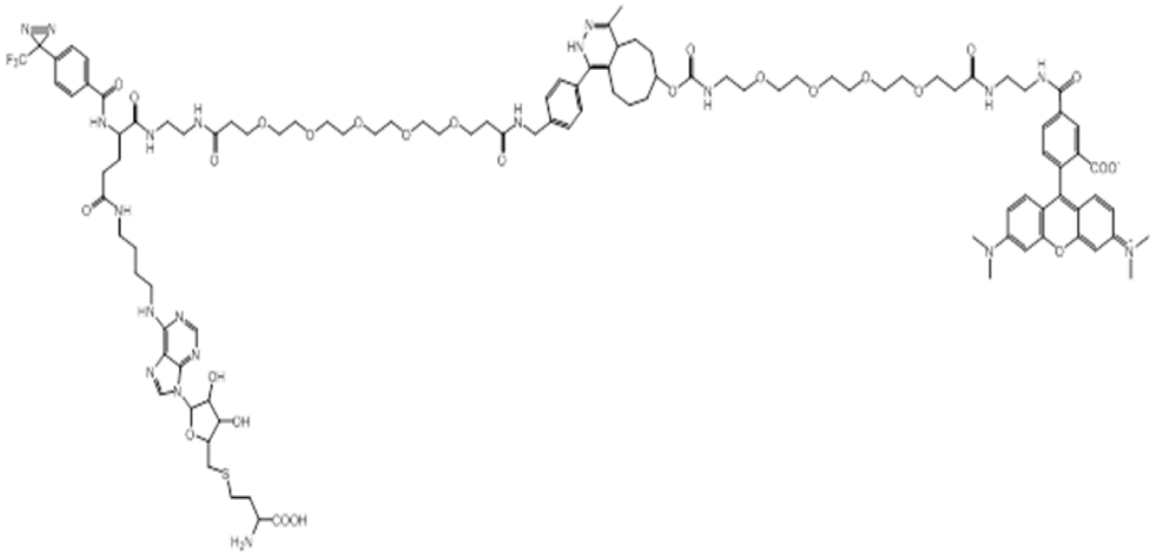

Figure 50. Product of click reaction. SAH based CC functionalized with TAMRA.

3.1.4. Pre-click capture experiment on M.TaqI

3.1.4.1. Interaction between SAH and M.TaqI

M.TaqI belongs to the family of DNA-modifying enzymes, which promote the transfer of methyl groups. For this process the known donor of methyl groups is *s*-adenosyl-L-methionine (SAM), the product of this transfer is *s*-adenosyl-L-homocycteine (SAH); the reaction scheme is shown in Figure 51. A high-potential of SAH as an affinity tag to methyltransferases was reported, because of the good affinity between them and the high stability of SAH in comparison with SAM. This is important for the successful synthesis and implementation of CC [109].

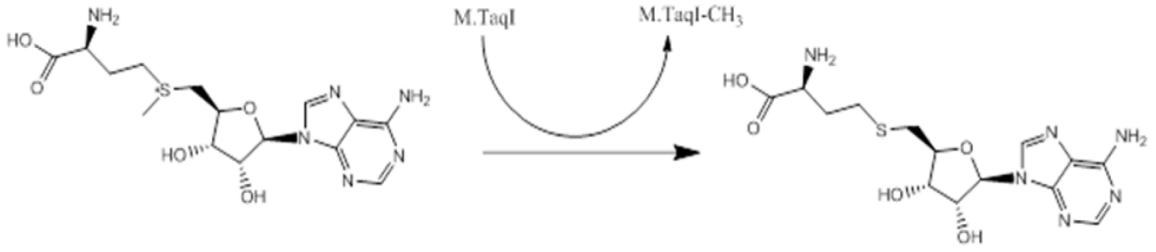

Figure 51. Methyl transfer from SAM, resulting in formation of SAH.

SAH-based CCs have been already synthesized and investigated in caprotec.[109][113] Several different attachment positions of selectivity function to the scaffold were tested, as well as various photocrosslinking groups (reactivity functions). Furthermore, the specific crosslinking was reported and the dissociation constant of the SAH-M.TaqI complex was determined via the titration. In addition, successful isolation of enzymes, which have affinity to SAH, from E-coli cell lysate was achieved via streptavidin-biotin interactions. For the previously reported experiments, biotin was used as a sorting function of CC that allows pull-out experiments with further MS/MS detection. For these investigations the reported crosslink yield had been in the range of 5-10%. As was also established with previous experiments, M.TaqI has the tendency to stick to the

walls of the reaction vessel; for this reason the standard capture buffer was slightly modified with the addition of detergent (Triton X).

During the capture experiment, the pre-clicked SAH based capture compound that carries metal tag or TAMRA as the detection functionality was incubated with the enzyme. After the equilibration was reached, the samples were irradiated with UV light to promote covalent crosslinking of the probe to the protein. It is important to mention that two types of control samples were utilized to assess that binding is specific (competition control) and to prove that compound is bound covalently exclusively due to the photocrosslink (UV irradiation control). Competition control samples were previously incubated with a tenfold excess of unmodified SAH. Under such conditions the CC was expected to crosslink mainly to unspecific protein. To control if crosslinking is taking place only under UV irradiation conditions, half of samples were not irradiated; moreover, to ensure that no exposition of UV light was taking place the samples were covered with aluminum foil. In case of no UV irradiation, no covalent attachment of CC to the protein was expected. All the probes were subjected to SDS-PAGE analysis. Samples were loaded into gel pockets in order to enable easy visual comparison of gel bands with fluorescence detection. The Figure 52 presents the results of in gel fluorescence detection.

3.1.4.2. Results of in gel fluorescence detection

As illustrated by the Figure 52, the fluorescence signal obtained from assay sample (lane 1) is notably higher than the one from the competition control sample (lane 2). As mentioned before, the addition of tenfold competitor (SAH) excess causes in majority the binding of SAH to the enzyme, while the probability that the selectivity function of CC will bind to a target protein is significantly lower; however, the minor crosslinking is taking place in spite of the excess of competitor. Because of this, the efficiency of the covalent crosslink of CC to the M.TaqI is notably lower. This is confirmed by the difference of the fluorescence signal intensity between the bands observed in lane 1 and in lane 2. Since MeCAT does not show any fluorescent properties, no fluorescence signal is observed in lanes 3 and 4. The intensity of the signal in the lane that contains a 1:1 mixture of assay labelled with fluorophore and of assay labelled with MeCAT (lane 5) can be estimated as half of signal intensity in comparison to that of the first lane, in agreement with the expectations. All the non-irradiated samples that are corresponding to lanes 7-12 show no fluorescence signal. This confirms that without photoactivation the CC is not attached covalently to the target protein.

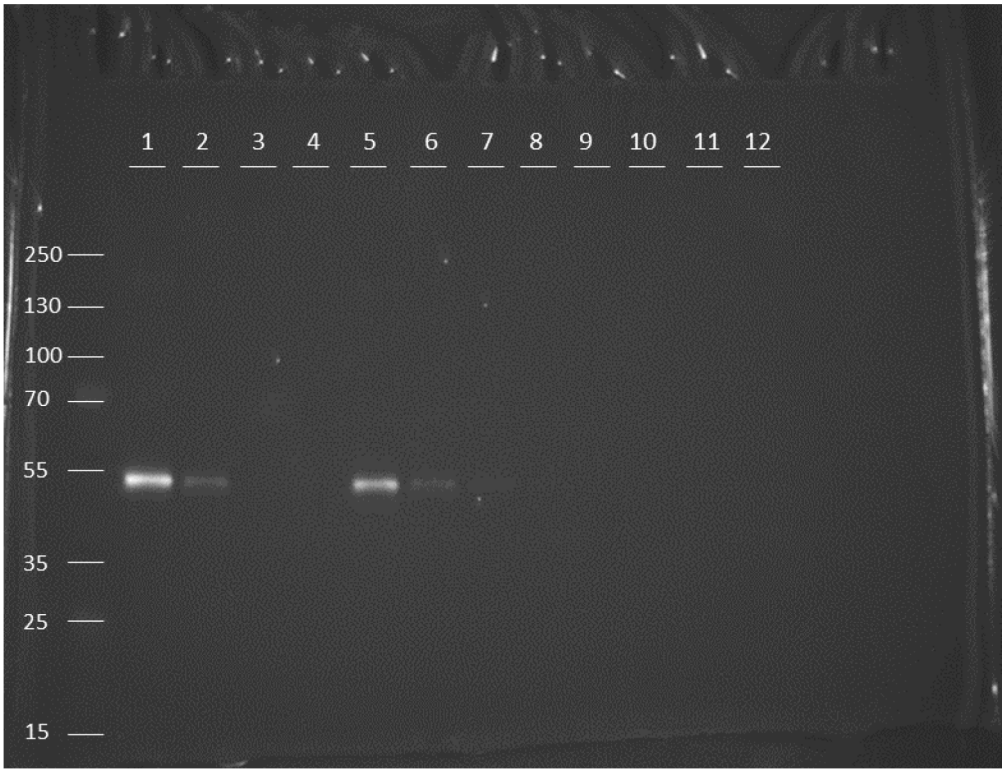

Figure 52. Results of in gel fluorescence detection. Pre-clicked capture experiment on M.TaqI. Lane 1 - corresponds to assay with CC that carries fluorophore (irradiated), lane 2 - competition control sample with CC that is labelled with fluorophore (irradiated), lane 3 - assay with CC that carries metal probe (irradiated), lane 4- competition control sample with CC that is labelled with MeCAT (irradiated), lane 5 - 1:1 mixture of assay samples with CCs that carry TAMRA and MeCAT (irradiated), lane 6 – 1:1 mixture of competition control samples with CCs labelled with TAMRA and MeCAT (irradiated), lane 7 - corresponds to assay with CC that carries fluorophore (non-irradiated), lane 8 - competition control sample with CC that carries fluorophore (non-irradiated), lane 9 - assay with CC that carries metal probe (non-irradiated), lane 10- competition control sample with CC that carries MeCAT (non-irradiated), lane 11 -1:1 mixture of assay samples with CCs that carry either TAMRA or MeCAT (non-irradiated), lane 12 – 1:1 mixture of competition control samples with CCs that carry either TAMRA or MeCAT (non- irradiated).

3.1.4.3. Sample preparation for ICP-MS detection

After in gel fluorescence readout, the visualization of the gel bands was done with Coomassie staining. The results are shown in the Figure 53. In addition to the bands that were corresponding to the molecular weight of M.TaqI, the shifted bands were observed for half of the samples, namely in lanes from 1 till 6. These shifted bands were assumed to correspond to the enzyme photocrosslinked to CC. This observation confirms that only under UV-irradiation conditions the covalent attachment of molecular probe to protein takes place. As is shown with the zoomed image on Figure 54, the shifted bands are present for samples corresponding to assay labelled with fluorophore, assay that carries a metal tag and to their mixtures. However, the shifts of labelled bands vary due to a different mass of TAMRA and MeCAT. For the CC that carries a lanthanide mass shift is notably higher in comparison to the one with the attached fluorophore. By the integration of the signal intensities in the image (ImageJ) it was

possible to make a rough estimation of crosslink yield for the assay labelled with MeCAT. For samples attached to TAMRA functionalized CC such evaluation was not feasible because of a very small distance between main and shifted bands.

For ICP-MS analysis, both shifted bands and main bands were extracted separately, in order to check if specific labeling was taking place. Shifted bands were expected to belong to a protein crosslinked to a CC, while main bands to the one that is not covalently attached to CC. Moreover, to ensure that the signal from lanthanide detected by ICP-MS is specific, and there is no disturbing background signal, the areas of the gel above the bands corresponding to MeCAT functionalized CC were extracted, the size of extracted blank area was approximately equal to the size of extracted band. These samples were taken as blanks. Also to find out if any external contamination is taking place during the sample preparation stage, the additional controls were done. These control samples did not contain initially any gel pieces, but they went through the same sample preparation procedure as the rest of the samples.

The gel bands were cut out manually and processed according to a standardized sample preparation protocol for ICP-MS detection developed in a working group of Prof. Linscheid. The main challenge that was faced during the sample preparation for ICP-MS quantification, was that due to a moderate crosslink yield and the presence of only one lanthanide ion per CC molecule the amount of lanthanide in the samples was not high. This required a relatively low dilution factor for the analysis. The standard sample preparation protocol (mineralization of extracted SDS-PAGE bands) for proteins labelled with MeCAT was designed initially for higher content of metal of interest in the samples; therefore a matrix effect was occurred. The matrix effect also caused very high blank control values. In order to solve this issue, the sample preparation protocol for the mineralization of extracted SDS-PAGE bands was optimized to decrease the final amount of nitric acid in samples before the dilution and addition of internal standard. After the adjustment of the mineralization protocol, the matrix effect was significantly reduced. Since, as was mentioned before, the initial concentration of terbium in samples was not high, a dilution factor of 10 was chosen for all the samples for ICP-MS detection.

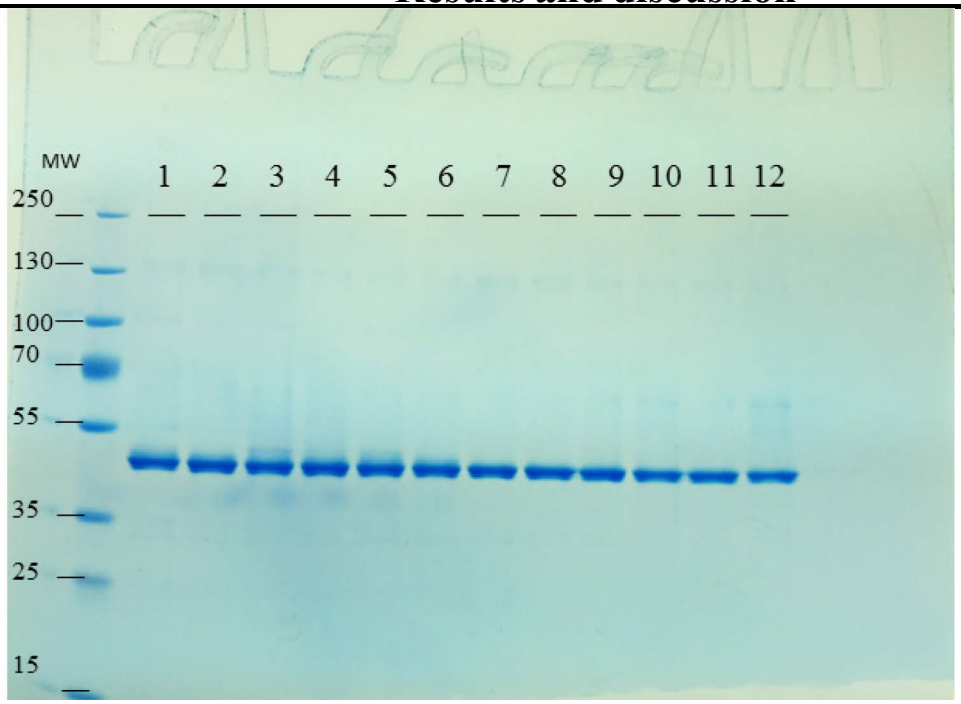

Figure 53. Results of Coomassie staining. Pre-clicked capture experiment on M.TaqI. Lane 1 - corresponds to assay with CC that carries fluorophore (irradiated), lane 2 - competition control sample with CC that is labelled with fluorophore (irradiated), lane 3 - assay with CC that carries metal probe (irradiated), lane 4- competition control sample with CC that is labelled with MeCAT (irradiated), lane 5 - 1:1 mixture of assay samples with CCs that carry TAMRA and MeCAT (irradiated), lane 6 – 1:1 mixture of competition control samples with CCs labelled with TAMRA and MeCAT (irradiated), lane 7 - corresponds to assay with CC that carries fluorophore (non-irradiated), lane 8 - competition control sample with CC that carries fluorophore (non-irradiated), lane 9 - assay with CC that carries metal probe (non-irradiated), lane 10- competition control sample with CC that carries MeCAT (non-irradiated), lane 11 -1:1 mixture of assay samples with CCs that carry either TAMRA or MeCAT (non-irradiated), lane 12 – 1:1 mixture of competition control samples with CCs that carry either TAMRA or MeCAT (non- irradiated).

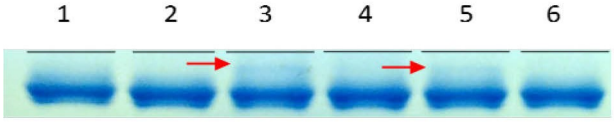

Figure 54. Results of Coomassie staining. Pre-clicked capture experiment on M.TaqI. . Lane 1 - corresponds to assay with CC that carries fluorophore (irradiated), lane 2 - competition control sample with CC that is labelled with fluorophore (irradiated), lane 3 - assay with CC that carries metal probe (irradiated), lane 4- competition control sample with CC that is labelled with MeCAT (irradiated), lane 5 - 1:1 mixture of assay samples with CCs that carry TAMRA and MeCAT (irradiated), lane 6 – 1:1 mixture of competition control samples with CCs labelled with TAMRA and MeCAT (irradiated). Red arrows are pointing to the shifted band that is corresponding to protein crosslinked to MeCAT functionalized CC.

3.1.4.4. Results of ICP-MS quantification

The results of ICP-MS quantification of the content of terbium in mineralized bands are shown in Figure 55. As demonstrated on the graph, the obtained numbers for the assay that carries metal probe as a detection function (blue bars) are in agreement with the results gained from the image conversion (orange bars). The conversion of shifted bands was done only for two lanes that were corresponding to irradiated assay labelled with MeCAT.

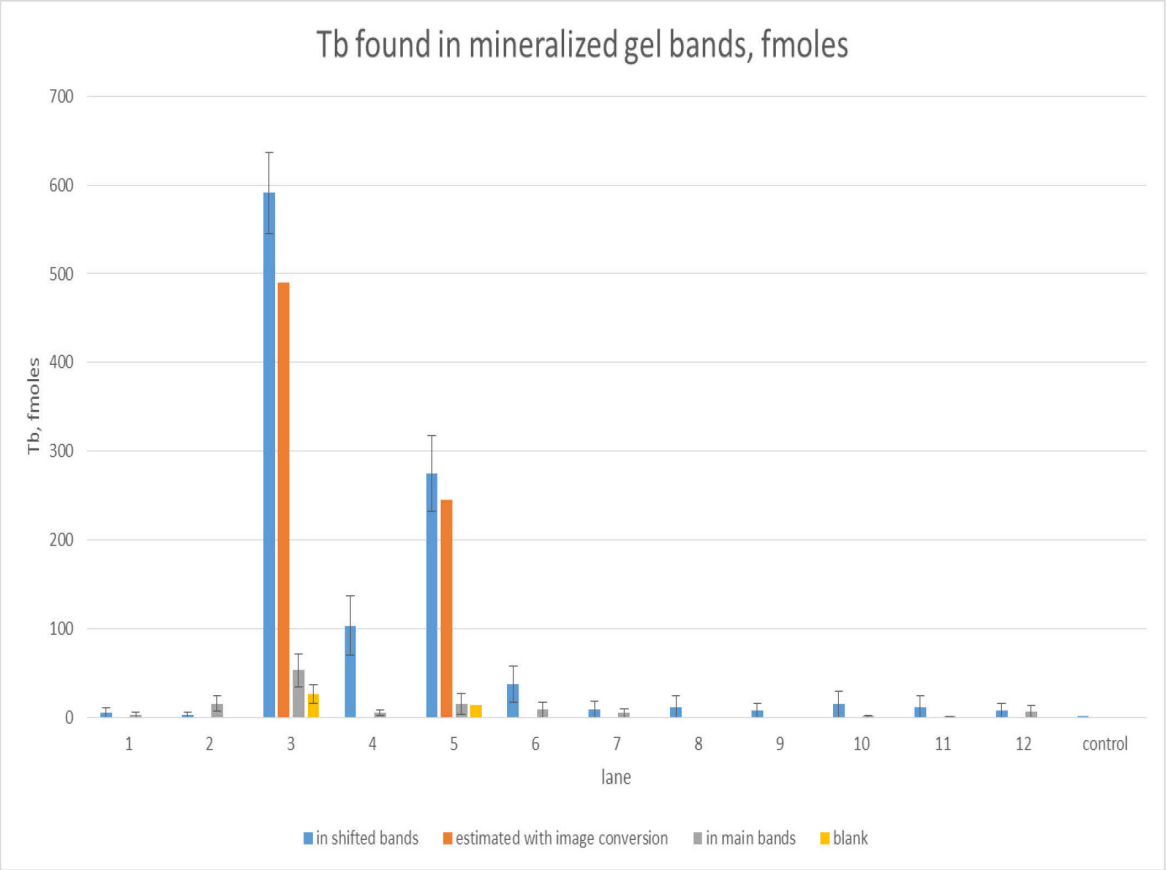

Figure 55. Results of ICP-MS quantification. Pre-clicked capture experiment on M.TaqI. . Lane 1 - corresponds to assay with CC that carries fluorophore (irradiated), lane 2 - competition control sample with CC that is labelled with fluorophore (irradiated), lane 3 - assay with CC that carries metal probe (irradiated), lane 4- competition control sample with CC that is labelled with MeCAT (irradiated), lane 5 - 1:1 mixture of assay samples with CCs that carry TAMRA and MeCAT (irradiated), lane 6 – 1:1 mixture of competition control samples with CCs labelled with TAMRA and MeCAT (irradiated), lane 7 - corresponds to assay with CC that carries fluorophore (non-irradiated), lane 8 - competition control sample with CC that carries fluorophore (non-irradiated), lane 9 - assay with CC that carries metal probe (non-irradiated), lane 10- competition control sample with CC that carries MeCAT (non-irradiated), lane 11 -1:1 mixture of assay samples with CCs that carry either TAMRA or MeCAT (non-irradiated), lane 12 - 1:1 mixture of competition control samples with CCs that carry either TAMRA or MeCAT (non- irradiated).

As expected, the amount of terbium found in a shifted band correwsponded to assay labelled with MeCAT (lane 3, blue bar) was significantly higher than the one from the competition control labeled with MeCAT sample (lane 4 blue bar). This result was in total agreement with the data obtained from in gel fluorescence readout for TAMRA

functionalized CC.

As anticipated, in main bands, and in bands that were standing for samples labeled with fluorophore, there was no signal of metal of interest or it was very low. Moreover, with the blank samples and control samples it was proven that there are no external contributions to the lanthanide signal from ICP-MS detection.

The reproducibility of the method was established, for the extracted bands that correspond to assay functionalized with MeCAT the RSD value was 7,7%. Taking into consideration pipetting of very small volumes and manual extraction of visualized SDS-PAGE band, the good reproducibility was achieved.

The absolute crosslink yield was calculated as a ratio of amount of metal, quantified with ICP- MS in a sample to an amount of lanthanide that would be quantified in case of 100% efficiency of crosslink, with the amount of input protein known. It is important to note that for the calculations it was considered that a single atom of lanthanide was corresponding to a single CC molecule.

The absolute crosslink yield quantified via ICP-MS was 6% that was in agreement with the estimations from the size ratio of shifted band to the main band, which is demonstrated on Figure
10. It is also coherent with the results obtained from previous investigations in caprotec when crosslink yield of 5-10% was reported.

3.1.5. *Conclusions and outlook*

The utilization of metal tag followed by ICP-MS the detection of the outcome of capture experiments on single purified protein is the first reported example of inorganic MS application in chemical proteomics. Also, within this project, MeCAT functionalized with the clickable moiety for the tetrazine ligation reaction was synthesized for the first time. Another novelty is the different approach for the attachment of the lanthanide tag to the protein. One of the trivial established MeCAT labeling methods is based on direct covalent attachment of the metal probe to thiol groups; it cannot provide specificity and cannot be controlled.

The successful application of a lanthanide tag as a detection function of CC has been demonstrated; the CC functionalized with MeCAT was proven to crosslink specifically to a target protein, via competition control experiments. Furthermore, the comparison with the reference method confirmed that the presence of the chelated lanthanide does not interfere with the specificity of binding. With the irradiation control it was established that the covalent attachment takes place exclusively under the controlled conditions (UV-irradiation); moreover, the formation of the covalent bond is necessary for the successful capture experiment. The results of absolute crosslink yield quantification (7,7% yield) are in agreement with those obtained from previous investigations on M.TaqI done in caprotec (5-10% yield) and with visual results obtained from Coomassie staining and the image integration (5% yield). Since the single purified protein was studies in this experimental setup, the question of selectivity of the metal functionalized CCs interaction with the target protein could not be addressed.

The important advantage of MeCAT application for the capture experiments is the provided accurate quantification of crosslink yield, which is not feasible via the trivial

CCMS approach, SDS-PAGE analysis and with the utilization of the fluorescent signal readout. It provides the complementary detection method to the already established ones.

However, it appears that the main restriction of the lanthanide tag as a detection moiety of CC is the limit of detection, provided by the readout via ICP-MS in comparison with fluorescence detection. The possible explanation for it is that every MeCAT molecule attached to the CC carries only one lanthanide atom. In addition to it, a low crosslink yield causes limitations in terms of sensitivity in comparison with the reference method. It was also found out that sample preparation protocol can become a source of matrix effect in case of relatively high content of acid in samples.

The possible way to improve the sensitivity, is the utilization of detection function with multiple metal cores, this can provide the noticeable enhancement of the signal. The matrix effect, as was mentioned before, can be significantly decreased with the optimization of sample preparation protocol, what was done in terms of this project.

3.2. Investigations of receptors. Capture experiment on a cell culture

3.2.1. The main concept and workflow

As shown in the experiments with the SAH-CC described in the previous section of the thesis, metal tags can be utilized as a detection functionality for chemo proteomic probes in order to enable absolute quantification. Based on the work reported in the first part of this thesis, metal tag allows absolute crosslink yield quantification; it is also not influencing the specificity of binding.

Nowadays, many studies suggest to use metal labeling also for imaging purposes. LA-ICP-MS was reported in numerous studies as a promising tool for bioimaging that allows visualization of elemental distribution on tissues [139] and even single cells [140] [141]. The utilization of LA- ICP-MS with MeCAT labeling for imaging and quantification purposes has been already reported [92]. However, the combination of metal labeling-based imaging with chemoproteomic probes has not been addressed so far and would, if successful, open an entire new field of applications in chemoproteomics with profound implications for target deconvolution in preclinical stage drug discovery. Due to the mentioned reasons, to perform further investigations of the potential benefits of MeCAT as a detection moiety of a capture compound, an experiment setup on living cells was selected.

The study that was addressing chemoproteomic targeting of receptors on living cells for the purpose of isolation and mass spectrometry-based identification was recently reported.[116] The main challenge that was successfully addressed in that study was to probe the target receptor by the capture compound in its native cellular environment, to avoid detergent-based extraction before binding and cross-linking. Successful targeting of cell surface receptors, in particular G- protein coupled receptors, is hard to achieve with the majority of chemoproteomic techniques other than CCMS. The case study reported by Blex et al. was based on sertindole CCs. [116] Sertindole-CC were used to target dopamine D2 receptors (DRD2) directly on the surface of living cells.

Three sertindole-based CCs with different attachment positions of the selectivity function to the CC scaffold were synthesized, and were tested for their binding and pharmacological efficacy. In the case study CCs functionalized with biotin as a pullout (isolation) function were utilized. By the experiments it was demonstrated that the sertindole- based CC in which sertindole was attached to the CC scaffold in an orientation that was suitable to bind DRD2 had an affinity to DRD2 on transfected cells and sertindole binding sites in rodent and porcine brain in the same range as an unmodified compound. Moreover, via molecular modelling study the binding patterns of the different sertindole-CCs to DRD2 was structurally rationalized.[116]

Nevertheless, the imaging challenge has not been addressed yet. Since DRD2 is a membrane receptor, it is of a great importance to detect if the sertindole-based CC crosslinks exclusively to the cell surface. In this study particular attention was paid to the imaging of cells, for this purpose such methods as fluorescence microscopy (as a reference method) and LA-ICP-MS were used. Another important question of interest was the quantification of a total cell population labeling yield. To address the quantitative challenge ICP-MS detection method with an internal standard was used. To perform these detection methods, in this project CCs functionalized with TAMRA or MeCAT as a detection function were utilized. The general workflow scheme is shown in Figure 56. During the first stage selectivity function (sertindole) is interacting with the target protein (DRD2) on the cell surface in a reversible way, at this stage competition with the other compounds is possible, since the binding is a non-covalent one before UV-irradiation. During the second stage CC is photo-crosslinked to the target via the reactivity function of the CC. After the CC is covalently attached to the cell surface, different sample preparation protocols were applied depending on the detection method of choice.

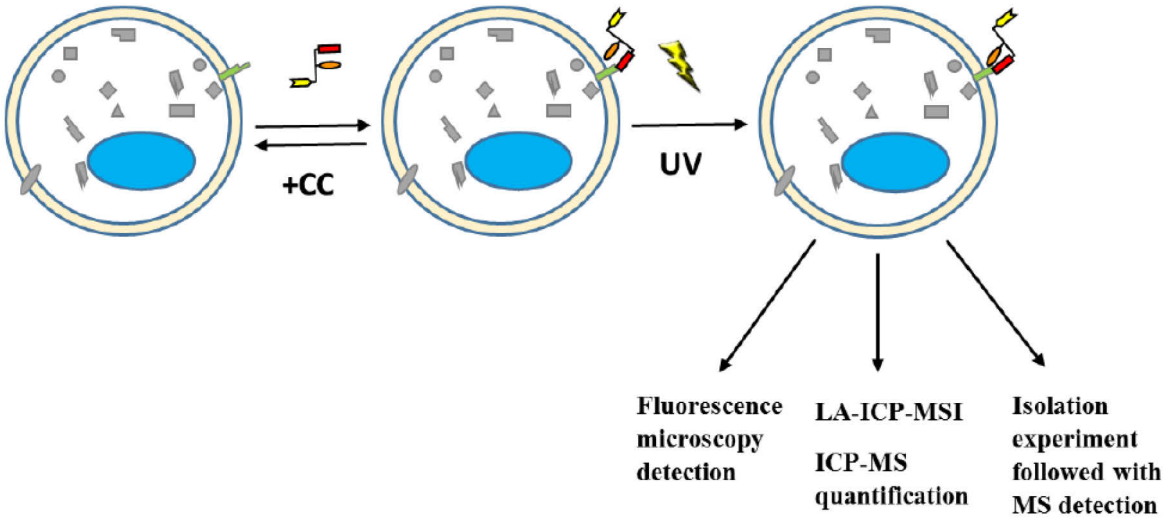

Figure 56. The general workflow of the capture experiment on living cells.

3.2.2. *Dopamine D2 receptor*

According to Beaulieu and Gainetdinov, dopamine plays a crucial role as a neurotransmitter in numerous functional processes in human brain. Because of this

role of dopamine, numerous human pathological conditions such as Parkinson's disease (PD), schizophrenia, etc. are influenced by the dysregulation of this compound. Dopamine activates several receptor classes, among them are G protein-coupled receptors. The family of dopamine receptors are named from D1 to D5. They have different affinities to the dopamine in the range from nanomolar to micromolar. This technology enabling study focused on one of the receptors from this family, the D2 receptor (DRD2), was investigated. In a human brain, DRD2 is expressed mostly in striarium, nucleus accumbens, olfactory tubercle, in a lower levels in the substantia nigra, vental tegmental area, hypothalamus, cortical areas, septum, amygdala, hippocampus, and in the pituitary gland. The D2 dopamine receptor is suggested to be the predominant type of autoreceptors that is involved into synthesis and release of dopamine. It is also worth noting that there are two different receptor isoforms: DRD2Sh (short) and DRD2Lh (long). They are reported to have different neuronal distribution, DRD2Sh is predominantly synaptic, DSD2Lh – postsynaptic. [142] [143][144]

The Figure 57 represents the results of a molecular modelling study of DRD2 performed at caprotec, in the frames of the case study of sertindole-based CC. During this case study, also the area where CC attaches to the protein was suggested, it is ligand binding pocket shown on Figure 57 on the right side. [116]

It is widely recognized, that pharmacological targeting of dopamine receptors is an efficient approach to affect deficient functions in case of some pathological conditions. Numerous drugs against PD and schizophrenia have been developed based on this strategy. It is also well known that a classic problem of drug development is on one hand finding out which one is the most relevant target in terms of therapeutic efficacy; on other hand uncovering the pathways leading to side effects. In terms of preclinical drug investigations CCMS can shed a light on these questions. [142][145] [146]

3.2.3. Sertindole

Sertindole is a phenylindole derivative, which is classified as a second generation antipsychotic drug. It has high affinity to DRD2, to serotonin 5-HT2 and to α1-adrenergic receptors. [146] The structural formula of sertindole is demonstrated in Figure 58. The affinity of sertindole to the dopamine D2 receptor is in the low nano-molar range.

Sertindole is used as a treatment against schizophrenia since 1996; however, due to suspects that this medication can increase the risk of sudden death from arrhythmias, and can be a risk factor of cardiovascular adverse events it was restrained from the commercial sale. This antipsychotic drug was reported as the potent antagonist of the Human Cardiac Potassium channel. [147] Nowadays it is on market in many countries with the safety disclaimer.

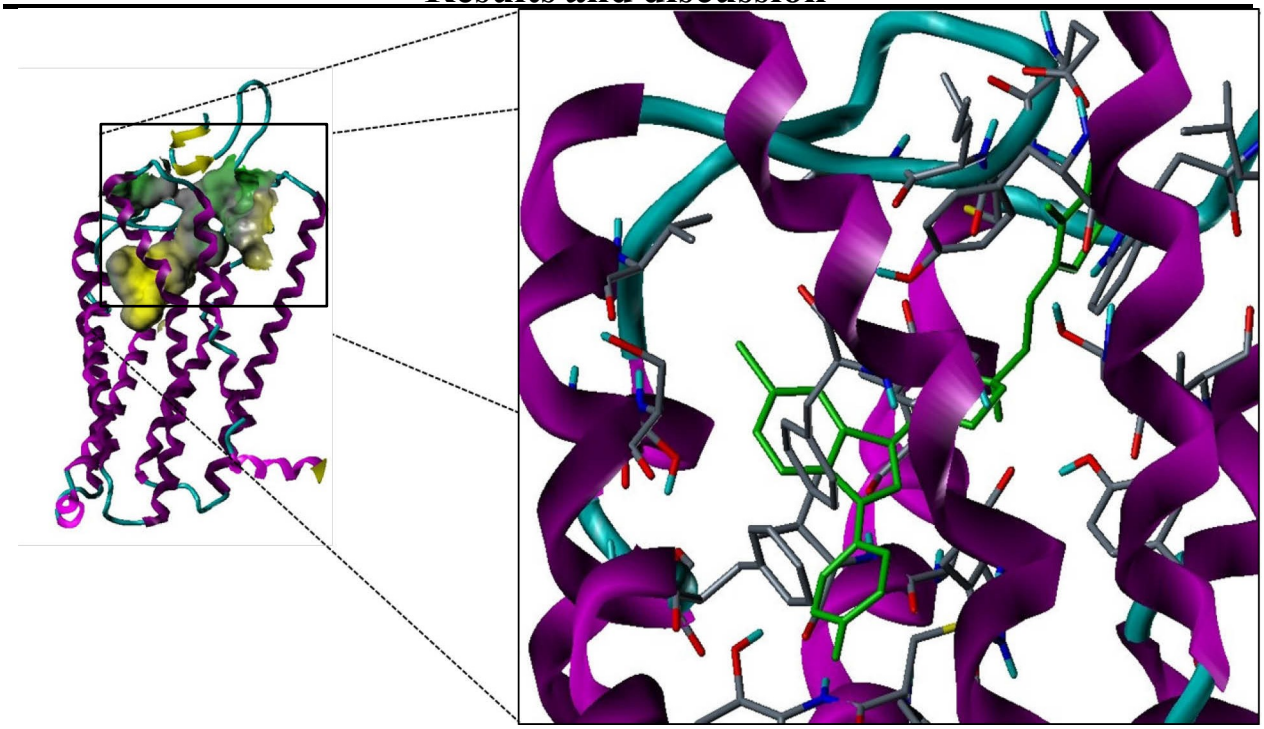

Figure 57. Molecular model of DRD2. On the right side the molecular pocket where CC attaches is shown.

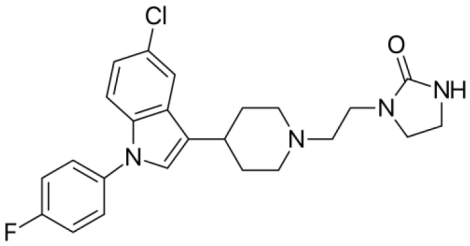

Figure 58. Structural formula of sertindole

3.2.4. Sertindole-based CC

After the successful completion of proof of concept stage, which was based on the investigation of interactions between SAH-based CC and the isolated enzyme M.TaqI, we aimed to perform a study of a more complex system – living cells. For the study addressing the living cell cultures the system sertindole-DRD2 was selected due to several reasons. First of all, as was mentioned previously, the sertindole-based CCs were already investigated in caprotec. [116] Secondly, addressing membrane receptors by chemical proteomics is a challenging but nevertheless an important task; this information might have the pharmacological relevance. The attachment of the selectivity moiety to the CC scaffold can lead to a significant drop of affinity of CC compared to unmodified drug molecule, due to the steric hindrance or other reasons. However, as was already reported [116], the sertindole-based CCs have a very high affinity to the target, in the same range as unmodified sertindole.

3.2.5. Transfection of cells with DRD2

For this experimental setup Human embryonic kidney 293 cell culture (HEK 293 or HEK cells) was selected for transfection with DRD2. HEK cells were originally

cultured from the kidney cells of a human embryo, they were transformed with sheared adenovirus DNA. HEK293 cells can be easily grown in culture and transfection kits are commercially available.

This cell line was selected for this experiment setup because the work on HEK293 was already done in caprotec. [116]

The stable transfection of the cells in culture with DRD2 cDNA was performed at caprotec, and reported already. [116] Of note, transfection with DRD2 led to a change of the adhesion properties of cells in a drastic way. A micrograph of transfected HEK cells is shown in Figure 59.

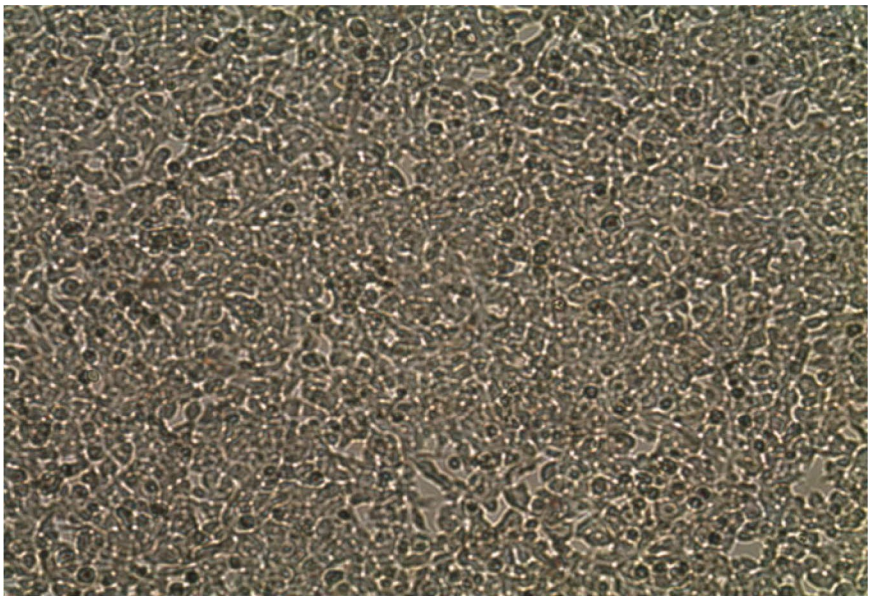

Figure 59. Micrograph of HEK293 cells transfected with DRD2 cDNA

3.2.6. Detection tags, synthesis and functionalization of CC

Similar to the strategy that had been used for the proof of concept experiment, for the experiments on the living cells the important task was to perform the comparison between the two detection moieties of the CCs: the metal tag, and the fluorescent tag.

The characterization of the capture experiment via imaging methods was to be performed for the first time. For this purpose, a sertindole CC functionalized with TAMRA was utilized. This CC had already been synthesized at caprotec, and the synthesis and purification of it were not done in the frames of this research project. The concentration of the CC was determined precisely based on the detection of the fluorophore.

Like in the case of the proof of concept experiments, the MeCAT moiety was decided to be attached to the CC via a click chemistry reaction. Due to this reason, there was a need in a similar reference CC, which carries the fluorophore tag. The CC was also functionalized with the fluorophore moiety via the same click chemistry reaction, to assure a reliable comparison between fluorescence and ICP-MS readouts. However, for this experiment setup, due to the availability of chemical compounds, the copper assisted azido-alkyne cycloaddition (CuAAC) was utilized as click chemistry.

3.2.6.1. *Fluorophore functionalized tag*

The detection moiety that carries fluorophore (TAMRA) and is functionalized with the azido group - CPT 381 was synthesized at caprotec, the structure of it is displayed in Figure 60. Neither the synthesis optimization, nor the purification were part of this dissertation project.

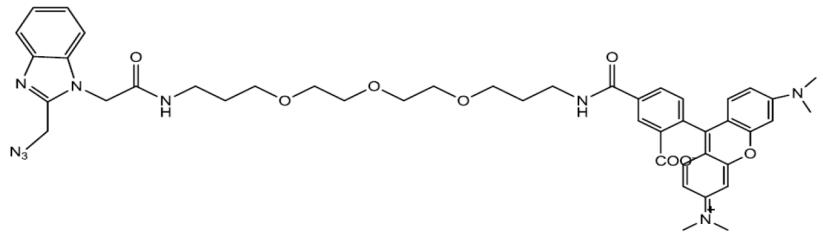

Figure 60. Structural formula of CPT-381

3.2.6.2.*Lanthanide functionalized tag*

For this experimental setup the DOTA chelate was functionalized with the azido moiety. For this part of studies, the additional synthesis to functionalize it with the azido group was not required, the DOTA with the attached suitable functional group was purchased commercially. To obtain the detection function that carries metal tag – MeCAT (DOTA -N_3-Tb) shown in Figure 61, the lanthanide was introduced inside the DOTA ring. The metalation of DOTA-N_3 was done based on a standard protocol, developed in a working group of Prof. Linscheid without any additional optimization. Terbium was selected among the other lanthanides since it is monoisotopic element, what simplifies the quantification task. As discussed previously, the obtained MeCAT does not demonstrate any fluorescence properties.

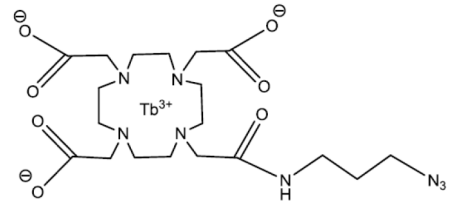

Figure 61. Structural formula of MeCAT

3.2.6.3. *Establishing and optimizing click chemistry reaction for sertindole-based CCs. Copper assisted azido-alkyne cycloaddition (CuAAC)*

Attachment of TAMRA

The main reason for the optimization of the reaction conditions for the attachment via the click chemistry approach, is that the concentrations determination based on the weight of the purified compound is not precise enough. In contrast, the concentration of the compounds, that carry the fluorophore, can be determined in an accurate way. Based on this, the optimization of the concentration of the CC, which carries the alkyne group was done. It is worth noting that no external copper-chelating ligand was required, since it was already included in the structure of the fluorescent detection function (CPT-381). This internal ligand has been reported as the one, that significantly improves the reaction kinetics because of its ability to promote the catalytic impact of

copper (I) [132]. The structure of the click reaction product is shown in Figure 62.

The results of the optimization of the click chemistry reaction are shown in Figure 63. With this experiment only the concentration of the CC functionalized with the alkyne group (CPT-549) was adjusted. As is illustrated by Figure 63, the highest reaction yield was obtained when the excess of the CC to the detection function was equal to 2,5. The full conversion of the CC that carries the sertindole selectivity function is crucial for this reaction. Any CC, which is photo crosslinked to a target but does not carry the moiety which enables the readout cannot be detected but could act as a competitor for the fully converted CC that carries the detection function, compromising the experiment. In contrast, the presence of a mild excess of unattached detection function, can only cause a background interferences, which can be monitored and controlled.

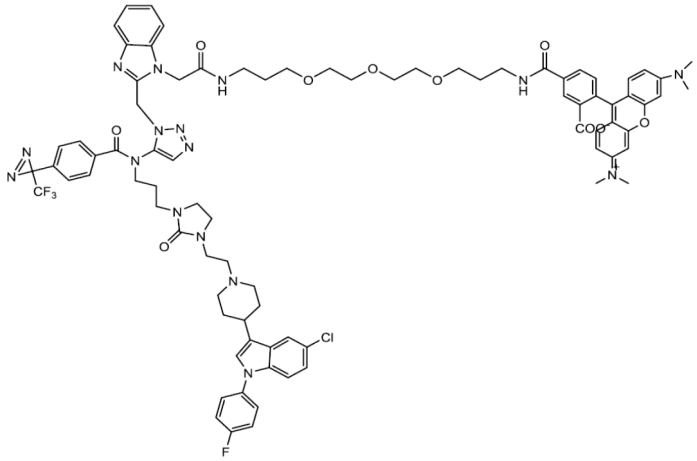

Figure 62. The product of click reaction. CPT 549-381

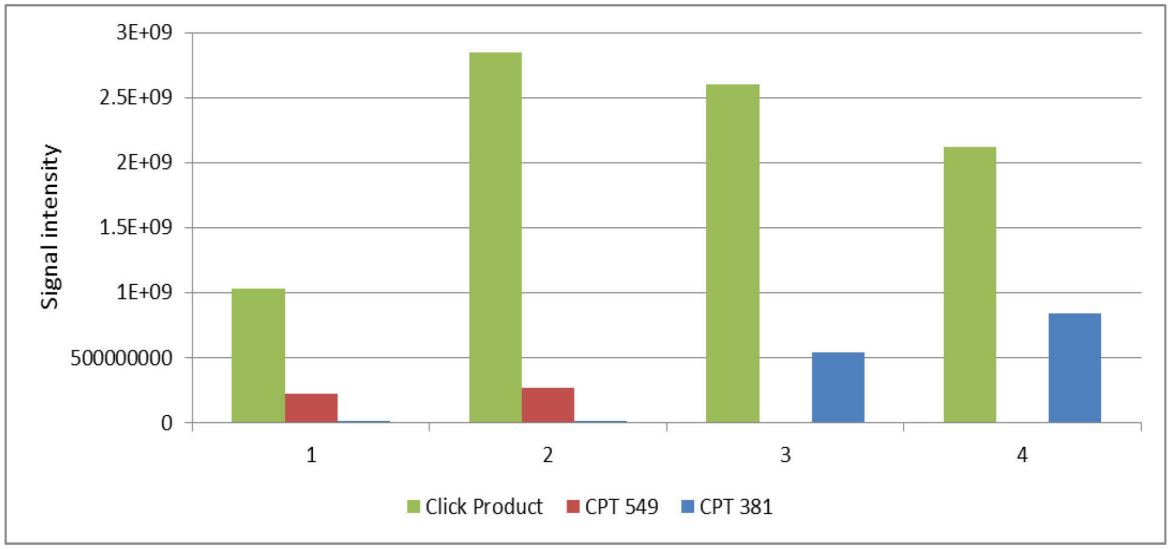

Figure 63. Optimization of click reaction conditions. 1 – 2 fold excess of CPT 549; 2 – 2,5 fold excess of CPT 549; 3 – 3 fold excess of CPT 549; 4 – 3,5 fold excess of CPT 549.

Attachment of MeCAT

The product of the inserting of the lanthanide inside the DOTA ring was not additionally purified. The calculations of the concentration of the obtained MeCAT were

based on the weight of the reaction product. Since the concentration of alkyne functionalized CC (CPT 549) was already evaluated, the further adjustments of the concentration of the metal tag were based on the established concentration of the CC. Since the MeCAT was for the first time attached to the CC via the copper promoted click reaction, several additional controls such as sample containing only MeCAT, sample containing mixture of MeCAT and sodium ascorbate, sample containing MeCAT in presence of sodium ascorbate and copper chelating ligand, and the reaction mixture with exclusion of MeCAT were done. Moreover, since the metal tag does include any internal copper chelating ligand, the external ligand was utilized to improve the reaction kinetics. The product of the click reaction is demonstrated in the Figure 64.

The results of the optimization of the click chemistry reaction conditions are illustrated with Figure 65. As is seen from the graph, the highest conversion yield was obtained when the excess of MeCAT was equal to 1,5. Further increase of its concentration did not affect the efficiency of the conversion. With the additional control it was established that the presence of the reducing and chelating agent did not interfere with the signal intensity of the MeCAT.

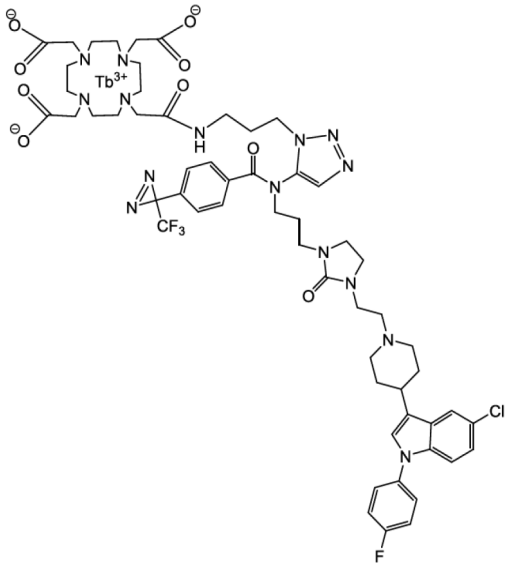

Figure 64. The product of click reaction. CPT 549-MeCAT

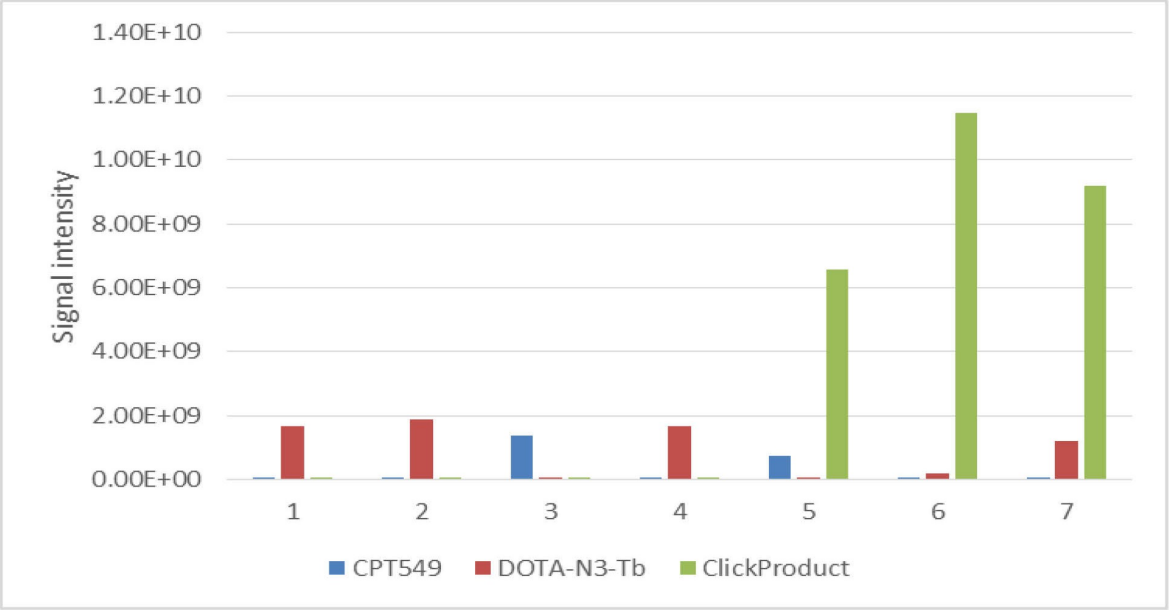

Figure. 65 Optimization of click reaction conditions. 1 – Control with DOTA-N_3-Tb only; 2 – Control with DOTA-N_3-Tb with the addition of sodium ascorbate; 3 – Control for the reaction mixture (CPT549, sodium ascorbate, copper sulfate and the external copper chelating ligand) without DOTA-N_3-Tb; 4 – Control with DOTA-N_3-Tb with the addition of sodium ascorbate and external copper chelating ligand; 5
– reaction mixture, 1 fold excess of DOTA-N_3-Tb; 6 – reaction mixture 1,5 fold excess of DOTA-N_3-Tb; 7 – reaction mixture 2 fold excess of DOTA-N_3-Tb.

3.2.7. Characterization of the capture experiment on the living cells

3.2.7.1. Cells grown on the glass slide: fluorescence microscopy detection

The system sertindole-DRD2 for target identification has already been studied and characterized with the CCMS approach by caprotec. [116] The application of the capture experiment to the imaging approach has not been performed yet, and, therefore, was one of the main challenges of this research project. Fluorescence microscopy was selected for the initial characterization of the system, because of the high sensitivity, high resolution and the availability of the fluorophore functionalized CC.

In the frames of this work capture experiment was defined with the fluorescence microscopy for the first time. For the initial depiction with the fluorescence microscopy it was crucial to exclude the possible side interferences. To provide this condition, the CC that was synthesized as a whole one (CPT-501) was selected, since it is a robust, well studied compound with the established concentration. The structure of CPT-501 is shown in Figure 66. To prepare the samples for the fluorescence microscopy detection, the transfected with DRD2 HEK cells were grown directly on the slide, treated with the CC, optionally irradiated and processed further by washing and fixation with PFA.

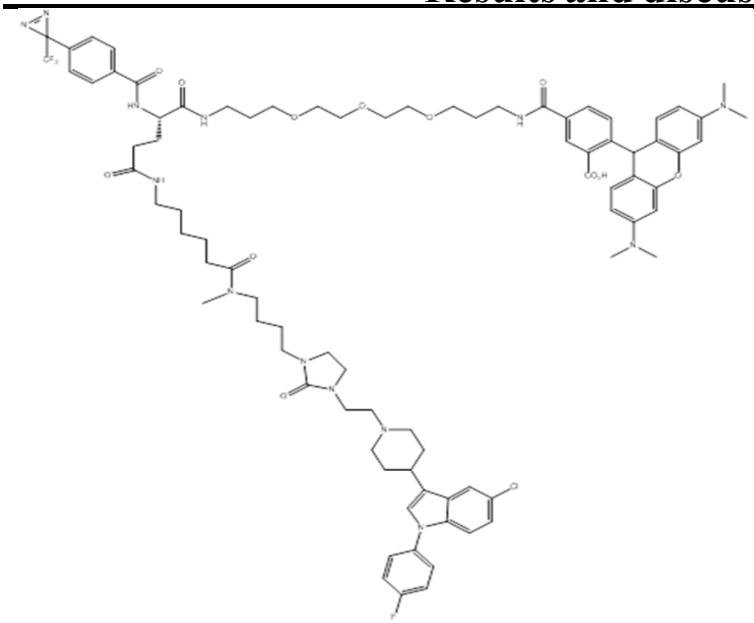

Figure 66. Structure of CPT-501

For this experiment setup cells were cultured directly in removable chambers mounted on a glass slide. The slide had been covered with polylysine. The picture of the glass slide, used in this experimental setup for fluorescent readout and in further experiments for fluorescence and LA- ICP-MS detection is shown in Figure 67.

Figure 67. The glass slide with removable chambers.

As was mentioned previously, the transfection of HEK cells with the Dopamine D2 receptor changed the cells adhesion to the polylysine coated surface in a drastic way; cells were easily detached after the simple rinsing. Due to this reason, the protocol of the cell treatment had to leave out the washing steps before the fixation by PFA. In the case the washing step was included, cells were simply "floating" in the culturing chamber, and almost all of them were lost for analysis. Because of this, after the capture experiment on the living cells, they were crosslinked to the polylysine coating of the culture wells with PFA, without the washing step and afterwards mounted with the coverslips. The results of the fluorescence microscopy readout are demonstrated on the Figure 68.

As is seen from the images demonstrated in Figure 68, the highest fluorescence signal was observed for the irradiated assay (1); however, the detected outcome from the non-irradiated assay (4), and all the competition control samples (2,5) were also relatively intense. Only in case of the control with no CC added (3,6), no signal was observed. Comparing irradiated assay with irradiated competition, or non-irradiated

assay with non-irradiated competition, the selectivity of the labeling DRD2 by the CC is already evident because the fluorescence intensities in the competition control samples are much lower than in the assay samples. Another important observation was, however, that the detected signal intensity was not distributed equally over the cell.

It is known that the target protein DRD2 is a membrane receptor [142]; moreover, the size of CPT-501 should not allow it to penetrate inside the cell. Therefore, it was foreseen to detect the highest localization of the signal on the cell surface. These expectations have been met for the irradiated assay samples (1), where the cell borders are outlined most intensively and the fluorescence signal is condensed in majority on the cell surface. For the non-irradiated assay (4) and the competition control samples (2,5), the residual signal was detected. However, the signal intensity was noticeably lower; and the observed signal can be attributed to CC that were non- covalently bound to DRD2.

With the results of this experiment it was confirmed, that the sertindole-based CC attaches to the surface of the transfected cell. Based on the difference between signal from assay (1,4) and competition control samples (2,5) and the non-irradiated assay (4), the specificity of the photo- induced covalent crosslinking was demonstrated; however, the specificity was not as high as anticipated.

In addition, the observed number of cells appears to be abundant for such experimental setup, especially due to their tendency to aggregate into the layers. This complicates the focusing and the detection in general, especially for the intended MeCAT readout via ICP-MS planned for further experiments. Therefore the further experiment the reduction of the number of cells was considered.

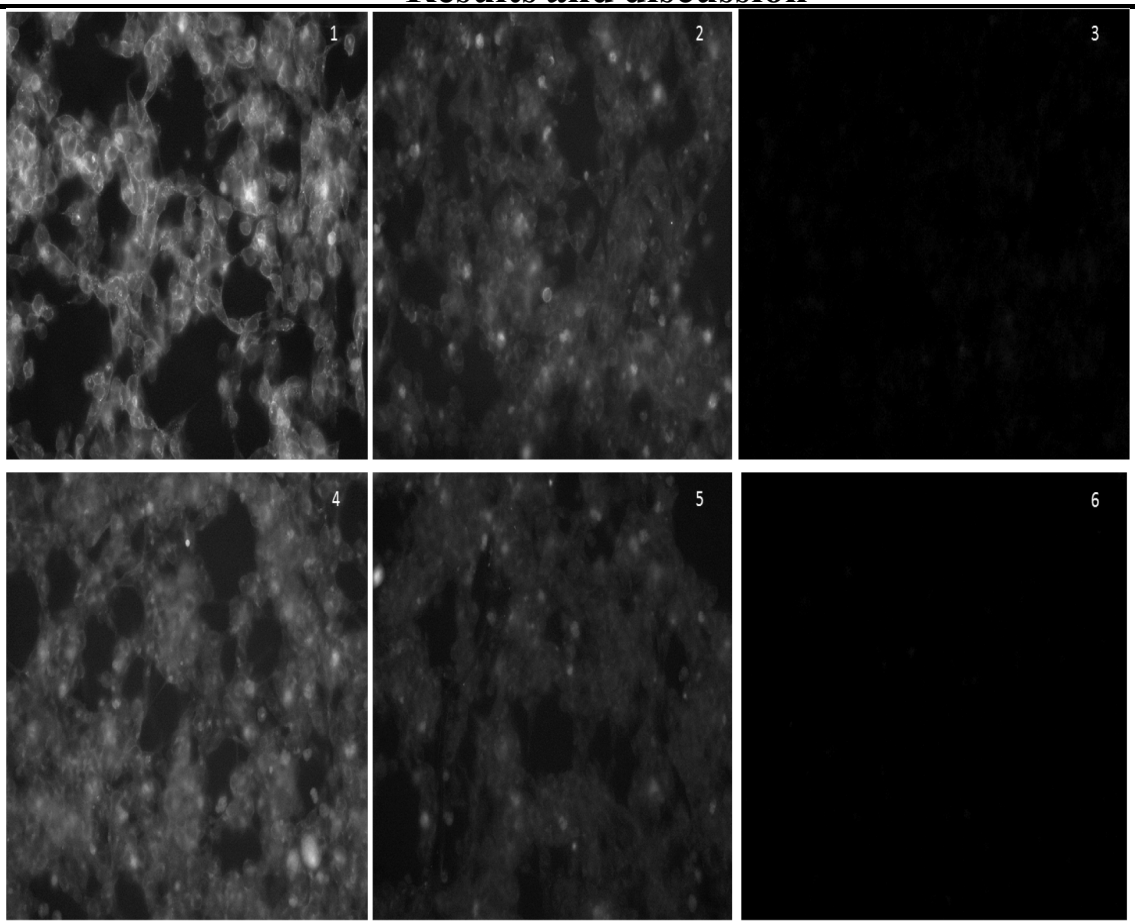

Figure 68. Fluorescence microscopy images, cy3, 40x objective immersion oil. Cells grown on the slide. Final concentration of CC (CPT-501) 50 nM 1 irradiated assay; 2 irradiated competition control; 3 irradiated control that contains no CC; 4. Non-irradiated assay; 5 non-irradiated competition control; 6 non-irradiated control that contains no CC.

3.2.7.2. Resuspended cells: fluorescence microscopy, WB immunoassay and isolation followed with the MS/MS analysis

For the cells grown on the glass slide, according to the procedure used for the first experiment, the fluorescence microscopy detection method was compromised by several factors, especially the exclusion of the washing step and the big number of cells aggregated in the multiple layers. In order to achieve the conditions, which enable the washing step after the crosslink of CC to the target; the protocol of the sample preparation via the resuspension of cells after was developed. The main idea of this approach was to enable substantial washing conditions so that only those CC, which are covalently attached to the target are remained; another challenge was to control the amount of cells that are transferred to the slide.

For this experiment setup cells were grown in six well culture dishes, and proceeded with the usual capture experiment protocol. After the photo crosslink, cells were harvested and resuspended several times under the physiological conditions. This treatment influenced the size and shape of cells; however, the cells integrities remained intact. An aliquot of resuspended cells was transferred to the glass slide with removable chambers as was used in previous experiment; the settled cells were crosslinked to the

polylysine coating of the slide with PFA, followed with the mounting of coverslips.

The results of the fluorescence microscopy detection are shown in Figure 69. With this sample preparation approach, the signal with a high intensity was observed only for the irradiated assay samples (1). The drastic difference of the fluorescence readout intensities between the cells grown on the glass slide and the resuspended cells can be explained with the washing of cells under the stringent conditions in the second case. Based on this result, we can conclude that only those tags, which were covalently attached to the target protein were detected in the case of the sample preparation via the resuspension protocol. Moreover, in comparison with the results obtained for the cells grown and treated in the 8 well slide dish, the average intensity of the signal was lower. The explanation for this observation is that with the previous experiment setup the detected signal consisted of two components: the signal of the CCs, which were covalently crosslinked to the target protein and the CCs which were attached to the target in a non-covalent way, with only selectivity function involved in binding. The reason for that a fraction of CCs bound to the target protein via the selectivity function, but did not crosslink covalently upon UV irradiation, is that the cross-link yield is never 100%, but considerably lower, similarly to the cross-link yield described above for the experiments on M.TaqI.

With this experiment setup it was demonstrated, that the binding of the sertindole-based CC to the cell membrane was not only specific, but also due to covalent cross-link of the CC to its target, because no significant fluorescence signal was detected in the competition control samples nor at all in the non-irradiated samples (2-5). Moreover, the signal was distributed exclusively on the cell surface.

Fluorescence microscopy was successfully utilized for the characterization of the signal distribution across the cell. The information describing and visualizing the localization of the CC binding to the living cell was of the great importance. However, it was still necessary to confirm the identity of the protein that was covalently crosslinked to the CC. In order to find out if the CC was attached to the protein of interest, DRD2, additional experiments were performed. The first reference method of choice was an anti-fluorophore western blot immunoassay. The results of the enhanced chemoluminescence (ECL) readout are demonstrated on the Figure 70. As is shown in Figure 70, a single fluorescence signal was detected in the samples corresponding to the irradiated assay (lanes 1,2), in case of irradiated competition control samples (lanes 3,4) the fluorescence signal was also observed; however, the signal intensity was noticeably lower. At the same time Ponceau staining confirmed the similar amounts of protein had been loaded to each gel lane. This observation showed that predominantly as single protein was labeled by the CC, and this gave rise to the fluorescence signal detected by fluorescence microscopy readout above. Moreover, the fluorescence signal that was detected was in the molecular weight range expected for glycosylated DRD2.

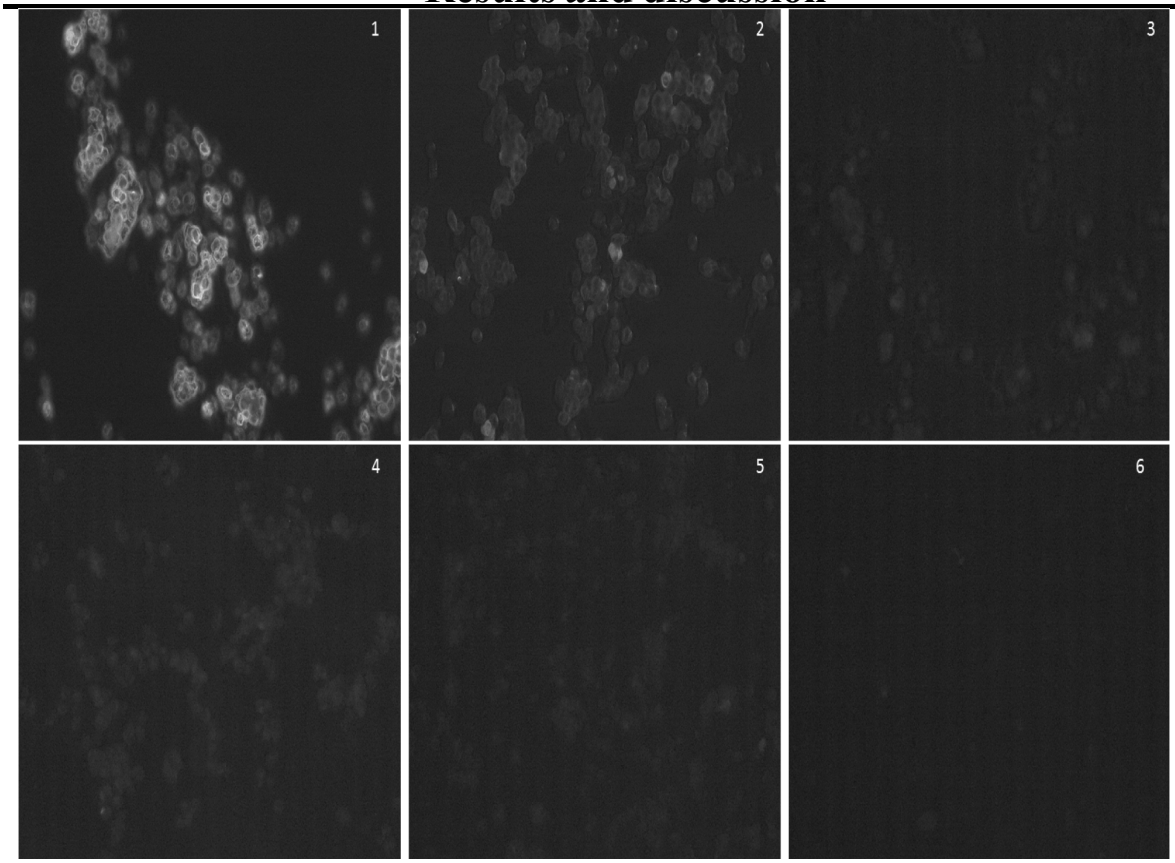

Figure 69. Fluorescence microscopy images, cy3, 40x objective immersion oil. Resuspended cells. final concentration of CC (CPT-501) 50 nM 1 Irradiated assay, 2 irradiated competition control, 3 irradiated control that contains no CC, 4. Non-irradiated assay, 5 non-irradiated competition control, 6 non- irradiated control that contains no CC.

The second task was to determine to which protein the CC was covalently attached. To perform this, the CC treated and pelleted cells were solubilized and exposed to the magnetic beads functionalized with the anti-fluorophore antibody to isolate CC-protein conjugates. Proteins on the beads were trypsinized, and the resulting peptides subjected to nano-LC-MS/MS analysis and relative quantification with MaxQuant. DRD2 was the outstanding specifically captured protein in these samples. The distribution of the signal intensity for DRD2 across the samples is shown in Figure 71. The highest signal intensity was detected from the irradiated assay samples (1, 2), significantly lower intensity was detected in the irradiated competition controls (3, 4). For the rest of samples the signal was at the level of the background. These results confirmed the fact that the sertindole-based CC was covalently crosslinked to the DRD2, the pattern of the photo- induced crosslink was consistent to the one observed with the ECL readout of the WB immunoassay and the fluorescence microscopy.

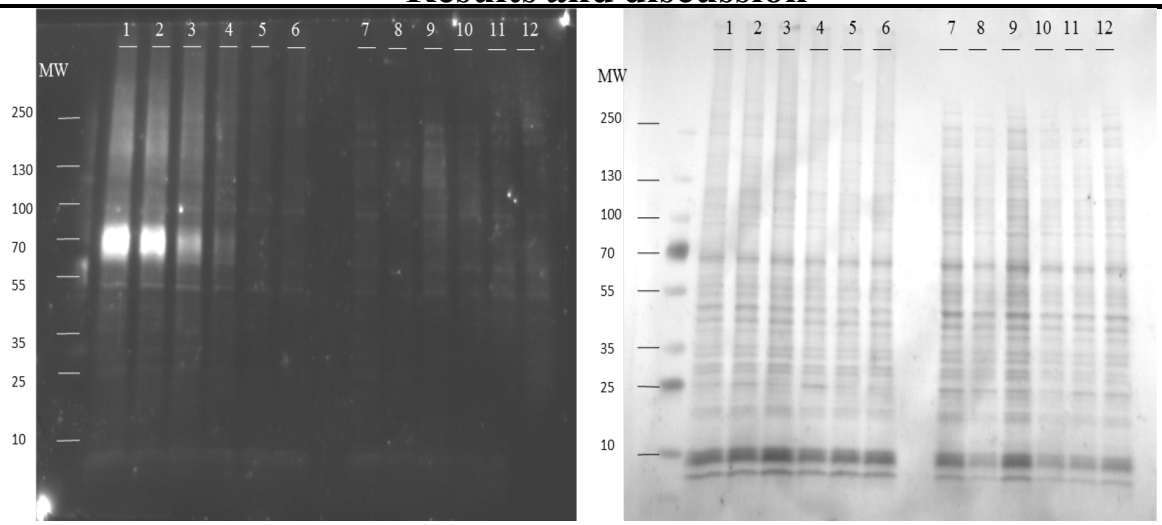

Figure 70. Anti TAMRA WB and Ponceau staining 1,2 – irradiated assay; 3,4 – irradiated competition control; 5,6 – irradiated control that contains no CC; 7,8 – non-irradiated assay; 9,10 – non-irradiated competition control; 11,12 – non-irradiated control that contains no CC.

In summary, the capture experiment on the HEK cells transfected with DRD2 was characterized with the imaging approach, which defined the spatial distribution of the signal over the cell. Moreover, with the ECL readout of the WB immunoassay experiment outcome, it was confirmed that only one protein was crosslinked by the CC. The results of the isolation experiment followed by the nano-LC-MS/MS detection and relative quantification, proved that was DRD2 that was covalently attached to the sertindole-based CC. In addition to this, with the new sample preparation approach the specificity of the photo induced crosslink was clearly demonstrated. With the utilization of the sertindole-based CC functionalized with the fluorophore (CPT-501) the selective and specific addressing of the target protein (DRD2) was proven to be successful.

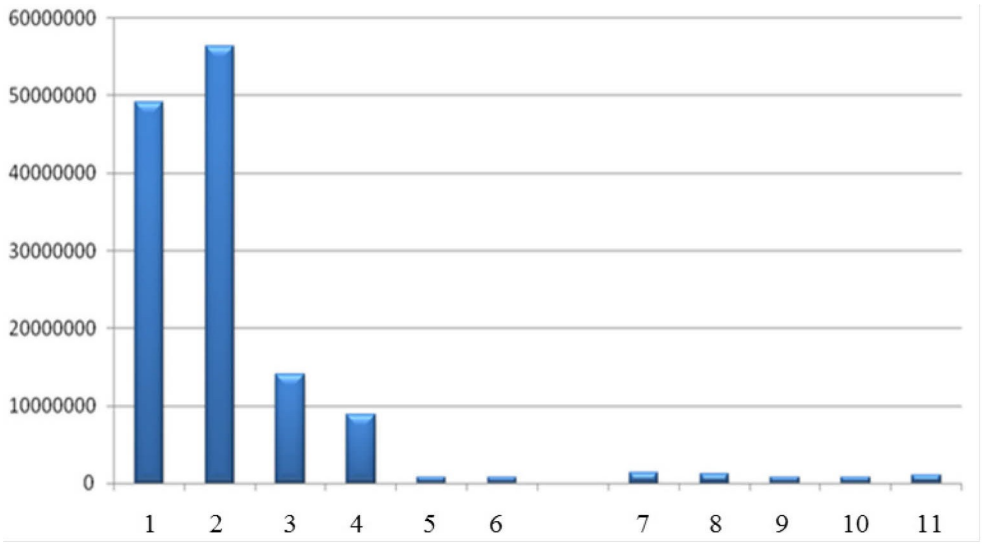

Figure 71. Relative quantification with MaxQuant. Signal intensities of Dopamin D2 receptor as determined by nano-LC-MS/MS. 1,2 – irradiated assay; 3,4 – irradiated competition control; 5,6 – irradiated control that contains no CC; 7,8 – non-irradiated assay; 9,10 – non-irradiated competition control; 11 – non-irradiated control that contains no CC.

3.2.8. Capture experiment with the pre-clicked CC

3.2.8.1. Establishing the concentration

After the successful targeting of dopamine D2 receptor with the fluorescent sertindole-based CC, which was synthesized as a whole one (CPT-501); another CC, functionalized with the detection function via the click chemistry approach, was tested. However, with the first trials when the concentration was equal to the one, which was used in the experiments with CPT-501, no signal was detected neither with the fluorescence microscopy, nor with the ICP-MS.

The determination of the concentration of the CPT-501 was done at caprotec based on the detection of the concentration of the fluorescent group. In the case when the CC was functionalized with the alkyne and did not have the fluorescent properties, this task was more challenging. The concentration was evaluated based on the weight of the purified compound, this evaluation of the concentration was done in caprotec. During the optimization of the click reaction conditions, the estimation of the concentration of alkyne functionalized CC (CPT 549) was performed. However, based on the outcome of the first trial with this CC structure, it was decided to do a capture experiment with a dilution series to evaluate the concentration of the CC that could allow the successful detection and the reasonable sensitivity.

The transfected HEK cells were treated with different concentrations of the sertindole-based CC functionalized with TAMRA via the click chemistry reaction. After the irradiation the cells were proceeded with the resuspension protocol. As the detection method the ECL readout of the anti- fluorophore WB immunoassay was selected. The results are shown in Figure 33.

With the previous experimental setup the final concentration of CC (CPT-501) was 50nM, which was sufficient to achieve the good sensitivity. The concentration of the CC (CPT-549-381), obtained via the click chemistry reaction, estimated as 50nM corresponds to first two lanes of the ECL readout. As is seen from the Figure 72, no signal from the samples treated with the CC of this concentration was detected. The concentration of the CC (CPT-549-381), evaluated as 100 nM, was at the LOD range. Based on the data shown in the Figure 72, the concentration of CC (CPT-549-381) estimated as 250 nM provided the necessary signal intensity for the detection in the anti-fluorophore western blot. Moreover, the competition control samples, which were treated with the CC of the 500nM concentration, demonstrated the lower signal intensity than that of samples, which were treated with the CC with the estimated concentrations of 250 nM and 500 nM. Based on this I concluded that in case of the utilization of the high concentrations of CCs, the specificity of the covalent crosslinking should remain in the similar range.

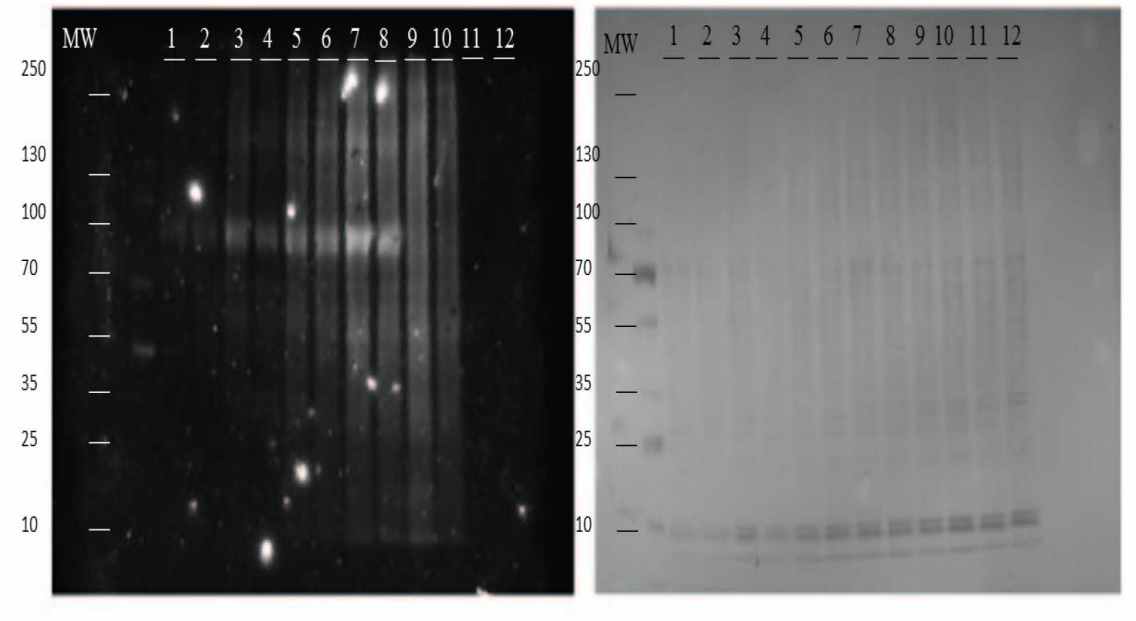

Figure 72. Anti TAMRA WB and Ponceau staining 1,2 – irradiated assay, final concentration of CC 50 nM; 3,4 – irradiated assay, final concentration of CC 100 nM; 5,6 – irradiated assay, final concentration of CC 250 nM; 7,8 – irradiated assay, final concentration of CC 500 nM; 9,10 –irradiated competition control, final concentration of CC 500 nM, concentration of competitor 1 uM; 11,12 –irradiated control that contains no CC.

With this experiment it was established that to provide the successful detection a higher concentration of the CC was required. This can be caused by the difference in structure. The linker of the CC, for CPT-501 (synthesized as a whole one) is longer in comparison with the one, which belongs to the CC functionalized with the alkyne group (CPT-549). This difference might influence the affinity of the CC to the target and the crosslinking ability of the compound. Another possible reason is that during the optimization of the conditions for the click chemistry reaction, the concentration of the alkyne functionalized CC was not calculated with appropriate precision.

3.2.8.2. Capture experiment followed with ICP-MS and fluorescence detection

With the previous experiment the working concentration of the CC, which was functionalized with the detection function via the click chemistry reaction, was established. After the determination of the LOD for the fluorescent detection, the first trials of LA-ICP-MS imaging of resuspended cells were performed.

Based on the results obtained from the proof of concept experiments on the isolated purified protein M.TaqI, the sensitivity provided by the fluorescence detection was expected to be higher than that provided by the ICP-MS readout.

To establish the LOD of the LA-ICP-MS imaging, the samples were treated with the lanthanide functionalized CCs at two different concentrations. The first one (250 nM) was established during the previous experiment as the one that allows the needed sensitivity for the ECL readout of WB immunoassay. The second concentration of

metal functionalized CC was two times smaller than the first one.

To provide the comparison with the reference method (fluorescence microscopy) the CC functionalized with the fluorophore was utilized, the concentration of it was equal to the highest concentration of the utilized MeCAT functionalized CC (250nM).

In the frames of this experiment no irradiation control was performed.

The main target of this experiment was to evaluate the LOD for the detection of the outcome of the capture experiment with the LA-ICP-MS, and to estimate the achievable resolution. To attain this, 3 different laser spot sizes were tested on the samples with the two different final concentrations of the MeCAT label. The initial purpose of the LA-ICP-MS imaging of cells in terms of this project, was to detect the distribution of the signal across the cell, similar to fluorescence microscopy. In case if sensitivity of the method would be high enough, it was planned to use the approach to ablate a single cell per laser shot and to estimate a signal value per cell.

For this experiment all the graphs, that were obtained by the LA-ICP-MS detection and showed the distribution of the signal of Tb across the ablated areas, were set to the maximal signal value of 250. This was done to simplify a visual comparison of the outcome with the utilization of different concentrations and laser spot sizes. All the areas on the images that are colored with the white color correspond to the signal intensity values higher than the established maximal signal intensity. Since no internal standard was utilized, the absolute quantification of via LA-ICP-MS was not possible.

The first laser spot size to be tested was of the size of 20um, which is approximately twice larger than the size of the transfected cell. The results of the LA-ICP-MS imaging of the cells with this laser spot size are demonstrated on the Figure 73 (final concentration of CC 125 nM) and the Figure 74 (final concentration of CC 250 nM). As is clearly seen from the figures, no signal was detected for any of the concentrations, the intensities of all the obtained signals were at the level of the background. Based on these results, it was concluded that the sensitivity of this method would not allow to achieve the resolution that was initially planned.

After it was established that the laser spot size of 20um cannot provide the detection with the required sensitivity, the laser spot size of 55 um was tested. The results are shown in Figure 75 (final concentration of CC 125 nM) and Figure 76 (final concentration of CC 250 nM). With the resolution provided by this laser spot size, a signal for both concentrations was detected; however, the difference between the control without CC, competition control and the assay samples was not as high as expected because of the low signal intensity in general. The low signal to noise ratio could lead to the misinterpretation of the obtained results. Because of this, the given resolution also had to be compromised to an even lower one.

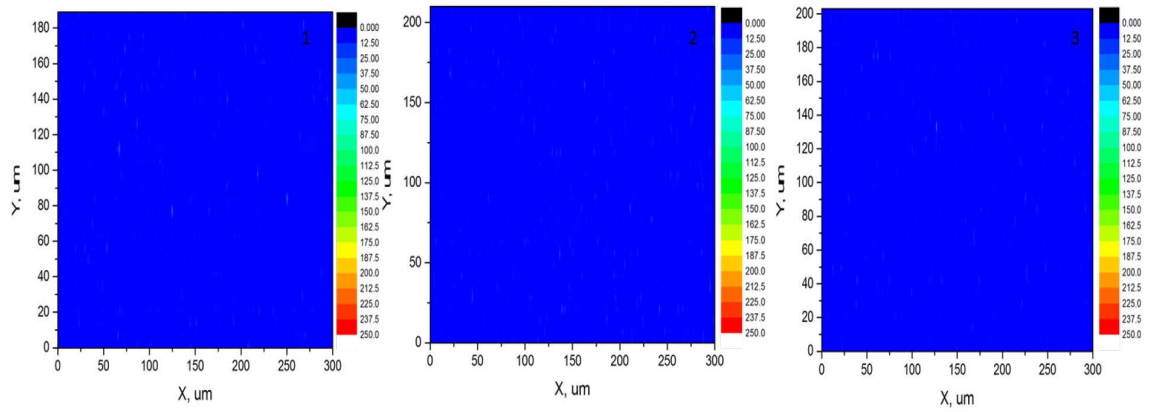

Figure 73. LA-ICP-MS imaging of terbium content, spot size 20um, laser energy 60%. Resuspended cells. Final concentration of CC 125 nM. 1 Irradiated assay, 2 irradiated competition control, 3 irradiated control that contains no CC.

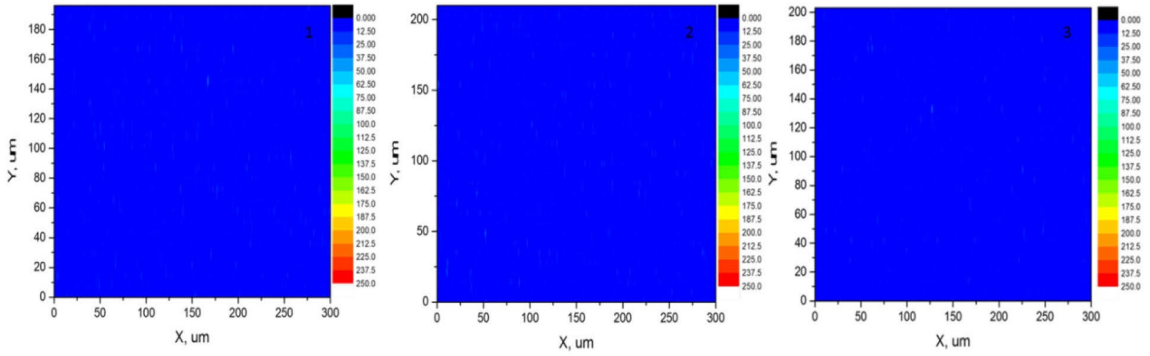

Figure 74. LA-ICP-MS imaging of terbium content, spot size 20um, laser energy 60%. Resuspended cells. Final concentration of CC 250 nM. 1 Irradiated assay, 2 irradiated competition control, 3 irradiated control that contains no CC.

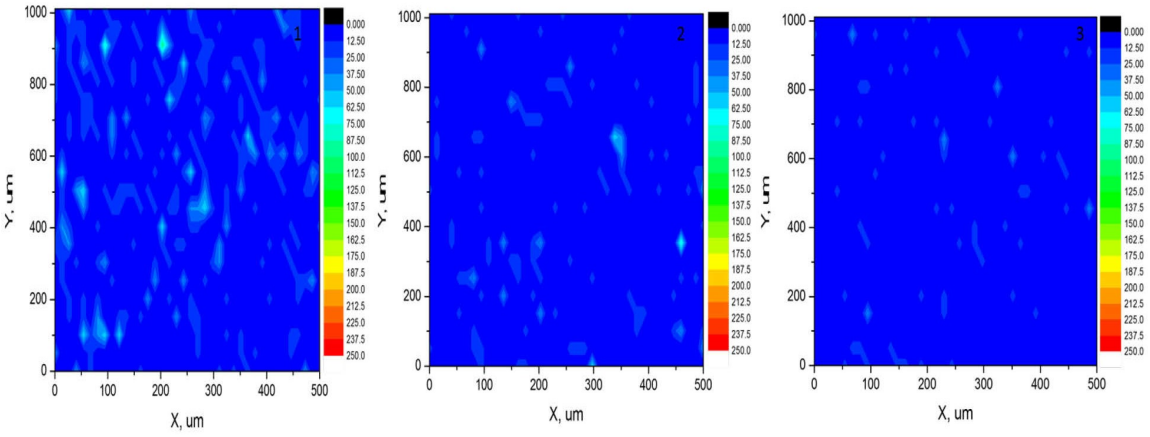

Figure 75. LA-ICP-MS imaging of terbium content, spot size 55um, laser energy 60%. Resuspended cells. Final concentration of CC 125 nM. 1 Irradiated assay, 2 irradiated competition control, 3 irradiated control that contains no CC.

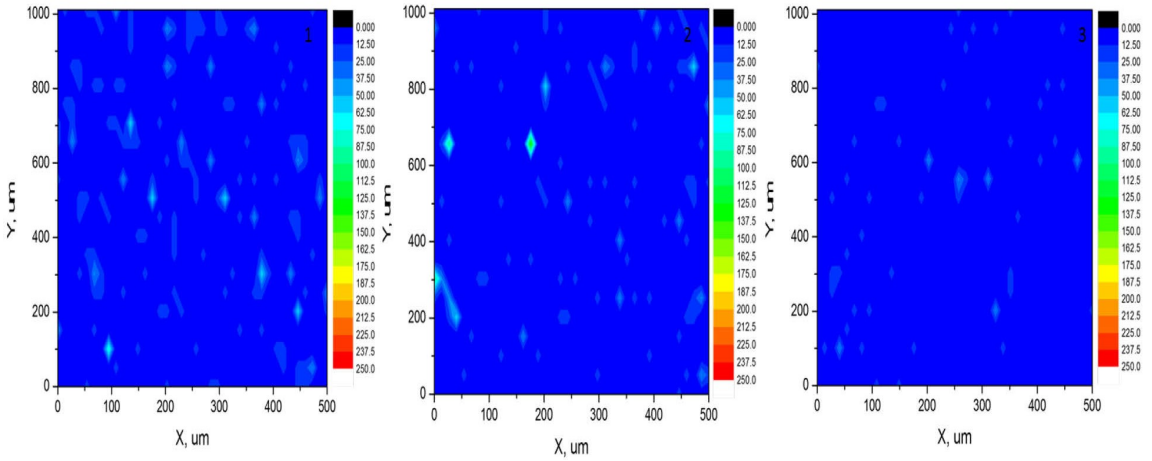

Figure 76. LA-ICP-MS imaging of terbium content, spot size 55um, laser energy 60%. Resuspended cells. Final concentration of CC 250 nM. 1 Irradiated assay, 2 irradiated competition control, 3 irradiated control that contains no CC.

The last laser spot size of 100um was tested. The results of LA-ICP-MS detection are shown in the Figure 77 (final concentration of CC 125 nM) and Figure 78 (final concentration of CC 250nM). As is demonstrated in the figures, in the case of the both concentrations the dynamic range was significantly higher in comparison with the results obtained with the spot size of 55 um. With this resolution only the signal detected from the control, which contains no CC sample was at the level of the background. However, based on signal intensities detected from the assay and competition control samples the conclusion about the specificity of the capture experiment cannot be done.

Because of the high signal to noise ratio obtained with the laser spot size of 100 um, it was decided to utilize it in the consecutive experiments.

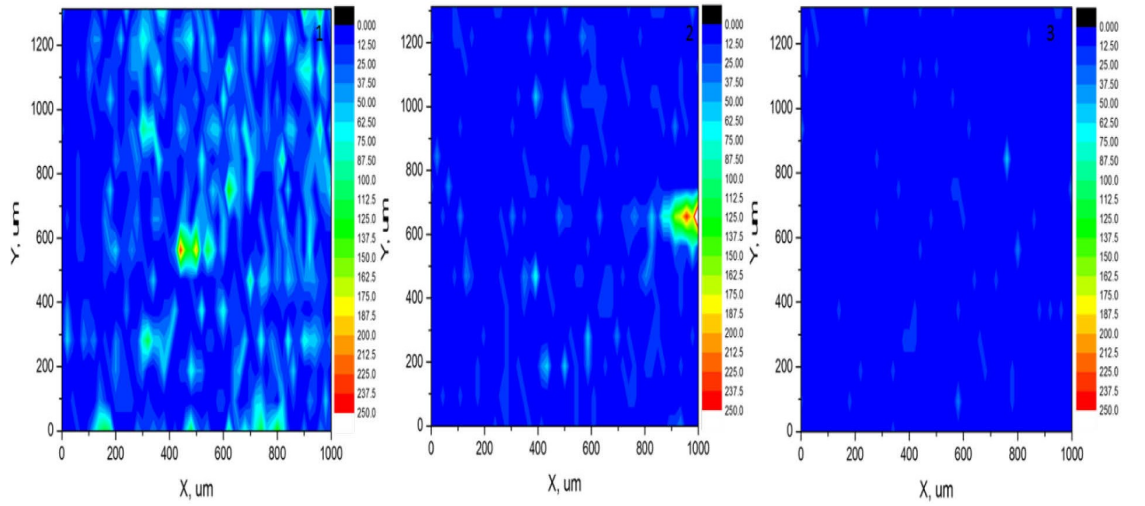

Figure 77. LA-ICP-MS imaging of terbium content, spot size 100um, laser energy 60%. Resuspended cells. .Final concentration of CC 125 nM. 1 Irradiated assay, 2 irradiated competition control, 3 irradiated control that contains no CC.

The results of the detection via the reference method – fluorescence microscopy are shown in the Figure 79.With the fluorescent microscopy some artefacts were detected both in the assay and competition control samples, most probably these artefacts are caused

by the collapsed cells, which could intake the CC inside. The concentration of the fluorophore functionalized CC was equal to the highest concentration of MeCAT functionalized CC (250nM). Overall, in case of the irradiated assay the cell membranes were far better defined, this observation confirmed the specificity of the photo crosslink.

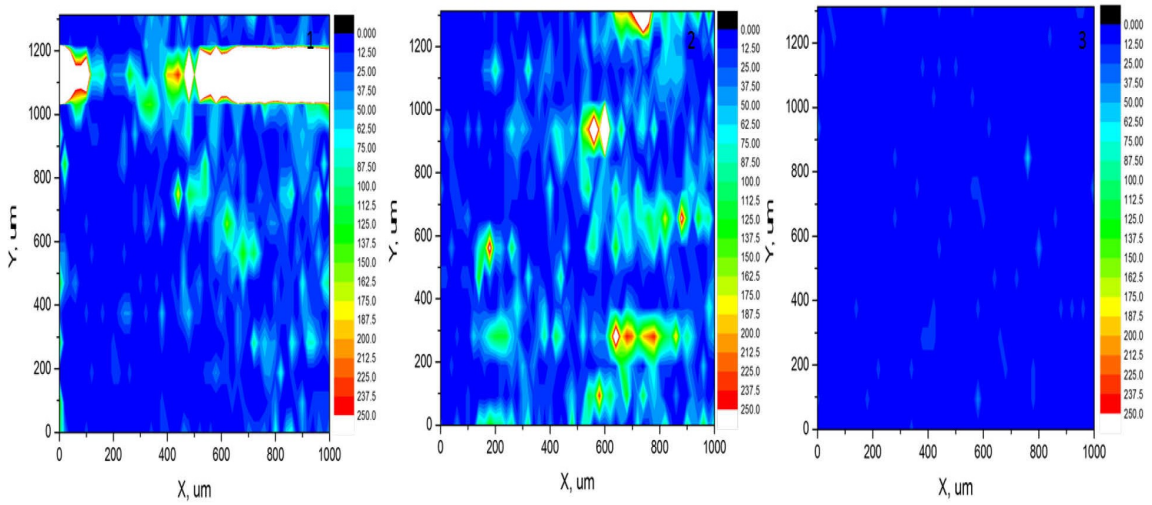

Figure 78. LA-ICP-MS imaging of terbium content, spot size 100um, laser energy 60%. Resuspended cells. Final concentration of CC 250 nM. 1 Irradiated assay, 2 irradiated competition control, 3 irradiated control that contains no CC.

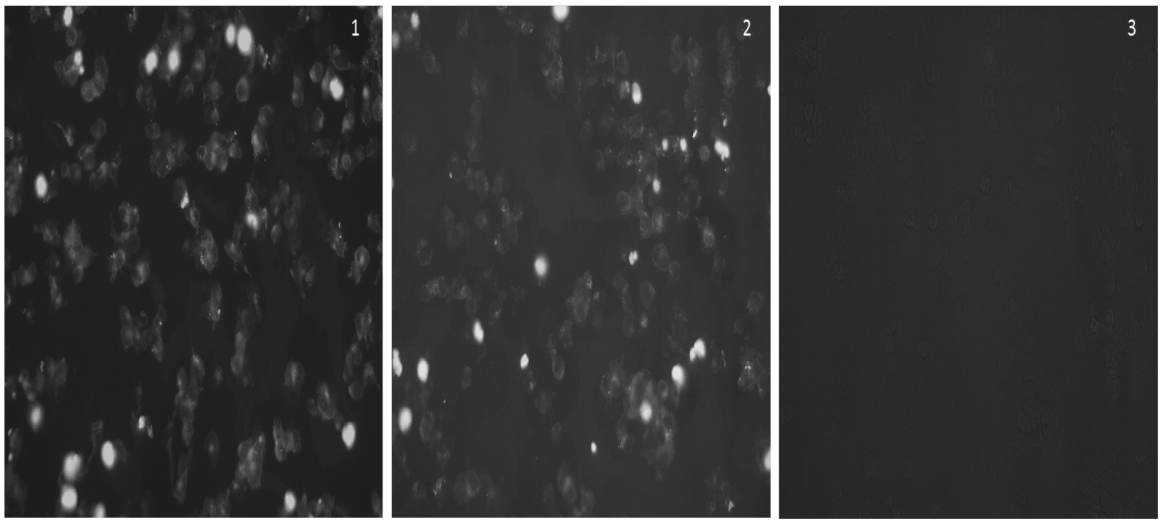

Figure 79. Fluorescence microscopy images, cy3, 40x objective immersion oil. Resuspended cells. Final concentration of CC 250 nM. 1 Irradiated assay, 2 irradiated competition control, 3 irradiated control that contains no CC.

With the LA-ICP-MS detection with the utilized laser spot size of 100um, the specificity of the photo crosslink was not demonstrated. The possible explanation for this could be the artefacts, which were observed with the fluorescence microscopy; they could cause the high signal detected from the competition control samples.

To complete the obtained results with the quantitative data, the remaining number of resuspended cells from the experiment were pelleted, mineralized and proceeded with the

direct injection ICP-MS detection. Praseodymium was utilized as an internal standard to allow the absolute quantification. The results of the quantification of the total cell population labeling are shown in the Figure 80.

As is shown graphically, the outcome of the total cell labeling quantification was equal for the assay and competition control samples in case of the lower final concentration of the CC (125nM). For the samples with the concentration (250nM), the quantified amount of Tb was even higher in the samples corresponding to the competition control, this can be explained with the one outlier among competition control samples. The results of the quantification of the terbium content in the control sample that contains no CC were significantly lower in comparison with the assay and competition control samples. As could be expected, in case of the treatment of the samples with the CC at higher concentration, the increase of the total cell population labeling outcome was observed.

Based on the results demonstrated in the Figure 41, within this experiment the photo-induced crosslinking appeared as not specific. Moreover, this data was in agreement with the results obtained from the LA-ICP-MS detection. However, according to the results of fluorescence microscopy readout, the artefacts that were detected in competition control samples could diminish the difference between the outcome of the assay and competition control samples.

3.2.8.3. Capture experiment with the control samples treated with the unattached detection function

To find out the reason of the presence of the artefacts in the assay and competition control samples, the experiment with the TAMRA functionalized CC was performed.

One of the possible reasons could be the presence of the detection function (fluorophore or MeCAT), which was not attached to the CC and could penetrated inside the cell. In this experiment the CC, which was synthesized as a whole one (CPT-501), was compared to the CC, which was obtained via the click chemistry reaction (CPT-549-381). The competition control was done for the both assays; moreover, the control that contains the detection function functionalized with an azido group (CPT-381) was performed. The comparison was done via the ECL readout of the WB immunoassay and by the fluorescence microscopy. The results of the ECL detection are shown in the Figure 81. As is seen from the image, the signal intensities obtained from the samples that were treated with the CPT-501 are noticeably higher in comparison with the samples treated with the CPT-549-381. However, the signal intensity of the competition control samples processed with CPT-501 was also noticeably higher than that of samples treated with CPT-549-381. From the control samples, which were containing only the detection function (CPT-381) no signal was detected.

The results of the fluorescence microscopy detection are in agreement with the data obtained from the WB immunoassay readout. The outcome of the fluorescence microscopy readout is shown in Figure 82. As is seen from the images, within the frames of this experiments some artefacts were detected in case of both capture compound assay and competition control samples. However, when the samples were treated exclusively with the detection function (CPT -381) no artefacts were detected. Moreover, the signal intensity of the samples treated only with the detection function, is in the same range as the

signal intensity of the control sample that contains no CC. Based on this observation, it can be concluded that the presence of the detection function, which is not attached to the CC, does not cause any artefacts. In spite of the smaller size of the detection tag, it was not confirmed that it penetrated inside the cell.

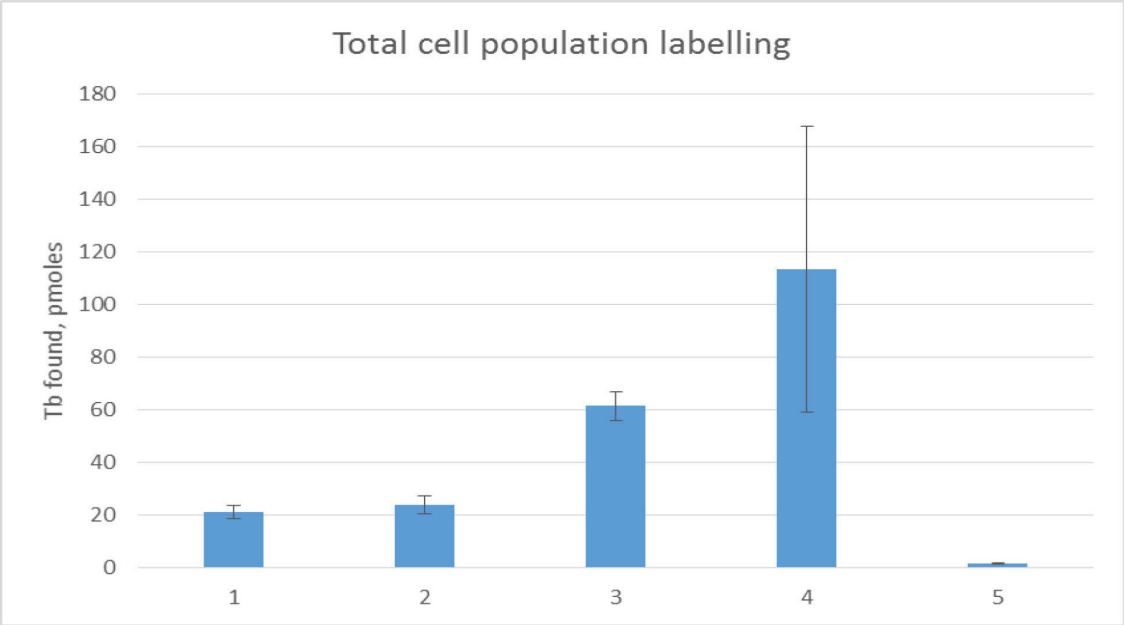

Figure 80. Results of the total cell population labeling quantification. 1 Irradiated assay, final concentration of CC 125 nM; 2 irradiated competition control, final concentration of CC 125 nM; 3 irradiated assay, final concentration of CC 250 nM; 4 irradiated competition control, final concentration of CC 250 nM; 5 irradiated control that contains no CC.

3.2.8.4. Capture experiment followed with LA-ICP-MS, ICP-MS and fluorescence microscopy detection, immunoassay approach for the LA-ICP-MS detection

With the previous experiment it was established, that the artefacts were not caused by the presence of the unattached detection function. Because of this, it was decided to perform the capture experiment with the higher concentration of CC in order to increase the dynamic range between the assay and competition control samples detection outcome. Fluorescence microscopy was used as a reference method. In addition to the capture experiment followed by the fluorescence detection of the fluorophore functionalized CC and the LA-ICP-MS detection of the CC, which carries the metal tag; the immunoassay labeling with the lanthanide of the cells treated with the fluorophore functionalized CC followed by ICP-MS detection was tested. The main idea behind this was to perform the comparison of the outcome of capture experiment with two different detection functions via the one detection method LA-ICP-MS. In the frames of this experiment, another important task was to perform the imaging of the outcome of the capture experiment under the optimized conditions, and to do the correlation of the optical images of the cells to the lanthanide signal distribution. Within this experiment setup no irradiation control was performed.

Part of the cells, which were treated with the fluorophore functionalized CC (CPT-501), were processed afterwards by the resuspension and the sample preparation protocols for the fluorescence microscopy detection. The results of the fluorescence

microscopy readout are shown in the Figure 83. As is seen from the images, the cells membranes are intensively outlined in case of the assay samples (1); however, for both assay and competition control samples some artefacts were detected. In spite of the presence of the artefacts, the clear pattern of the specific covalent crosslink was detected.

Another part of cells, which were exposed to the CPT-501, were resuspended and incubated with the anti-TAMRA primary antibody; after that they were resuspended again and incubated with the secondary anti-mouse antibody labelled with the europium. After the second incubation, cells were resuspended and processed with the sample preparation protocol for LA-ICP-MS detection. The rest of cells were pelleted, in order to perform the total cell population labeling quantification with the direct injection ICP-MS.

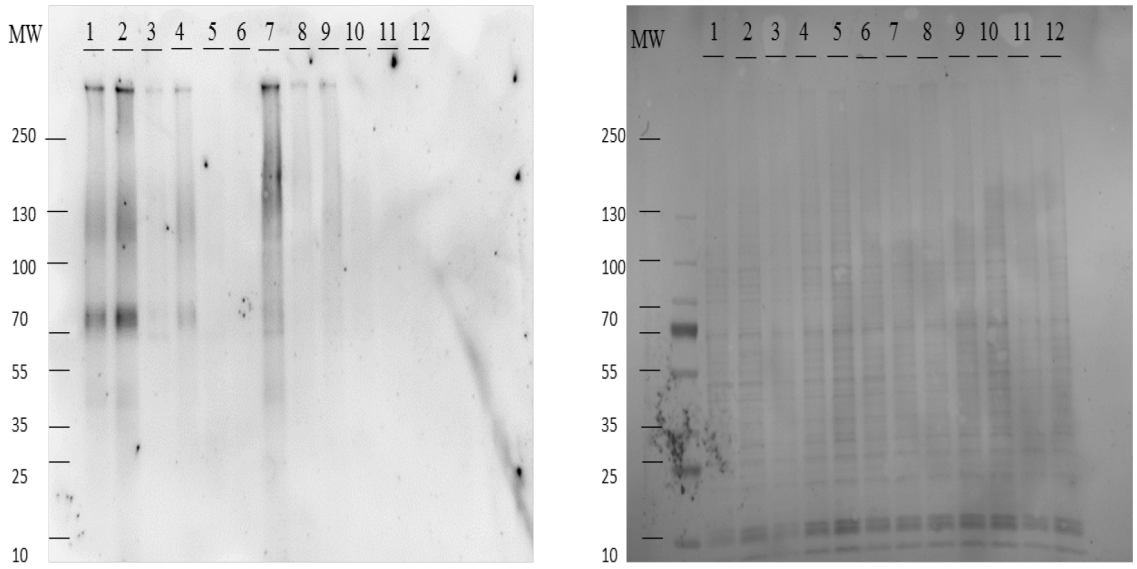

Figure 81. Anti TAMRA WB and Ponceau staining 1,2 – irradiated assay (CPT-501), final concentration of CC 250 nM; 3,4 – irradiated assay (CPT-549-381), final concentration of CC 250 nM; 5,6 – irradiated control that contains only fluorophore tag (CPT -381), final concentration 250 nM; 7– irradiated competition control (CPT-501), final concentration of CC 250 nM , final concentration of competitor 1 uM; 8, 9 – irradiated competition control (CPT-549-381), final concentration of CC 250 nM, concentration of competitor 1 uM; 10 – irradiated control that contains only fluorophore tag (CPT -381), final concentration 250 nM, concentration of competitor 1 uM; 11,12 –irradiated control that contains no CC.

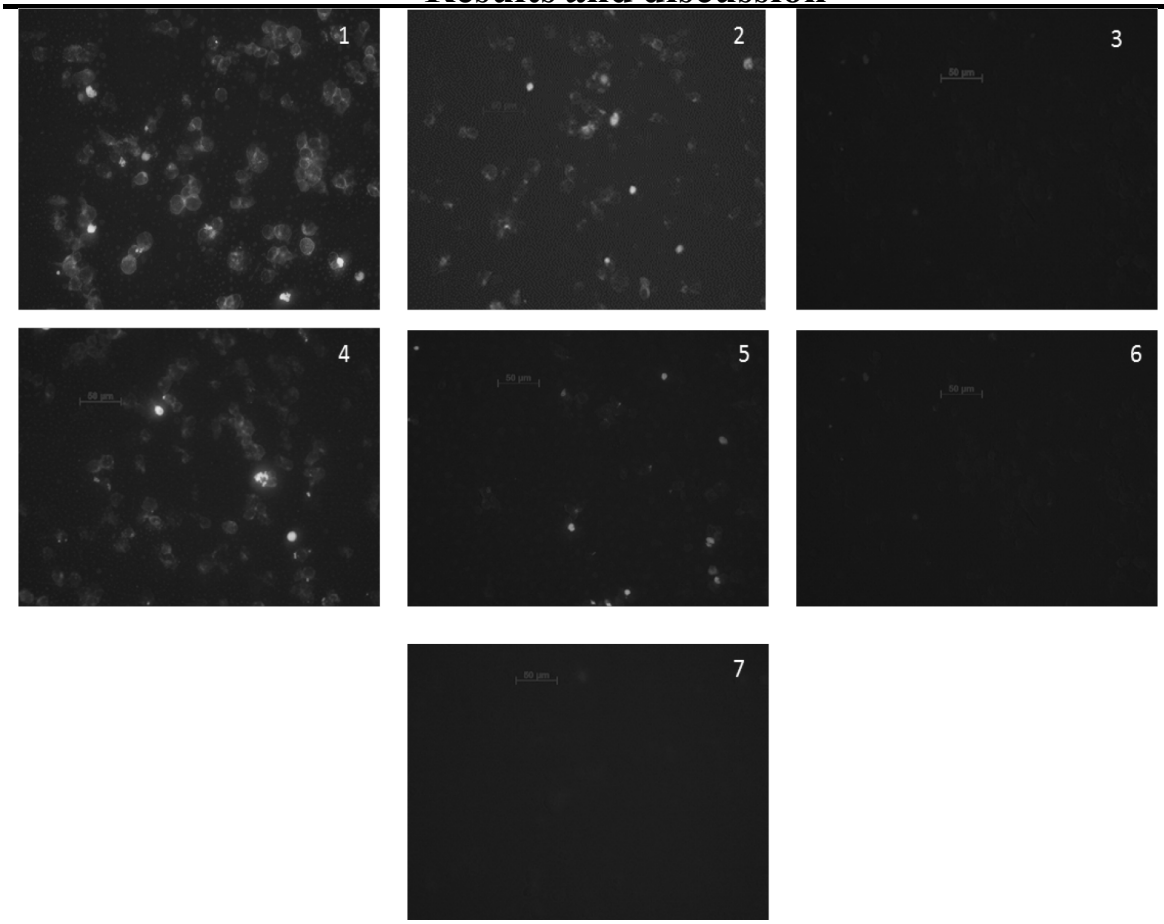

Figure 82. Fluorescence microscopy images, cy3, 40x objective immersion oil. Resuspended cells. 1 Irradiated assay (CPT-501), final concentration of CC 250 nM; 2 irradiated competition control (CPT- 501), final concentration of CC 250 nM; 3 irradiated control that contains only fluorophore tag (CPT - 381), final concentration 250 nM; 4 irradiated assay (CPT-549-381), final concentration of CC 250 nM; 5 irradiated competition control (CPT-549-381), final concentration of CC 250 nM; 6 irradiated control that contains only fluorophore tag, 7 irradiated control that contains no CC.

The main disadvantage of this immunoassay approach was that most of the cells were lost during the numerous washing steps. As the result, the obtained cells pellets were very small in comparison with the ones produced in the previous experiments. Due to the very small amount of cells obtained after the resuspension, the total cell population labeling quantification was not performed.

The results of the LA-ICP-MS imaging of the europium distribution are shown in Figure 84, the detection was done under the optimized conditions. For this experiment setup all the images obtained from LA-ICP-MS detection were set to a maximal signal value of 500 to provide a visual comparison of the signal intensities of samples. All the areas on the images that are colored with the white color correspond to the signal intensity values higher than the established maximum. Since no internal standard was utilized, the absolute quantification of via LA-ICP-MS was not possible. From the Figure 84 it is clearly seen that the detected signal intensities were at the level of noise, in spite of the big size of the laser spot. It can be suggested that the huge loss of the cells was the reason for this result. Another possible explanation is the detachment of the labelled antibody during the washing steps.

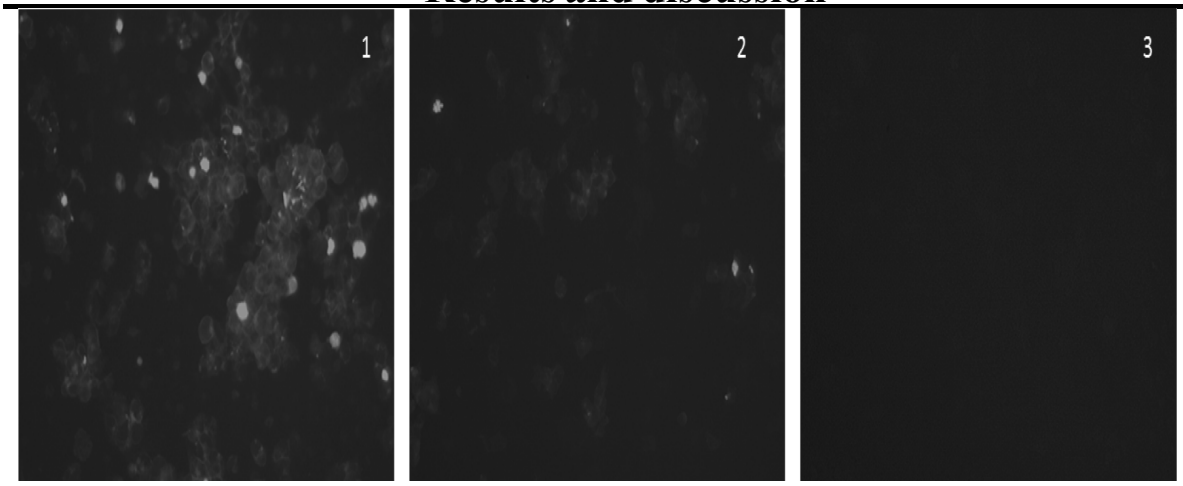

Figure 83. Fluorescence microscopy images, cy3, 40x objective immersion oil. Resuspended cells. Final concentration of CC (CPT-501) 250 nM.1 Irradiated assay, 2 irradiated competition control, 3 irradiated control that contains no CC.

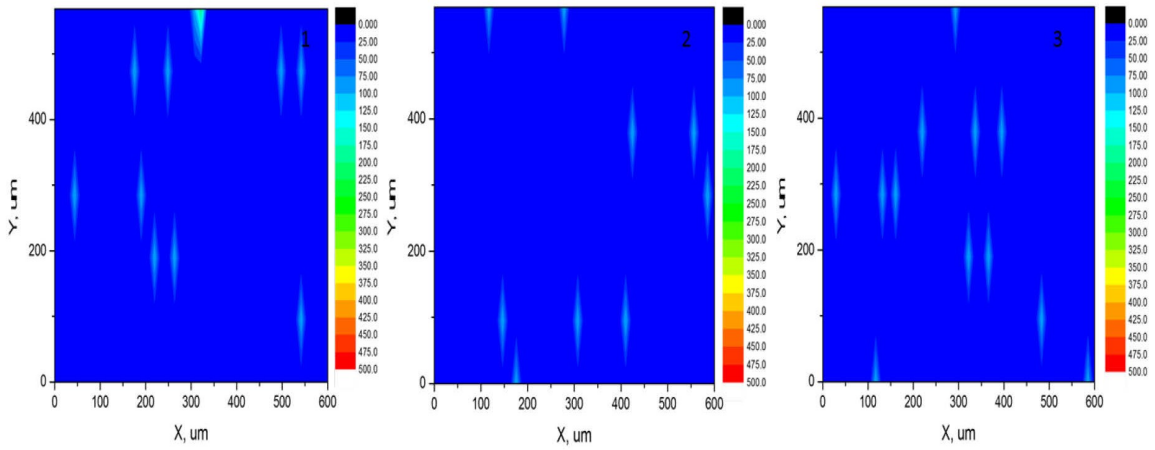

Figure 84. LA-ICP-MS imaging of europium content, spot size 100 um, laser energy 60%. Resuspended cells. Final concentration of CC 1uM. 1 Irradiated assay, 2 irradiated competition control, 3 irradiated control that contains no CC.

The cells that were treated with the MeCAT functionalized CC, were resuspended and processed according to the sample preparation protocol for LA-CP-MS detection and ICP-MS quantification. The results of the LA-ICP-MS imaging are shown in the Figure 85. All the images were set to the same maximal signal intensity value of 500. As is seen from the graphs, there is a noticeable difference of the signal intensity between the assay and competition control samples. This observation reflected the specificity of the capture experiment; moreover, it was in total agreement with the results obtained from the fluorescence microscopy readout.

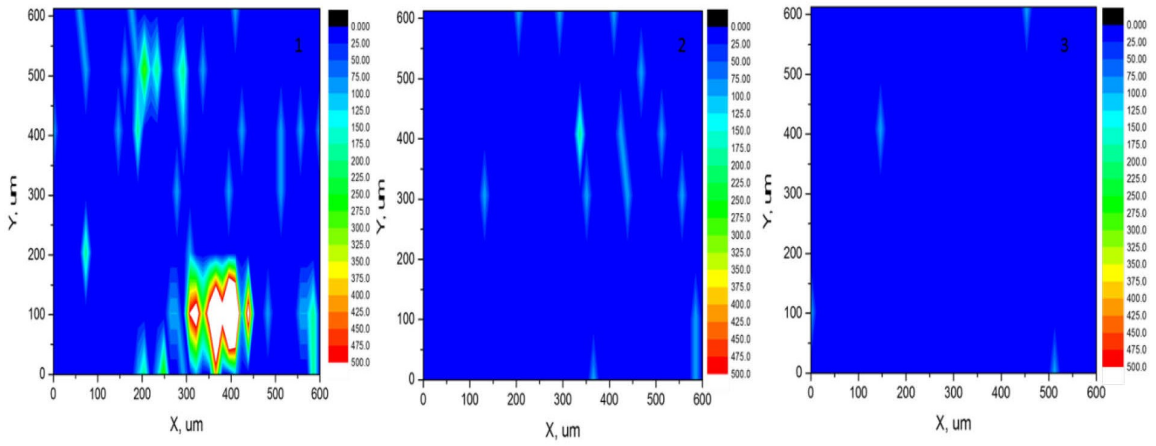

Figure 85. LA-ICP-MS imaging of terbium content, spot size 100 um, laser energy 60%. Resuspended cells. Final concentration of CC 1uM. 1 Irradiated assay, 2 irradiated competition control, 3 irradiated control that contains no CC.

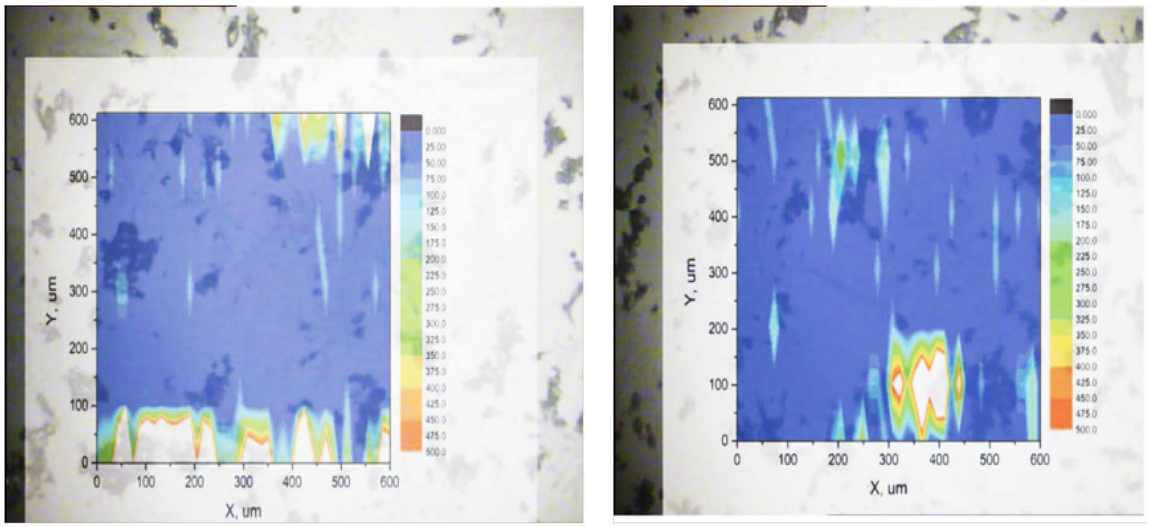

Figure 86. Combined LA-ICP-MSI results with the bright field images of cells, spot size 100 um, laser energy 60%. Resuspended cells. Final concentration of CC 1uM. Irradiated assay samples.

In order to compare the distribution of the cells on the slide to the detected signal intensity of the lanthanide, merging of the optical image of cells before the ablation with the LA-ICP-MSI graphs was performed. Figure 86 shows the results for the two irradiated assay samples. As is seen from the images, the localization of the hotspots and cells are coinciding; however, it is also seen that the distribution of signal was not homogeneous. For some cells the signal intensity was significantly higher than for the others. This observation can be explained with the low resolution of the detection method, and with the probable presence of the artefacts, that may be the reason for the detection the signal from the hotspots.

Similar to the previous experiments, the resuspended cells, which were treated with the MeCAT functionalized CC, were pelleted, mineralized and proceeded with the direct injection ICP-MS detection. Praseodymium was utilized as an internal standard to allow the absolute quantification. The results of the quantification of the total cell population

labeling are shown in Figure 87. Here the difference between the amount of lanthanide found in assay and competition control samples was significantly higher in comparison with the previous results. In the samples corresponding to the control that contained no CC and to the control of the mineralization, which contained no cells, but were processed according to the mineralization protocol, a non-significant amount of terbium was detected. These results confirmed the good signal to noise ratio for this concentration of the sertindole-based CC, it is also in a good agreement with the data obtained from the LA-ICP-MSI.

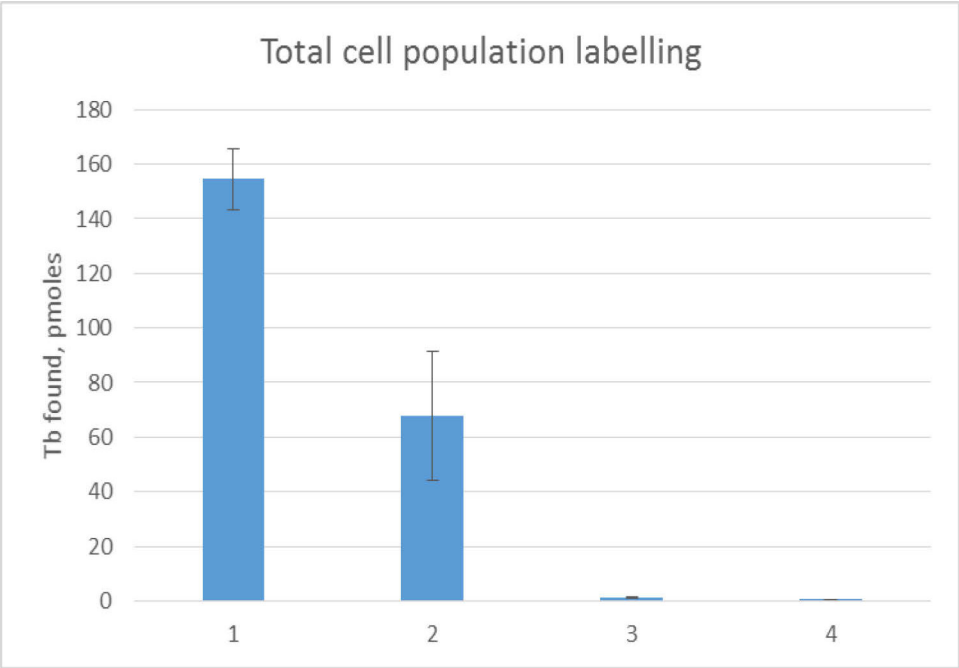

Figure 87. Results of the total cell population labeling quantification. Final concentration of CC: 1uM. 1 Irradiated assay; 2 irradiated competition control; 3 irradiated control that contains no CC; 4 blank control for the mineralization.

During the sample preparation via the resuspension protocol, the amount of cells can vary drastically from one sample to another. In order to minimize the influence of this factor, normalization of the results of the ICP-MS quantification of the total cell population labeling to the mass of the dried cell pellet was applied. This approach had already been reported as an efficient one to minimize the impact of the cell number variation for the determination on the metal content in cells with ICP-MS.[148]

In order to perform the normalization the detected amount of the lanthanide was normalized to the weight of the dried cell pellet. The results of the normalization are shown in Figure 88. According to the graph, if the variation of the mass of the cells is taken into account, it results in the increase of the difference between the assay and competition control samples. Moreover, the reproducibility of the results obtained for the competition control samples improved significantly.

Based on these results, one can conclude that the sertindole-based CC attaches to the target protein DRD2 in a selective way; moreover, the CC photo-crosslinks to the target protein in a specific way.

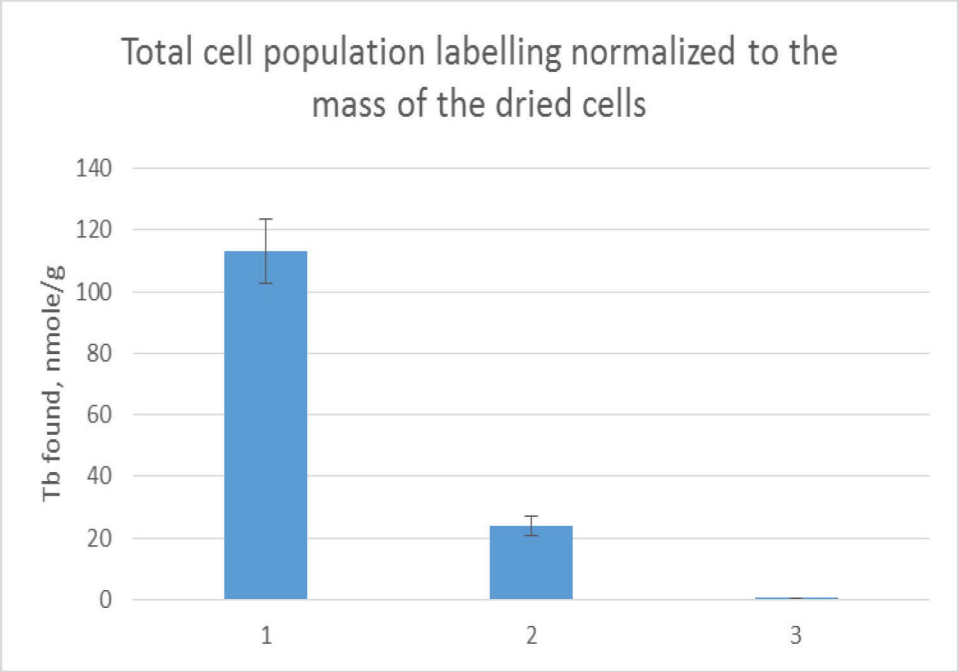

Figure 88. Results of the total cell population labeling quantification. Final concentration of CC 1uM. 1 Irradiated assay; 2 irradiated competition control; 3 irradiated control that contains no CC

3.2.9. *Conclusions and outlook*

We report successful selective cross link of the sertindole-based capture compound functionalized with metal chelate to a target membrane receptor. We could also prove that the studied CC, covalently cross links to the protein of interest; moreover, the binding was confirmed to be specific. The results obtained for CC compound that carries the MeCAT as a detection moiety via the ICP-MS readout, were in complete agreement with the results obtained from fluorescence microscopy detection of the reference CC functionalized with the fluorophore.

For the attachment of detection function of choice to the CC, the click chemistry approach was used; however, for the first experimental trials the utilized CC was synthesized as a whole already carrying a fluorophore as a detection function. It was observed that this CC functionalized with the fluorophore that was synthesized as a whole one, and the one to which the detection function was attached via click chemistry reaction, show significant difference in sensitivity for the ECL readout of the WB immunoassay. For the one that was a product of the click chemistry reaction, significantly higher concentrations were needed to provide the LOD. There are several possible explanations for this, the first one is a different length of the linker (spacer). This can make a certain impact on the affinity of CC to the target. Therefore, a clickable sertindole CC that does not differ in the spacer length and chemistry between the sertindole selectivity function and the CC central core atom should be synthesized and tested to clarify this aspect. The second possible reason is the difficulties with the establishing the actual concentration of the alkyne functionalized CC.

Results of the fluorescence microscopy detection confirmed that the attachment of the CC to the target protein takes places on the surface of cell. It has confirmed our expectations since firstly, the CC was designed in such a way, that it does not

penetrate inside a cell, because of its big size. Secondly, the target protein DRD2 is a membrane receptor. Moreover, the results with the competition control and with the non-irradiated samples proved the specificity of the crosslinking and that it takes place only under the UV irradiation conditions. Thus, the use of CCs for target imaging by fluorescence microscopy was demonstrated.

During the fluorescence microscopy detection of cells that were grown directly on the slide low adhesion of cells to the polylysine coated glass surface was noticed, also the number of cells was noticeably higher than it had been wished for the LA-ICP-MS detection. Because of the mentioned reasons a novel sample preparation protocol for the treatment of cells was developed. According to this protocol the cells were resuspended and washed under the physiological conditions. The results obtained from the fluorescence microscopy detection, ECL readout of the WB immunoassay, and the immunoassay based isolation experiment followed by the nano-LC- MS/MS detection and the relative quantification, proved that via this sample preparation approach only those CC were detected, which were covalently crosslinked to the cell membrane target protein. Moreover, this sample preparation method allowed to control the number of cells on a glass slide in a more efficient way.

With LA-ICP-MS the mapping of Tb distribution was performed, unfortunately, due to the lack of internal standard the utilization of this method for absolute quantification was not possible. Another limitation that was faced, was the low sensitivity in comparison with the fluorescence detection. The low sensitivity can be explained with the non-sufficient content of metal in probes attached to a cell to achieve the higher signal intensity. Because of this, high resolution for the detection of lanthanide was not achievable; the laser spot size had to be in the range of 100um for signal detection.

The cell resuspension protocol gave the opportunity to quantify the total cell population labeling via the direct injection ICP-MS of the mineralized cell pellets. The normalization of the detected amount of metal to the weight of dried cell pellet showed significant improvement in the reproducibility of results. The results obtained from the detection of a total cell population labeling also confirmed that the cross linking of the sertindole-based CC to the target was specific and that covalent attachment took place only under the UV irradiation conditions.

The results of probing metal tags as a detection function of CC are as following: metal chelate as a detection function allows absolute quantification what was not achievable so far with any other reported detection function. Moreover, the MeCAT attached to a CC does not influence the specificity of crosslinking, it is also not influencing the affinity of the CC to the target. The metal tags are allowing elemental imaging via LA-ICP-MS; however, the sensitivity is a limiting factor here, what results in a low resolution. The possible way to overcome this problem is to synthesize a novel tags with higher metal content, for this multiple metal core can be utilized, another alternative detection moieties that could provide the high sensitivity of the ICP-MS detection are the nanoparticles. This work reports for the first time the successful utilization of chemoproteomic probes containing a metal tag for the detection and quantification of labelled target proteins.

4. Materials and methods

4.1. Chemicals

Name	Molecular Formula	Supplier
(+)-Sodium L-ascorbate	$C_6H_7NaO_6$	Sigma Alldrich
1,4,7,10-Tetraazacyclododecane-1,4,7-tris(acetic acid)-10-(azidopropyl ethylacetamide)	$C_{19}H_{34}N_8O_7$	Macrocyclics, USA
2,2`,2``-(10-(4-((2-aminoethyl)amino-)-1-carboxy-4-oxobutyl)-1,4,7,10-tetraazacyclododecane-1,4,7-triyl)triacetic acid	$C_{21}H_{38}N_6O_9$	CheMatech, France
Acetonitrile (HPLC grade)	C_2H_3N	J.T. Baker,
Ammonium bicarbonate (AMBIC)	NH_4HCO_3	Sigma Alldrich
B-mercaptoethanol	C_2H_6OS	AppliChem,
Bromphenole blue, sodium salt	$C_{19}H_9Br_4NaO_2S$	Serva, Germany
Copper (II) sulphate pentahydrate	$CuSO_4*5H_2O$	Alpha Caesar
Dimethylformamide	C_3H_7NO	Sigma Alldrich
Dimethyl sulfoxide	C_2H_6OS	Acros, Germany
Formic acid	CH_2O_2	Fluka, Germany
Glycerol	$C_3H_8O_3$	Gerbu, Germany
Glycine	$C_2H_5NO_2$	Carl Roth,
Hepes	$C_8H_{18}N_2O_4S$	Gerbu, Germany
Hydrogene peroxide	H_2O_2	Sigma Alldrich
IGEPAL CA-630	$(C_2H_4O)_nC_{14}H_{22}O$	Sigma Alldrich
Magnesium acetate tetrahydrate	$C_4H_{14}MgO_8*4H_20$	Sigma Alldrich
Methanol (HPLC grade)	CH_4O	J.T. Baker,
Multi Element ICP standard solution	-	Carl Roth,
Nitric acid, ultra-quality	HNO_3	Carl Roth,
Paraformaldehyde	CH_2O	Sigma Alldrich

Praseodymium ICP standard solution	Pr_6O_{11}	Carl Roth,
Potassium acetate	$C_2H_3KO_2$	Sigma Alldrich
S-(5′-Adenosyl)-L-homocysteine	$C_{14}H_{20}N_6O_5S$	Sigma Alldrich
Sertindole	$C_{24}H_{26}ClFN_4O$	Sigma Alldrich
Skim milk powder	-	Saliter,
Sodium acetate	$C_2H_3NaO_2$	Fluka, Germany
Sodium chloride	NaCl	Carl Roth,
Sodium deoxycholate	$C_{24}H_{39}NaO_4$	Sigma Alldrich
Sodium dodecyl sulphate	$C_{12}H_{25}NaO_4S$	Carl Roth,
Terbium ICP standard solution	Tb_4O_7	Carl Roth,
Terbium(III) chloride hexahydrate	$TbCl_3 \cdot 6H_2O$	Sigma Alldrich
Trans-Cyclooctene-PEG4-NHS esther	$C_{24}H_{38}N_2O_{10}$	Jena Bioscien
Triethylamine	$C_6H_{15}N$	Carl Roth,
Tris base	$C_4H_{11}NO_3$	Gerbu, Germany
Tris hydrochloride	$C_4H_{12}ClNO_3$	Gerbu, Germany
Triton X-100	$C_{14}H_{22}O(C_2H_4O)_n$, n=9-10	Sigma Alldrich
Trypan blue	$C_{34}H_{24}N_6Na_4O_{14}S_4$	Sigma Alldrich
Trypsin	-	Roche,
Tween 20	-	VWR, USA

4.2. Analytical instruments and equipment

Instrument type	Name/Model	Manufacturer
Analytical balance	Sartorius CP225D	Sartorius, Germany
Analytical balance	Mettler Toredo XP105DR	Mettler Toledo, USA
Caprobox	Broadband UV lamp 310nm	Caprotec bioanalytics, Germany
CaproMag	-	Caprotec bioanalytics, Germany
Centrifuge	Micro centrifuge AL	Carl Roth, Germany
Centrifuge	Universal 320R	Andreas Hettich GmbH,
Electrophoresis	EPS-300 X. Power supply	C.B.S. Scientific, USA
Electrophoresis	EBX-700.Mini western blotting system with temperature control	C.B.S. Scientific, USA
Electrophoresis	Novex Mini-Cell	Thermo Fisher Scientific,
Electrophoresis	Novex Power supply, 300V	Thermo Fisher Scientific,

Fluorescent microscope	Axio observer A1	Carl Zeiss, Germany
Glass cutter	Dremel Multi	Dremel, The Netherlands
Ice machine	ZNE1250	Zierga, Germany
Imaging device	Syngene G:BOX Chemi XT4	Syngene, Cambridge, UK
Incubator	Hera cell 150	Thermo Fisher Scientific,
Laser ablation	UP213 deep-UV YAG Laser Ablation System	New wave Research Inc., USA
Laser ablation cell	SuperCell	New wave Research Inc., USA
Mass Spectrometer	Element XR	Thermo Fisher Scientific,
Mass Spectrometer	LTQ Velos	Thermo Fisher Scientific,
Mass Spectrometer	amaZon	Bruker, USA
Microscope	Inverted Microscope DM IL	Leica Microsystems, Germany
Nano-HPLC	Dionex UltiMate 3000	Thermo Fisher Scientific,
Nebulizer	Meinhard, 0,2 ml/min	MicroMist, Glass Expansion, Australia
pH meter	SevenEasy pH meter S20	Mettler Toledo, USA
Preparative HPLC	Waters 2487 Prep HPLC System	Waters Corporation, USA
Sonication bath	Sonorex Super	Bandelin, Berlin
Vacuum centrifuge	SpeedVac AES 1000	Savant Instrumetns, India
Vacuum centrifuge	Genevac EZ-2	Genevac, UK
Vortex	Vortex 4 basic	Carl Roth, Germany
Water purification system	Milli-Q Plus	Millipore, Merk, Germany
Water purification system	Purelab Plus	ELGA LabWater, UK

4.3. Consumables and kits

Category	Name	Manufacturer
Antibody	Anti-TAMRA [G71-DC7]	Hybrotec, Germany
Antibody	Anti-mouse HRP	Hybrotec, Germany
Cell adhesion agent	L-polylysine	Merk Millipore, Germany
Cell culture plates	VWR Multiwell-Cell culture plates	VWR, USA
Chambered coverslip	8 Well Chamber, removable: microscopy glass slide, sterilized	Ibidi, Germany
Enhanced chemiluminescent substrate (ECL)	ECL Western Blotting Substrate	Thermo Scientific Pierce, Germany

Endonuclease	Benzonase Endonuclease	Merk, Germany
Gel staining	Colloidal Coomassie Blue	Fluka, Germany
Immersion oil	Immersoil 518F	Carl Zeiss, Germany
Nitrocellulose blotting membrane	Amersham™ Protran® Premium Western blotting membranes, nitrocellulose	GE Healthcare, UK
Magnetic beads	DynaBeads (Tosyl activated)	Thermo Fisher Scientific,
Membrane staining	Ponceau S	Sigma Alldrich, Germany
Molecular weight marker	PageRuler Plus Prestained Protein Ladder	Thermo Scientific Pierce, Germany
Mounting medium	Mounting Medium for fluorescence microscopy	Ibidi, Germany
Polyacrylamide gels	Progel Tris Glycin 4 – 20%	Anamed Elektrophorese,
Protease inhibitor	cOmplete Protease Inhibitor Cocktail	Roche, Germany
Protein digestion agent	ProteaseMAX Surfactant	Promega, USA
Whatman Gel Blotting Paper	Whatman Gel Blotting Papers GB003, GE Healthcare	GE Healthcare – Whatman, UK

4.4. Cell culture and materials

Cell line	HEK293, DSMZ, Germany
Plasmid	Plasmid encoding human DRD2, Origene (RC2024776T), USA
Transfection agent	Fugene, Roche, Germany
Medium	Earler´s Balanced Salt solution, Sigma Alldrich,
Resuspention buffer	Dulbecco´s Phosphate-buffered saline, Biochrom,

4.5. Buffers

Name	**Stock solution preparation**	**Working**
Blocking buffer	2% skim milk powder in TBST	Same as stock
Blotting buffer (transfer buffer)	10x: 478 mM Tris base, 390 mM glycine, 0,4% SDS	100 mL methanol, 100 mL 10x stock,
Laemmli buffer (loading buffer)	4x: 50mM Tris-HCl, 2,5% SDS, 10% glycerol, 320mM β-mercaptoethanol, 0,05% bromphenole blue, pH6.8	Same as stock
Radioimmunoprecipitation assay (RIPA) buffer	1x: 150 mM sodium chloride, 1.0% IGEPAL CA-630, 0.5%	Same as stock

	sodium deoxycholate, 0.1% SDS, 50 mM Tris-HCl, pH 8.0	
Reaction buffer	1x: 20nM HEPES, 10 mM magnesium acetate, 50mM potassium acetate, 10% glycerol, 0.1% Triton-X-100, pH 7.9	Same as stock
SDS Running buffer	10x: 250 mM Tris, 1,92M glycine, 1% SDS	100 mL of 10x stock,
Sodium acetate buffer	1x: 100mM sodium acetate	Same as stock
Tris buffered saline (TBS)	10x: 500 mM Tris, 1,5M sodium chloride, pH7.5	100 mL of 10x stock,
Tris buffered saline with Tween 20 (TBST)		100 mL of 10x TBS stock, 1mL

4.6. Structures

4.6.1. MeCAT

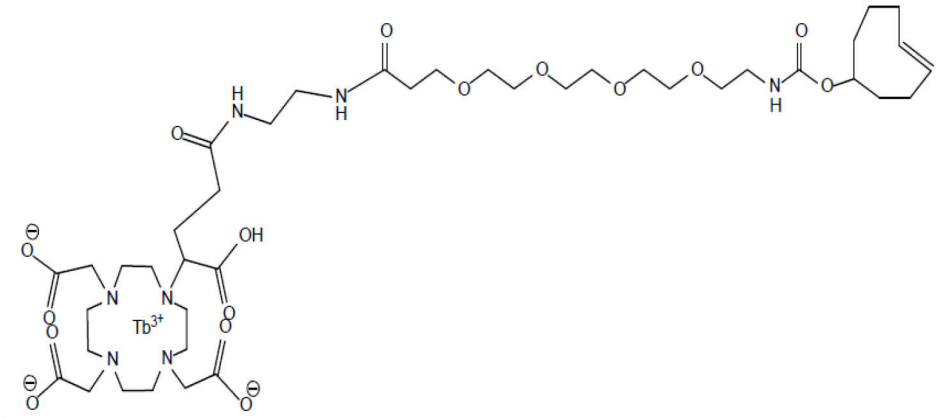

Clickable DOTA-TCO-Tb

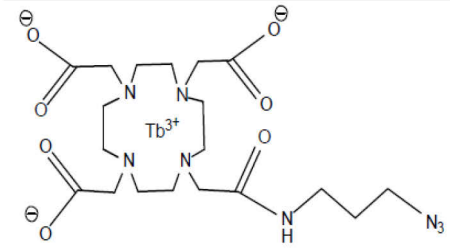

Clickable DOTA-N_3-Tb

4.6.2. Capture compounds, ligands

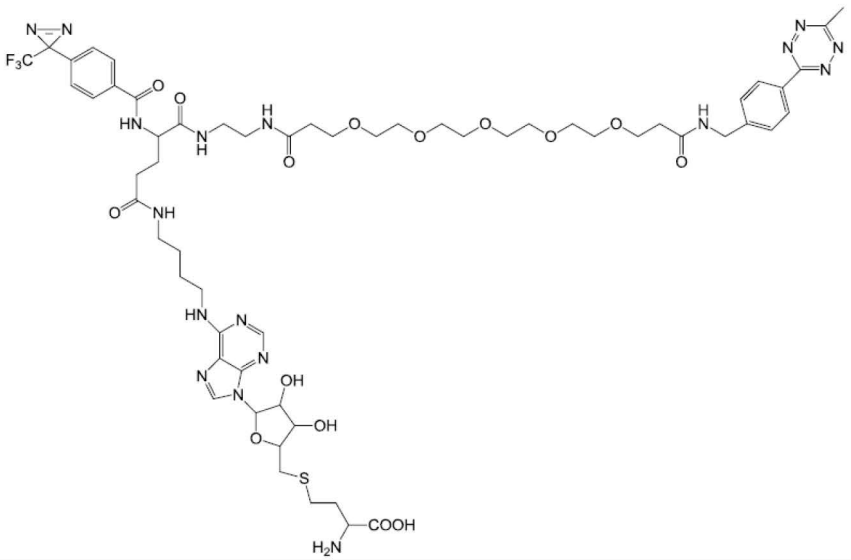	**CPT594** Clickable SAH based CC, that carries tetrazine group
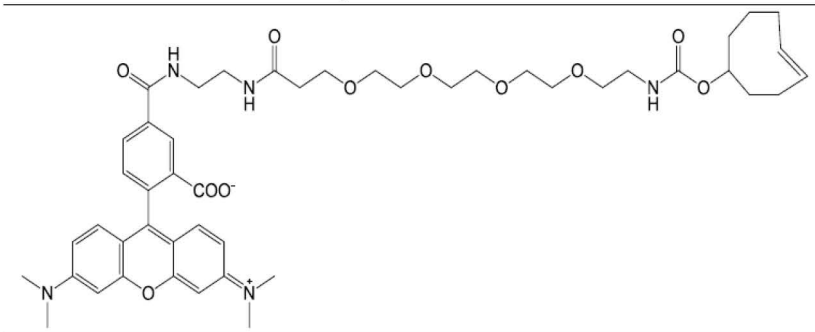	**CPT 533** Clickable TAMRA TCO
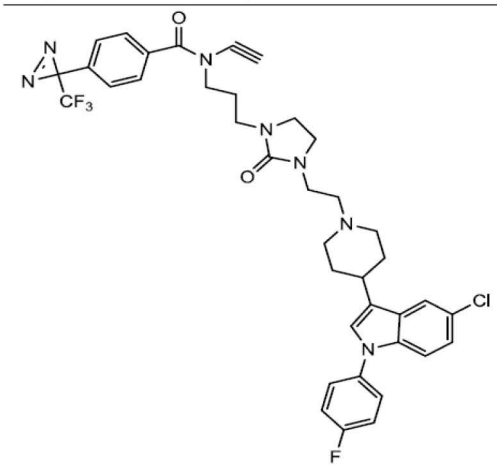	**CPT 549** Clickable Sertindole based CC, that carries alkyne group

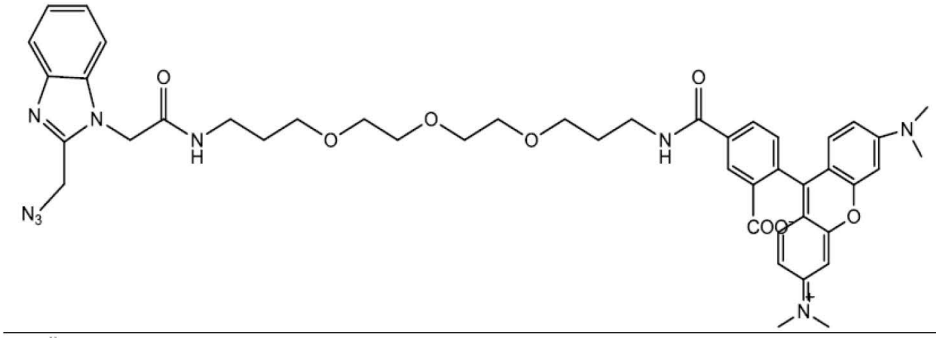	**CPT 381** Clickable TAMRA azide
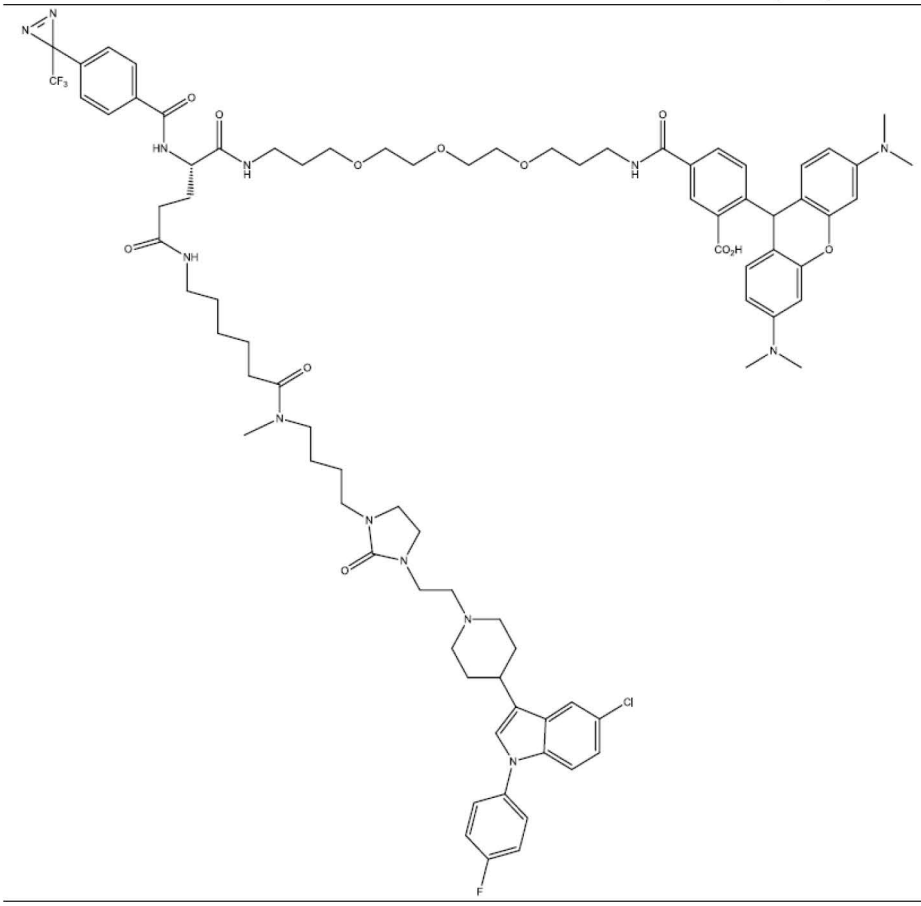	**CPT 501** Sertindole based CC functionalized with TAMRA
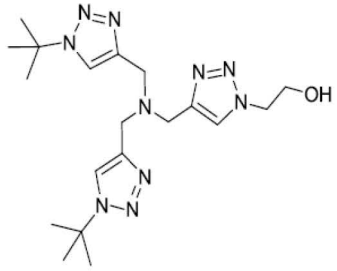 2-(4-((bis((1-(tert-butyl)-1H-1,2,3-triazol-4-yl)methyl)amino)methyl)-1H-1,2,3-triazol-1-yl)ethanol	**CPT 338** Copper chelating ligand

4.7. MeCAT synthesis

4.7.1. Optimization of the synthesis of DOTA-TCO-Tb

4.7.1.1. Solvent composition

In order to optimize the solvent composition, DOTA-NH_2-GA was probed to be dissolved in a following solvents: water; mixture of DMF (90%) and water (10%); DMF; methanol; mixture of methanol (90%) with water (10%). The amount of the chelate loaded to the every solution was 0,2 umoles.

In order to improve solubility of the chelate in the tested solvents, all the samples were vortexed, stirred for 2 hours, heated up to the temperature of 50°C.

4.7.1.2. Reaction time

To optimize the reaction time for the coupling reaction resulting in the formation of DOTA- TCO, 24uL of 10 mM NH2-DOTA-GA (dissolved in a mixture of methanol (90%) and water (10%)) was mixed with the 12 uL of solution of TEA (40mM dissolved in water), and with 3 uL of 20mM TCO-NHS esther dissolved in DMF. The aliquots of the reaction mixture of the volume of 6,5 uL were taken after 30 minutes, 60 minutes, 120 minutes and 240 minutes after the mixing of the starting compounds. The reaction was running at the room temperature. The samples were diluted with the mixture of acetonitrile (20%)/water (80%) and proceeded to LC- MS analysis on amaZon.

4.7.1.3. Impact of concentration of TEA in water

To establish the influence of the concentration of TEA on the reaction yield, 4uL of 10 mM NH2-DOTA-GA (dissolved in a mixture of methanol (90%) and water (10%) was mixed with 0,5uL of 20mM TCO-NHS esther dissolved in DMF. 2 uL of solution of TEA in water was added to the samples, the concentrations of the added amine varied as following: 200mM, 300mM, 400mM, 500mM. The reaction was running at the room temperature for the one hour.
The samples were diluted with the mixture of acetonitrile (20%) with water (80%) and proceeded to LC-MS analysis on amaZon.

4.7.1.4. Impact of concentration of TEA in DMF

To establish the influence of the concentration of TEA on the reaction yield, in case the organic base was dissolved in DMF, 4uL of 10 mM NH2-DOTA-GA (dissolved in a mixture of methanol (90%)/water (10%) was mixed with 0,5uL of 20mM TCO-NHS esther dissolved in DMF. After that 2 uL of solution of TEA in DMF was added to the samples, the concentrations of amine were as following: 200mM, 400mM, 800mM, 1,6M, 3,2M,6,4M,7,2M. The reaction was running at the room temperature for the one hour. The samples were diluted with the mixture of acetonitrile (20%) with water (80%) and proceeded to LC-MS analysis on amaZon.

4.7.2. DOTA-TCO-Tb synthesis under optimized conditions

DOTA-TCO-Tb (Figure 1.B) was synthesized from 2,2`,2``-(10-(4-((2-aminoethyl)amino-)-1- carboxy-4-oxobutyl)-1,4,7,10-tetraazacyclododecane-1,4,7-triyl)triacetic acid (NH_2-DOTA-GA) and Trans-Cyclooctene-PEG4-NHS esther (TCO-NHS esther).

NH2-DOTA-GA (2,6 mg, 10 µmol) was dissolved in 50 µL of distilled water (Milli-Q Plus) and vortexed, 452 µL of methanol was added afterwards and vortexed again. To the obtained solution 186 µL of TEA (1,6M) dissolved in DMF was added, later 46,5 µL of TCO-NHS esther (20mM) dissolved in DMF (Figure 89 A). The reaction was lasting for a one hour at the room temperature, then it was quenched with the liquid nitrogen. After that the solvent was removed under the reduced pressure. The reaction product was used directly in the next step without any other purification.

The further treatment of DOTA-TCO was done with 372 µL of Terbium (III) chloride (100mM) dissolved in sodium acetate buffer (Figure 89 B). The mixture was stirred for 2 hours at room temperature, afterwards it was dried overnight under reduced pressure. Yielded DOTA-TCO-Tb as a solid, was later purified on a preparative reverse-phase liquid chromatography system with mass fractionation (Waters), equipped with YMC Triart C8 column using 12 minutes gradient.

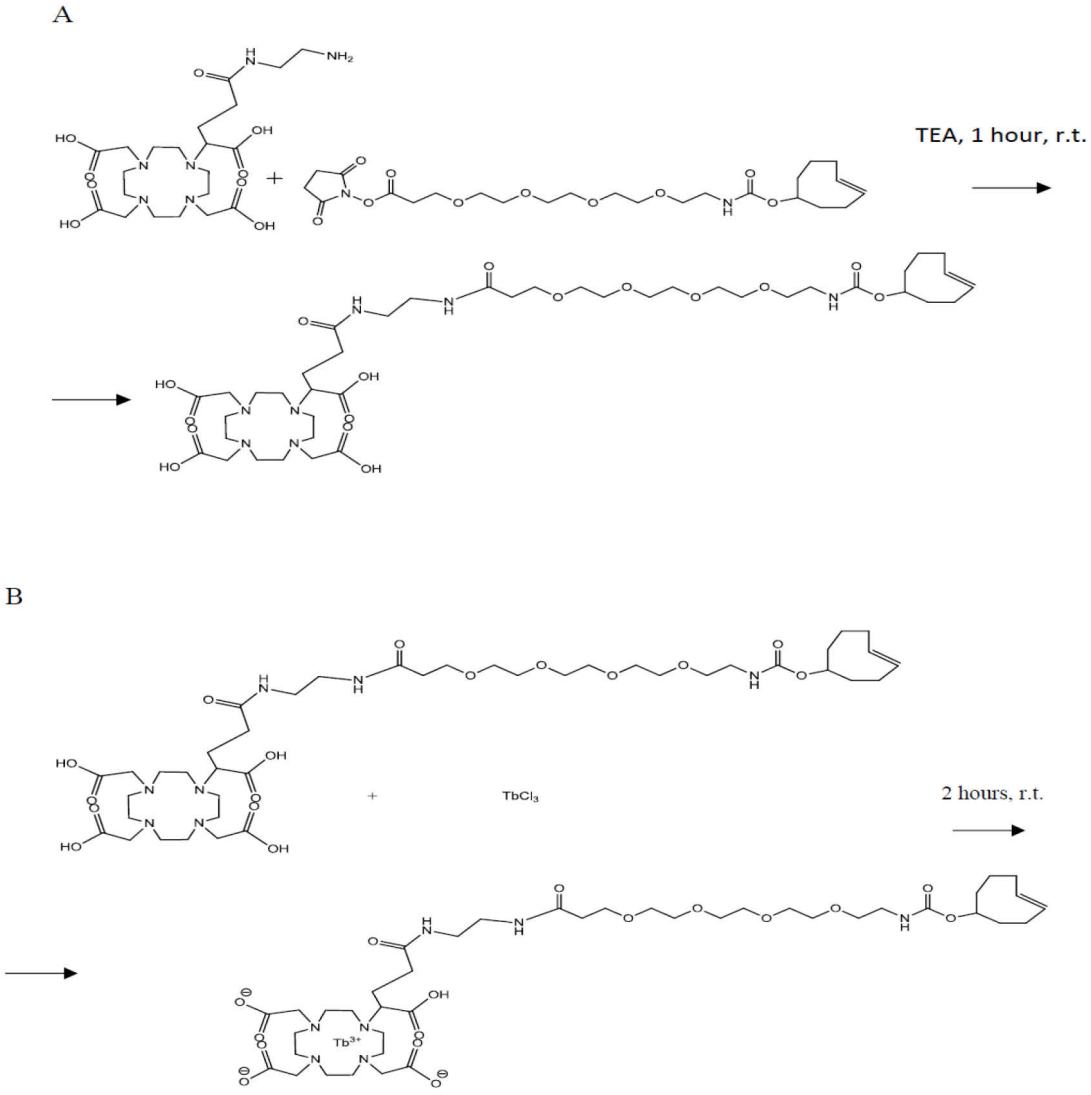

Figure 89. Scheme of the synthesis of DOTA-TCO-Tb: A. Coupling of TCO-NHS ester with NH_2- DOTA-GA. B. Metallation of DOTA-TCO with Terbium.

4.7.3. DOTA-N_3-Tb synthesis

DOTA-N_3-Tb (Figure 2) was synthesized from 1,4,7,10-Tetraazacyclododecane-1,4,7-tris(acetic acid)-10-(azidopropyl ethylacetamide) (DOTA-N_3).

1,51 mg of Terbium (III) chloride was dissolved in 200 µL of sodium acetate buffer. 162 µL of the solution was added to 1,44 mg of DOTA-N_3 (Figure 90). The mixture was stirred for 2 hours at the room temperature, afterwards it was dried overnight under the reduced pressure. The reaction product was used directly in the next step without any other purification.

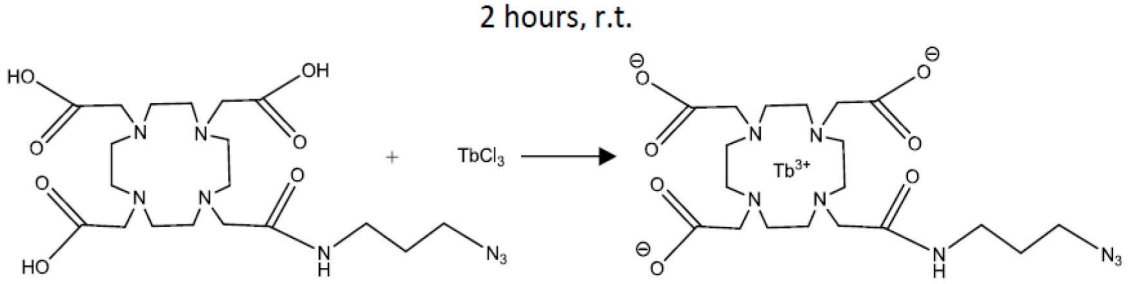

Figure 90. Scheme of the synthesis of DOTA-N_3-Tb.

4.8. Click chemistry reactions

4.8.1. Optimization of the tetrazine ligation reaction conditions

Since the concentration of purified DOTA-TCO-Tb was established according to the weight of the obtained compound, the reaction trials were performed in order to evaluate the efficient concentration of the TCO-functionalized MeCAT.

The batch of the purified compound with the weight of 0,86 mg was dissolved in 40uL of DMSO, the mass-based calculated concentration of the MeCAT solution was 20mM. 1uL of the obtained solution was mixed with 39uL of DMSO in order to achieve the 500uM concentration.

To the 1uL of 500uM solution of CPT-594 (tetrazine functionalized CC) in DMSO, 500uM DOTA-TCO-Tb was added the amounts were as following: 1uL, 2uL, 4 uL. In case of the control samples the equal volume of DMSO was added instead of the compound of interest. The reaction was taking place for 5 minutes under the room temperature. After that, half of each sample was diluted with acetonitrile (20%)/water (80%) mixture and proceeded to LC-MS analysis on amaZon. The detected conversion rate was not sufficient to the last two samples, which were containing MeCAT in 2 and 8 fold excess. Because of it, 500mM DOTA-TCO-Tb was added to these two samples in amounts of 7ul and 8 uL. The reaction was taking place at the room temperature for the time of five minutes. After that the samples were diluted with the mixture of acetonitrile (20%) with water (80%) and proceeded to LC-MS analysis on amaZon.

4.8.2. Tetrazine ligation

Conducted for the purpose of attachment of TAMRA as a detection function: 1,35 µL of 25 µM CPT594 (synthesized in caprotec) in DMSO was mixed with 0,506 µL of CPT533 (100 µM) (synthesized in caprotec) in DMSO, solutions were vortexed and incubated for 5 minutes at the room temperature (Figure 91).

Conducted for the purpose of attachment of MeCAT as a detection function: 1,35 µL of 25 µM CPT594 (synthesized in caprotec) in DMSO was mixed with 0,506 µL of DOTA-TCO-Tb (3mM-titrated concentration) in DMSO, solutions were vortexed and incubated for 5 minutes at the room temperature (Figure 92).

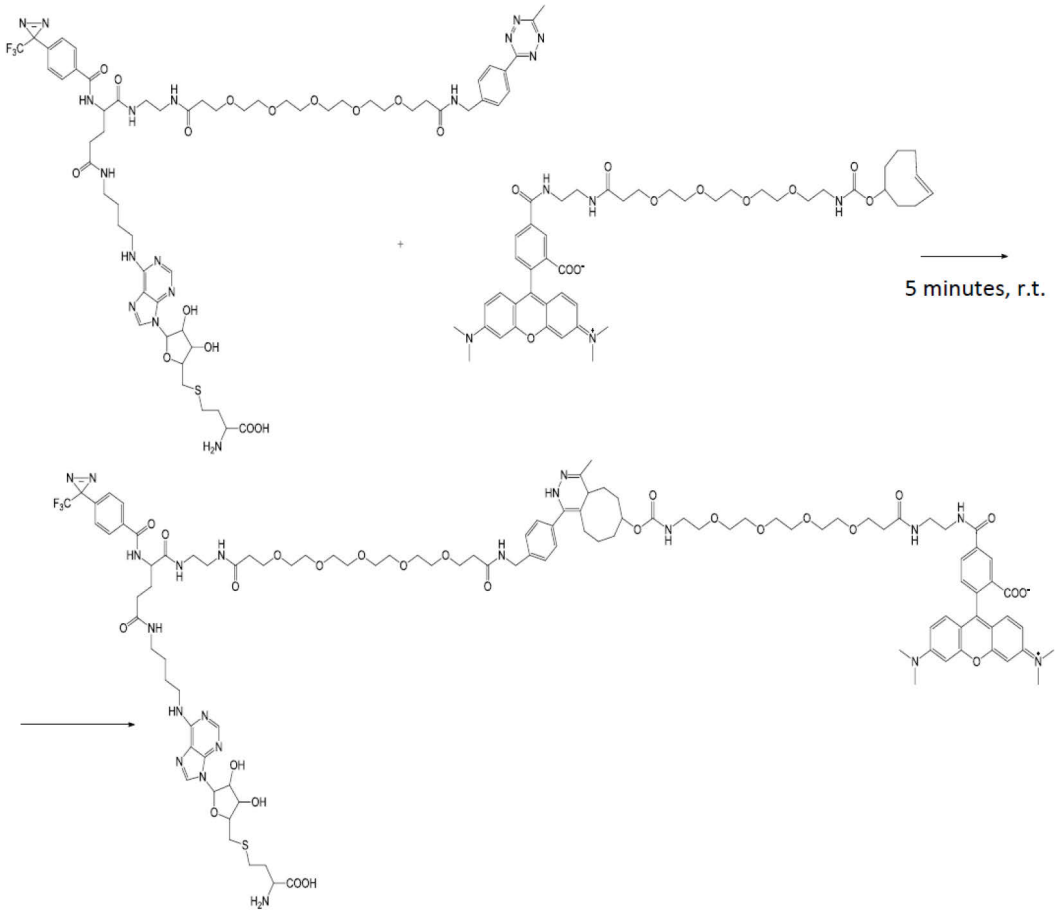

Figure 91. Scheme of the click reaction. Attachment of fluorescent detection function (TAMRA) to the CC via tetrazine ligation.

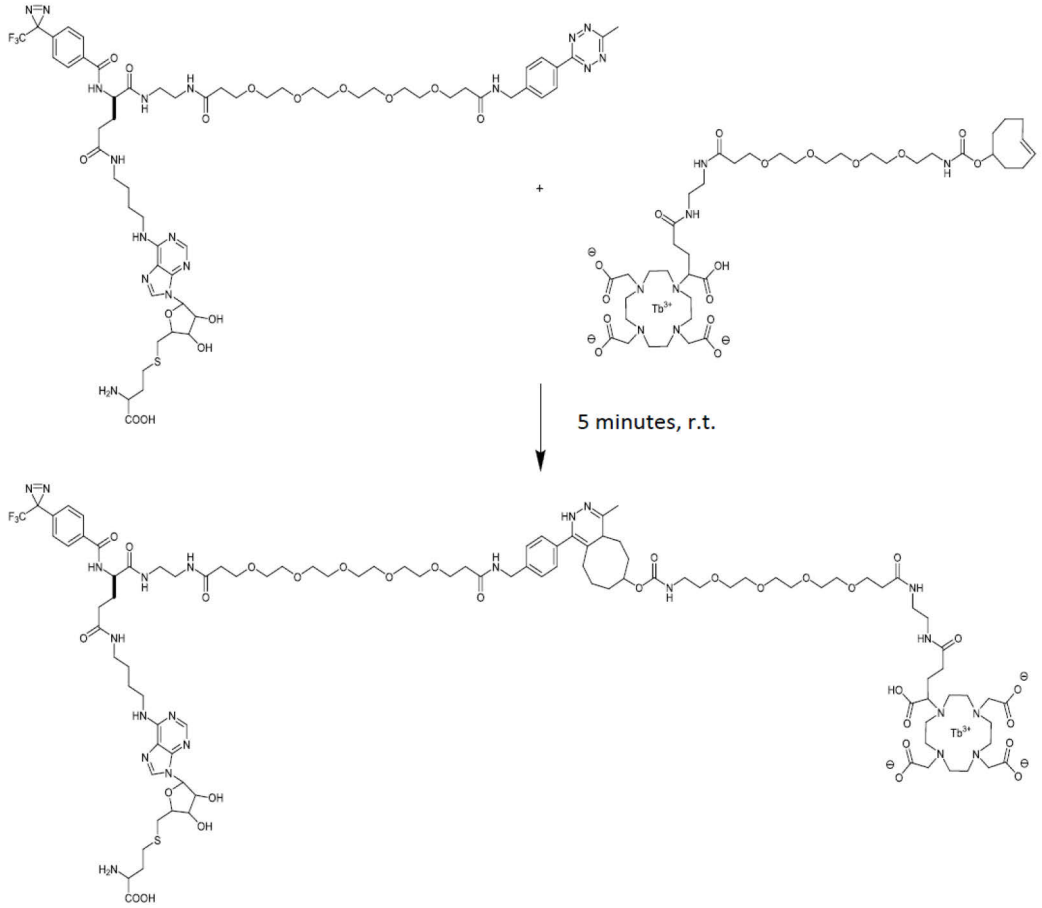

Figure 92. Scheme of the click reaction. Attachment of MeCAT to the CC via tetrazine ligation.

4.8.3. Optimization of the Huisgen-(3+2)-cycloaddition reaction conditions

4.8.3.1. Optimization for TAMRA-functionalized detection function

To establish the concentration of the alkyne functionalized CC (CPT 549) that will provide a high reaction yield, a different amounts of its solution in DMSO with the estimated 20mM concentration were taken: 2 uL, 2,5 uL, 3 uL and 3,5 uL. To all of the aliquots 2,5 uL of the TAMRA-based detection function functionalized with azido group (established concentration 10mM) was added. After that, 0,2 uL of 100mM solution of copper sulfate was added to the reaction mixture and incubated for the five minutes at the room temperature. Afterwards to each sample 0,4 uL of 0,5M sodium ascorbate was added and incubated at the room temperature for fifteen minutes. 0,5uL of each sample was diluted with the mixture of acetonitrile (10%) and water and proceeded to LC-MS analysis on amaZon.

4.8.3.2. Optimization for MeCAT-functionalized detection function

To establish the concentration of DOTA-N_3-Tb that will allow high conversion yield, 1,67 uL of the MeCAT dissolved in DMSO and water with the estimated concentration of 15mM was mixed with the 2,5 uL of the CC functionalized with the alkyne group, and with 1,3 uL of the 15,4 mM solution of the external copper chelating ligand in water. In case of control samples the equal volume of solvent was added instead of the compound of interest. The reaction mixture was incubated for the five minutes at the room temperature. Afterwards to each sample 0,4 uL of 0,5M sodium ascorbate was added and

incubated at the room temperature for fifteen minutes.
0,5uL of each sample was diluted with the mixture of acetonitrile (20%) and water and proceeded to LC-MS analysis on amaZon.

Since the detected conversion yield was not sufficient 1,7 uL of MeCAT and 0,4 uL of 0,5M sodium ascorbate were additionally added to the sample of interest, the obtained reaction mixture was incubated for the fifteen minutes. Afterwards, the aliquote of 0,5uL was taken and diluted with the mixture of acetonitrile (20%) and water and analyzed via LC-MS analysis on amaZon.

Because the tested access of MeCAT did not provide the required conversion rate again, the addition trial was done. 2,5 uL of the MeCAT dissolved in DMSO and water with the estimated concentration of 10mM was mixed with the 2,5 uL of the CC functionalized with the alkyne group (9mM) and with 1,3 uL of the 15,4 mM solution of the external copper chelating ligand in water. The reaction mixture was incubated for the five minutes at the room temperature.
Afterwards 0,4 uL of 0,5M sodium ascorbate was added to the sample and incubated at the room temperature for fifteen minutes. The sample aliquote of 0,5uL diluted with the mixture of acetonitrile (20%) and water and analyzed via LC-MS analysis on amaZon.

4.8.4. Huisgen-(3+2)-cycloaddition

4.8.4.1. Attachment of the fluorophore-based detection function

Conducted for the purpose of attachment of TAMRA as a detection function (Figure 93) under optimized reaction conditions: 2,5 uL of 9mM (titrated concentration) CPT549 (synthesized in caprotec) in DMSO was mixed with 2,5 uL of 10mM CPT381 (synthesized in caprotec) in DMSO, 0,20 uL of 100 mM copper sulphate in water was added, solutions were vortexed and incubated for 5 minutes at the room temperature. After that 0,4 uL of 500nM sodium ascorbate in water was added, solutions were vortexed and incubated for 15 minutes at the room temperature.

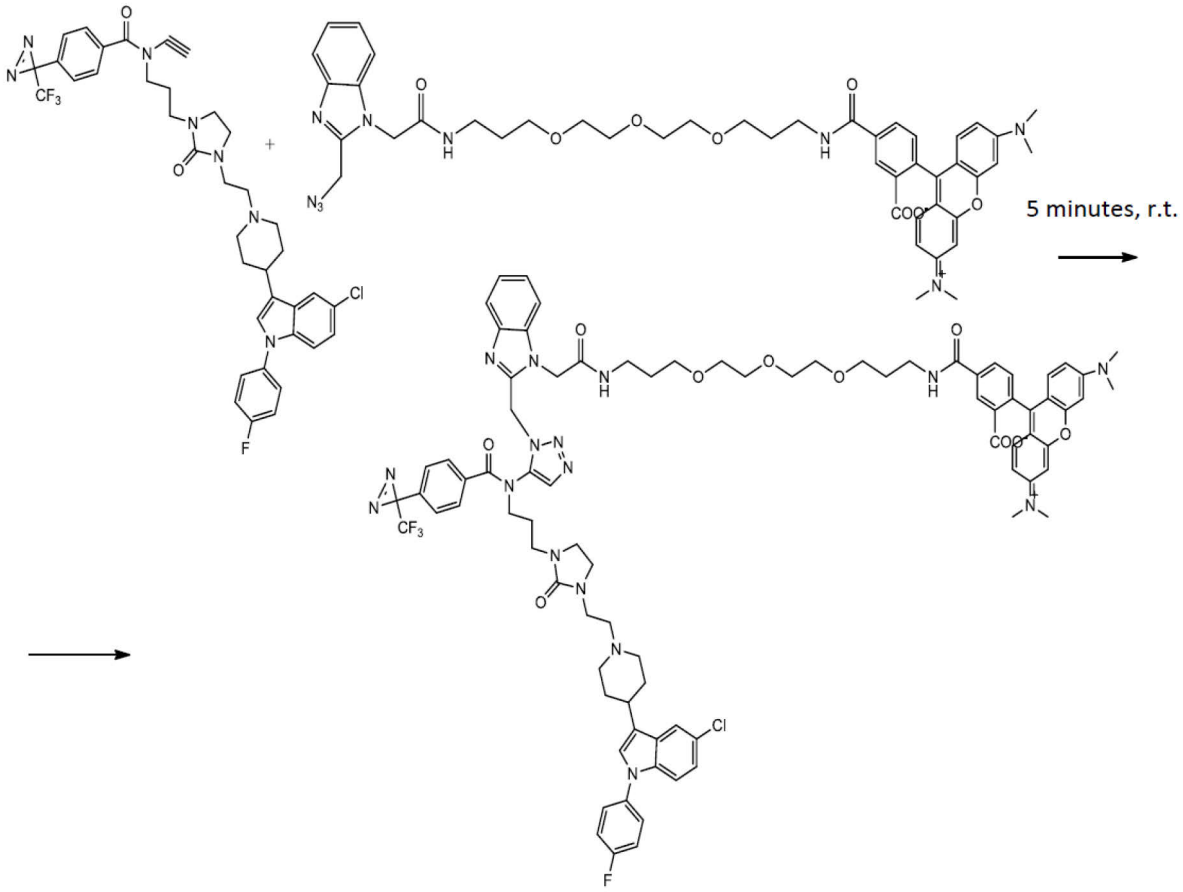

Figure 93. Scheme of the click reaction. Attachment of fluorescent detection function (TAMRA) to the CC via Huisgen-(3+2)-cycloaddition

4.8.4.2. Attachment of the detection function that carries lanthanide

Conducted for the purpose of attachment of MeCAT as a detection function (Figure 94) under optimized reaction conditions: CuSO4-CPT338: 107,9 uL of 20mM CPT338 (external ligand) was mixed with 9 uL 200mM copper sulphate. 2,5 uL of 9mM CPT549 (synthesized in caprotec) in DMSO was mixed with 2,5 uL 10mM DOTA-N_3-Tb in DMSO and water (2:1, titrated concentration), 1,30 uL of 15,4 mM CuSO4-CPT338 in water was added, solutions were vortexed and incubated for 5 minutes at the room temperature. After that 0,4 uL of 500nM sodium ascorbate in water was added, solutions were vortexed and incubated for 15 minutes at the room temperature.

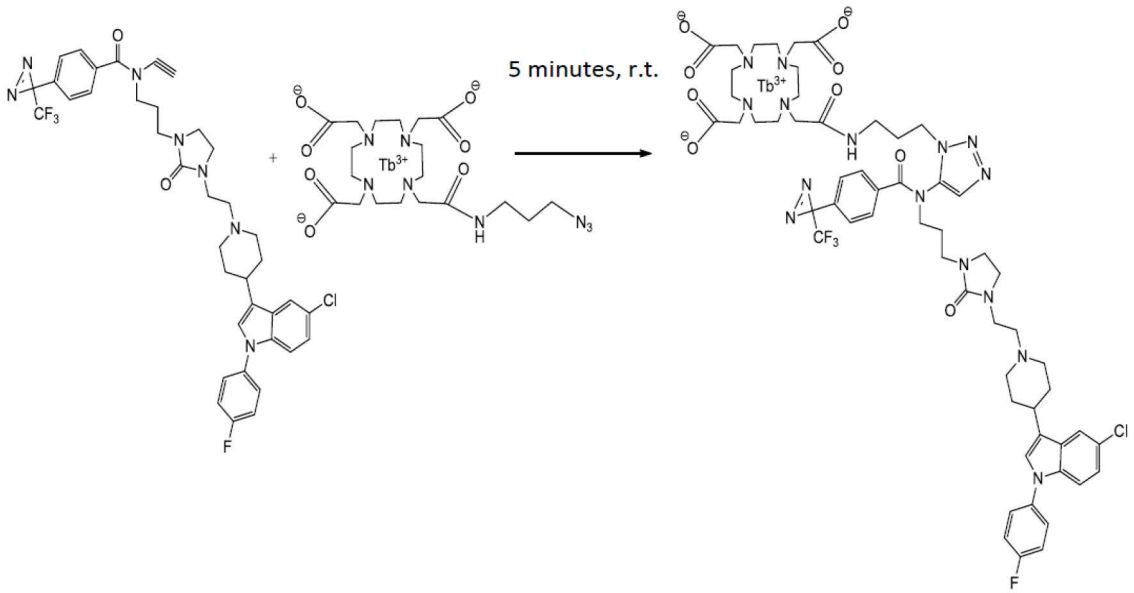

Figure 94. Scheme of the click reaction. Attachment of MeCAT to the CC via Huisgen-(3+2)-cycloaddition

4.9. Capture experiment on a single purified protein with following fluorescence and ICP-MS detection

DNA adenine N6 MTase from Termus aquaticus (M.TaqI) was overexpressed and purified as described elsewhere [149] [150]. M.TaqI (25 µM) was ten times diluted in reaction buffer (20nM HEPES, 10 mM $Mg(OAc)_2$, 50mM KOAc, 10% glycerol, 0,1% Triton-X-100, pH 7,9).

To ensure the specificity of the capture experiment competition control control samples were utilized: 39,5 µL of diluted M.TaqI was mixed with 1,125 µL of SAH (10mM). To achieve the same sample volume for the capture assay samples 39,5 µL of diluted M.TaqI was mixed with 1,125 µL of distilled water. 13,5 µL of assay and competition control samples were added to the preclicked fluorophore and MeCAT functionalized CC, what was resulting in 4 samples: assay that carries TAMRA, assay that carries a metal tag, competition control that carries fluorophore, competition control that carries MeCAT. Placed in thin-walled tubes (0.2 mL) of a 12-tube strip (Thermo-Strip, Thermo Scientific) 7,5 µL of each sample was irradiated with UV light (310nm, Caprobox)) for 5 minutes under the temperature of 4°C. Another 7,5 µL of each sample were not irradiated. In total 8 samples were obtained (irradiated: capture assay that carries TAMRA, capture assay that carries a metal tag, competition control that carries fluorophore, competition control that carries MeCAT; non-irradiated capture assay that carries TAMRA, non-irradiated
capture assay that carries a metal tag, non-irradiated competition control that carries fluorophore, non-irradiated competition control that carries MeCAT).
For SDS-PAGE separation 5 µL of sample was mixed with SDS sample buffer (50mM Tris-HCl, 2,5% SDS, 10% glycerol, 320mM β-mercaptoethanol, 0,05% bromphenole blue, pH6.8) and heated for 5 minutes (95°C). Samples were loaded to the pockets of precast gel (4 - 20 % Tris- Glycin-Gels).

After electrophoresis (300V, 30minutes) in gel fluorescence detection was done with

G:BOX (Green LED sourse, UV06 filter, GeneSys software, manual capture), afterwards protein bands were visualized with Colloidal Coomassie Blue (Fluka, Germany) and Prestained Protein Ladder, 10 to 180 kDa marker (PageRuler™, Thermo Scientific) was used for molecular weight estimation. The image conversion of gel bands was done with ImageJ software.

Visualised target bands from the electrophoretic gel were cut and mineralized adding 100 µl HNO_3 (68%, OPTIMA grade) and 40 µl H_2O_2 (30%) and incubated overnight at 95 °C. The aliquots of fractions of mineralized bands were spiked with 5 µL 141Pr (100 µg/L) as internal standard for 159Tb and the volume was adjusted to 500 µL with 3.5% HNO3.

The samples were then analyzed by direct infusion ICP-MS (Element XR, Thermo Fisher Scientific, Germany) employing a Meinhard-type nebulizer (MicroMist, Glass Expansion, Australia). Isotopes were measured in low resolution (R≈40). 3.5% HNO_3 was used for between- run cleaning to avoid carryover. The ICP was tuned daily for maximum ion intensity. Instrument parameters: cool gas flow 15 L/min, auxiliary gas flow 0,90 L/min, sample gas flow 1,651 L/min, RF power 1482W.

4.10. Cell culture and transfection

HEK293, established from a human primary embryonal kidney transformed by adenovirus type 5, were obtained from the DSMZ (German Collection of Microorganisms and Cell Cultures) Braunschweig, Germany. The transfection of the cell culture with human DRD2was done in caprotec. The plasmid encoding human DRD2 was gained from Origene (RC2024776T). The transfection was done using Fugene (Roche). Expression of DRD2 was verified by anti-FLAG tag Western blotting.

4.11. Capture experiment on cells

4.11.1. Capture experiment on cells (cells grown on slide – chambered coverslip) with following fluorescent detection

In an attempt to perform detection with fluorescence microscopy cells were seeded in open µ- Slide (which consists of removable silicone chamber, mounted on a glass slide) with 8 wells, coverslips were treated with L-polylysine. For capture assay samples, treatment with sertindole- CC (CPT501) was done for one hour at the final concentration of 50nM by direct addition of CC stock solution in DMSO. For competition control samples, cells were previously incubated for 10 minutes with unmodified sertindole (final concentration 500nM). For control samples that contain neither capture compound, no competitor the equal volume of DMSO instead of CC stock was added. Afterwards, cells were irradiated for 10 minutes under 4°C using the Caprobox (310 nm). In case of irradiation control samples cells were not irradiated. After irradiation, the cell medium was removed, then 3 times concentrated PFA was added to each well and left for 10 minutes to allow fixation. Finally PFA was removed, the chambers were removed as well. To allow fluorescence microscopy detection with high magnification (immersion oil objective) the coverslips were mounted.

4.11.2. Capture experiment on cells (resuspension protocol) with following fluorescent detection, Western Blot analysis and isolation experiment

To enable the stringent washing conditions and to facilitate the control over the number of

cells per well, the new resuspension protocol was developed. Cells were seeded in six-well plates (VWR Multiwell-Cell culture plates) and grown to near confluence. For capture assays, treatment with sertindole-CC was for 30 minutes by direct addition of CPT501 solution in DMSO to the culture medium (final concentration 50nM). For competition control samples, cells were incubated for 30 minutes with unmodified sertindole (final concentration 500nM). For control samples that contain neither capture compound, no competitor the equal volume of DMSO instead of CC stock was added. Afterwards, cells were irradiated for 10 minutes under 4°C using the Caprobox (310 nm). In case of irradiation control cells were not irradiated. After irradiation cells were harvested by rinsing them off with the entire cell medium and afterwards with PBS (500 uL). The combined harvest was centrifuged for 10 minutes in a table centrifuge (4°C, 500 x g). After that cells were resuspended in 1mL of PBS, centrifuged and resuspended again.

For the SDS-PAGE separation followed with the Western blot immunoassay analysis, 50uL of the suspension was taken. To these aliquots 16 uL of 4x concentrated Laemmli sample buffer was added, after that 1 uL of benzonase was added to each tube. Samples were shaken for 15 minutes in order to allow complete DNA digestion. Afterwards they were heated (55°C) for 10 minutes. Samples were loaded to the pockets of precast gel (4 - 20 % Tris-Glycin-Gels), electrophoresis was conducted under following conditions: 300V, 30minutes. The transfer to the nitrocellulose membrane and immunoassay treatment are described in a section Western blot.

For the fluorescence microscopy detection aliquots of resuspended cells (50uL) were transferred to an open µ-Slide (chambered coverslip) with 8 wells, covered with L-polylysine, each well was containing already 150 uL of PBS. Cells were left for 15 minutes in order to let them settle down, after that 100 uL of PFA (9% in PBS) was added for fixation that was allowed to proceed for 30 minutes. Afterwards, the liquid was removed from the chambers, the chambers were removed as well. To allow fluorescence microscopy detection with high magnification (immersion oil objective) the coverslips were mounted.

The remaining 900 uL of resuspended cells suspension was centrifuged for 10minutes (4°C, 500 x g). The supernatant was removed, cell pellets were shock-frozen in liquid nitrogen and stored at -80°C. To prepare samples for nano-LC-MS/MS analysis, to each cell pellet 500 uL of RIPA buffer, 2 uL benzonase and 2 uL of protease inhibitor were added. Samples were vortexed and rotated for an hour. After that samples were centrifuged (full speed) for 20 minutes. The washed Anti-TAMRA beads (with RIPA buffer 6 times) were added to the supernatant, the incubation took place overnight under rotation. Afterwards the beads were collected and transferred to PCR tubes. Samples were washed 3 times with RIPA buffer, 2 times with 100 mM AMBIC. Samples were digested with Trypsin in 10uL 50mM AMBIC/0,05% ProteaseMAX for one hour. After the digest and supernatant recovery 20 uL of water was added for washing and was pooled with initial supernatant. Beads were magnetically isolated using the caproMag.

4.11.3. Capture experiment on cells (resuspension protocol) optimization for pre-clicked CC

To enable the stringent washing conditions resuspension protocol was utilized. Cells were seeded in six-well plates (VWR Multiwell-Cell culture plates) and grown to near

confluence. For capture assays, treatment with sertindole-CC was for 1 hour by direct addition of CPT549-381 solution in DMSO to the culture medium (final concentrations 50nM, 100mM, 250nM, 500nM). For competition control samples, cells were incubated for 30 minutes with unmodified sertindole (final concentration 1uM). For control samples that contain neither capture compound, no competitor the equal volume of DMSO instead of CC stock was added. Afterwards, cells were irradiated for 10 minutes under 4°C using the Caprobox (310 nm). After the irradiation cells were harvested by rinsing cells off with the entire cell medium and afterwards with PBS (500uL). The combined harvest was centrifuged for 10 minutes in a table centrifuge (4°C, 500 x g). After that cells were resuspended in 1mL of PBS, centrifuged and resuspended again.

For the SDS-PAGE separation followed with the Western blot analysis 50uL of the suspension was taken. To these aliquots 16 uL of 4x concentrated Laemmli sample buffer was added, after that 1 uL of benzonase was added to each tube. Samples were shaken for 15 minutes in order to allow complete DNA digestion. Afterwards they were heated (55°C) for 10 minutes. Samples were loaded to the pockets of precast gel (4 - 20 % Tris-Glycin-Gels), electrophoresis was conducted under following conditions: 300V, 30minutes. The transfer to the nitrocellulose membrane and immunoassay treatment are described in a section Western blot.

4.11.4. Capture experiment on cells (resuspension protocol) for comparison of pre-clicked CC and synthesized CC

To enable the stringent washing conditions and to facilitate the control over the number of cells per well, the resuspension protocol was utilized. Cells were seeded in six-well plates (VWR Multiwell-Cell culture plates) and grown to near confluence. For capture assays, treatment with sertindole-CC was for 1 hour by direct addition of CPT501 solution in DMSO (final concentration 250nM), CPT549-381 solution in DMSO (final concentration 250nM), or CPT381 solution in DMSO (final concentration 250nM) to the culture medium. For competition control samples, cells were incubated for 30 minutes with unmodified sertindole (final concentration 2,5uM). For control samples that contain neither capture compound, no competitor (NoCC) the equal volume of DMSO instead of CC stock was added. Afterwards, cells were irradiated for 10 minutes under 4°C using the Caprobox (310 nm). After irradiation cells were harvested by rinsing cells off with the entire cell medium and afterwards with PBS (500 uL). The combined harvest was centrifuged for 10 minutes in a table centrifuge (4°C, 500 x g). Cells were resuspended in 1mL of PBS, centrifuged and resuspended again.

For the SDS-PAGE separation followed with the Western blot analysis 50uL of the suspension was taken. To these aliquots 16 uL of 4x concentrated Laemmli sample buffer was added, after that 1 uL of benzonase was added to each tube. Samples were shaken for 15 minutes in order to allow complete DNA digestion. Afterwards they were heated (55°C) for 10 minutes. Samples were loaded to the pockets of precast gel (4 - 20 % Tris-Glycin-Gels), electrophoresis was conducted under following conditions: 300V, 30minutes. The transfer to the nitrocellulose membrane and immunoassay treatment are described in a section Western blot.

For the fluorescence microscopy detection aliquots of resuspended cells (50uL and 25 uL) were transferred to an open µ-Slide (chambered coverslip) with 8 wells, covered with L-polylysine, each well was containing already 150 uL or 125 uL of PBS. Cells were left

for 15 minutes in order to let them settle down, after that 100 uL of PFA (9% in PBS) was added for fixation that was allowed to proceed for 30 minutes. Afterwards, the liquid was removed from the chambers, the chambers were removed as well. To allow fluorescence microscopy detection with high magnification (immersion oil objective) the coverslips were mounted.

4.11.5. Capture experiment on cells (resuspension protocol) with following fluorescent detection, LA-ICP-MS detection and direct injection ICP-MS quantification

To enable the stringent washing conditions and to facilitate the control over the number of cells per well, the resuspension protocol was utilized. Cells were seeded in six-well plates (VWR Multiwell-Cell culture plates) and grown to near confluence. For capture assays, treatment with sertindole-CC was for 1 hour by direct addition of CPT501 solution in DMSO (final concentration 250nM) or CPT549-DOTA-Tb solution in DMSO (final concentration 1uM) to the culture medium. For competition control samples, cells were incubated for 30 minutes with unmodified sertindole (final concentration 10uM). For control samples that contain neither capture compound, no competitor (NoCC) the equal volume of DMSO instead of CC stock was added. Afterwards, cells were irradiated for 10 minutes under 4°C using the Caprobox (310 nm). In case of irradiation control cells were not irradiated. After irradiation cells were harvested by rinsing cells off with the entire cell medium and afterwards with PBS (500 uL). The combined harvest was centrifuged for 10 minutes in a table centrifuge (4°C, 500 x g). Cells were resuspended in 1mL of PBS, centrifuged and resuspended again. Cell counting was done with Neubauer Chamber, Trypan Blue staining.

For fluorescence microscopy and LA-ICP-MS detection, the aliquots of resuspended cells (25uL) were transferred to an open µ-Slide (chambered coverslip) with 8 wells, covered with L- polylysine. Each well was containing already 175 uL of PBS. Cells were left for 15 minutes in order to let them settle down, after that 100 uL of PFA (9% in PBS) was added for fixation that was allowed to proceed for 30 minutes. Afterwards, the liquid was removed from the chambers, the chambers were removed as well. For the fluorescence measurements the coverslips were mounted. For LA-ICP-MS detection, the slide was cut in order to fit the laser ablation cell (SuperCell).

The remaining cell suspension was centrifuged for 10 minutes (4°C, 500 x g). Afterwards, the supernatant was removed and cell pellets were dried under reduced pressure for 2 hours. To allow detection by direct infusion ICP-MS dried samples were mineralized adding 200 µl HNO_3 (68%, OPTIMA grade) and 200 µl H_2O_2 (30%) and incubated for 4 hours at 70 °C. The aliquots of fractions of mineralized bands were spiked with 5 µL 141Pr (100 µg/L) as internal standard for 159Tb and the volume was adjusted to 500 µL with 3.5% HNO_3.

The samples were then analyzed by direct infusion ICP-MS (Element XR, Thermo Fisher Scientific, Germany) employing a Meinhard-type nebulizer (MicroMist, Glass Expansion, Australia). Isotopes were measured in low resolution (R≈40). 3.5% HNO3 was used for between- run cleaning to avoid carryover. The ICP was tuned daily for maximum ion intensity. Instrument parameters: cool gas flow 15 L/min, auxiliary gas flow 0,90 L/min, sample gas flow 1,651 L/min, RF power 1482W.

4.12. Fluorescence microscopy

All fluorescence microscopy work was done in the working group of Prof. Dr. Oliver Seitz.

Images were taken with the Zeiss Axio Observer A1 inverted stand microscope equipped with an 40x (N.A.1,3) oil immersion objective (Zeiss EC Plan-NEOFLUAR) at rt. Wavelengths (ex,em) of 550/25, 605/70 nm (Filter Set 43 HE, Carl Zeiss, Germany) were applied for Cy3. Images were taken using Axiocam MRm and Carl Zeiss AxioVision 4.8 software (Carl Zeiss, Germany).

4.13. Western blotting

The transfer was done immediately after electrophoretic separation. Nitrocellulose membrane and a filter paper were previously incubated in a transfer buffer for 15 minutes. After the sds- based polyacrylamide gel was extracted out of the chamber, the "sandwich" was assembled in a following order: sponge, gel blot paper, blotting membrane, gel, gel blot paper, and sponge. It was locked in a cassette, the transfer of proteins to a nitrocellulose membrane (Amersham Protan, 0,45um) took place under the following conditions: 20V, overnight, wet-transfer in a blotting buffer (EBX-700 Blot Chamber, C.B.S. Scientific). Afterwards Ponceau S staining was done. After destaining, the membrane was incubated for an hour with blocking buffer (2% milk in TBST), afterwards the 1 hour incubation in primary antibody (anti-TAMRA [G71-DC7], 1:1000 in 2% blocking buffer) took place. Then membrane was washed 3 times with TBST, 5 minutes for each wash. Finally the membrane was incubated with secondary antibody (anti- mouse HRP, 1:1000 in blocking buffer) for an hour and afterwards it was washed 3 times with TBST (10 minutes every wash). After a final wash with TBS for 5 minutes, membrane was treated with enhanced chemiluminescence (ECL) detection reagent, ECL readout has been done in G:BOX (6x6 binning, GeneSys software, manual capture).

4.15. LA-ICP-MS

A commercial LA system (New wave research), equipped with a beam expander and yielding laser spot sizes between 4 and 100 um, was coupled to an ICP sector field mass spectrometer (Element XR, Thermo Fisher Scientific, Germany). The ICP-MS was synchronized with the LA unit in external triggering mode.
Fixed cells were mounted onto microscope glass slides and inserted into the SuperCell (New wave research). The aerosol was transported by helium at a flow rate of 0,2 L/min, and Ar was added at a typical flow rate of 1.3 L/min before the ICP torch. The ICP was tuned daily for maximum ion intensity. Samples were completely ablated by adjacent single line scans under optimal LA-ICP-MS conditions: the spot size 100 um, speed 100 um/s, Energy 35%. The isotope 159 Tb was selected for analysis.

LA-ICP-MS data were exported to Origin 9.0 (Originlab Corporations, Northampton, USA), where either intensity time profiles or color coded images can be produced by converting the scan speed into a micrometer scale. Signal intensities were color coded in a way that low intensities are depicted in blue and high intensities in red.

4.16. Label free quantification

4.16.1. Nano-LC-MS/MS

Samples from tryptic digest were analyzed with online nanoflow liquid chromatography tandem mass spectrometry (nano LC-MS) with UltiMate 3000RSLC nano-LC system coupled to an LTQ-Orbitrap Velos instrument (Thermo Fisher Scientific, Germany) through a Proxeon nano- electrospray ion source (Thermo Fisher Scientific, Germany). For chromatographic separation, samples were first loaded on a reversed phase (RP) precolumn (Acclaim PepMap100 C18) and separated on a RP analytical column using a 132 min gradient (Acclaim PepMap RSLC C18, Dionex, Thermo Fisher Scientific, Germany).

Mass spectrometric analysis was performed in the data-dependent top-10 mode allowing automatic switching between Orbitrap-MS and LTQ-MS/MS acquisition for a full scan with subsequent collision-induced dissociation (CID) fragmentation. Full scan MS spectra (m/z 300– 1700) were acquired in the Orbitrap analyzer. The 10 most intense ions were sequentially isolated and fragmented in the linear ion trap using collision-induced dissociation (CID).

4.16.2. *Peptide and protein identification via automated database search*

All MS/MS data were analyzed using the search engine Andromeda implemented in MaxQuant (www.maxquant.org, release 1.5.2.8, Cox & Mann 2008). Automated database searching against the human UniProtKB/Swiss-Prot database (release 2016_02 contains 20186 reviewed sequence entries) was performed with 4.5 ppm precursor tolerance, 0.5 Da fragment ion tolerance, full trypsin specificity allowing for up to 2 missed cleavages and methionine oxidation, acetylated N- termini and deamidation on asparagine and glutamine as variable modification. The maximum false discovery rates were set to 0.01 both on protein and peptide level and 7 amino acids were required as the minimum peptide length. The label-free quantification option was selected for alignment between LC-MS/MS runs. The output of the MaxQuant analysis was post-processed according to a standardized procedure implemented at caprotec bioanalytics to normalize protein intensities, and subsequently calculate fold changes and p-values.

5. References

[1] J. Reinders and A. Sickmann, *Proteomics. Methods and protocols*. Humana Press,

2009. [2] B. Michalke, *Metallomics*. Wiley, 2016.

[3] B. J. Lederberg and A. T. McCray, " Ome Sweet Omics-- A Genealogical Treasury of Words," *Sci.*, vol. 15, no. 7, p. 8, 2001.

[4] E. S. Lander *et al.*, "Initial sequencing and analysis of the human genome," *Nature*, vol. 409, no. 6822, pp. 860–921, 2001.

[5] M. R. Wilkins *et al.*, "Progress with Proteome Projects: Why all Proteins Expressed by a Genome Should be Identified and How To Do It," *Biotechnol. Genet. Eng. Rev.*, vol. 13, no. 1, pp. 19–50, 1996.

[6] A. Persidis, "Proteomics," *Nat. Biotechnol.*, vol. 16, pp. 393–394, 1998.

[7] P. Picotti, B. Bodenmiller, and R. Aebersold, "Proteomics meets the scientific method," *Nat. Methods*, vol. 10, no. 1, pp. 24–27, 2012.

[8] M. Dreger, "Emerging strategies in mass-spectrometry based proteomics," *Eur. J. Biochem.*, vol. 270, no. 4, p. 569, 2003.

[9] H. Ovaa and F. van Leeuwen, "Chemical biology approaches to probe the proteome.,"*Chembiochem*, vol. 9, no. 18, pp. 2913–2919, 2008.

[10] A. D. Weston and L. Hood, "Systems Biology , Proteomics , and the Future of Health Care : Toward Predictive , Preventative , and Personalized Medicine Introduction : Paradigm Changes in Health Care," *J. Proteome Res.*, vol. 3, pp. 179–196, 2004.

[11] R. Aebersold and M. Mann, "Mass spectrometry-based proteomics," *Nature*, vol. 422, no. March, pp. 198–207, 2003.

[12] M. Moche, B. Heßling, and M. Hecker, "From the genome sequence to the protein inventory of Bacillus subtilis," *Proteomics*, vol. 11, pp. 2971–2980, 2011.

[13] T. Bennike, S. Birkelund, A. Stensballe, and V. Andersen, "Biomarkers in inflammatory bowel diseases : Current status and proteomics identification strategies," *World J. Gastroenterol.*, vol. 20, no. 12, pp. 3231–3244, 2014.

[14] S. Hess, "The emerging field of chemo- and pharmacoproteomics," *Proteomics*, vol. 7, pp. 171–180, 2013.

[15] M. Schirle, M. Bantscheff, and B. Kuster, "Review Mass Spectrometry-Based Proteomics in Preclinical Drug Discovery," *Chem. Biol.*, vol. 19, no. 1, pp. 72–84, 2012.

[16] Y. M. Jhanker, M. F. Kadir, and R. I. Khan, "Proteomics in Drug Discovery," *J. Appl. Pharm. Sci.*, vol. 2, no. 8, pp. 1–12, 2012.

[17] U. Rix and G. Superti-Furga, "Target profiling of small molecules by chemical proteomics," *Methods Mol. Biol.*, vol. 1394, no. 9, pp.211–218, 2016.

[18] F. Huang, B. Zgang, S. Zhou, X. Zhao, C. Bian, and Y. Wei, "Chemical proteomics:

terra incognita for novel drug target profiling," *Chin. J. Cancer*, vol. 31, no. 11, pp. 507–518, 2012.

[19] M. Bantscheff, A. Scholten, and A. J. R. Heck, "Revealing promiscuous drug-target interactions by chemical proteomics," *Drug Discov. Today*, vol. 14, no. 21–22, pp. 1021– 1029, 2009.

[20] P. K. Ghosh, *Protein Mass Spectrometry*. 2016.

[21] S. Y. Han and H. K. Seong, "Introduction to chemical proteomics for drug discovery and development," *Arch. Pharm. (Weinheim).*, vol. 340, no. 4, pp. 169–177, 2007.

[22] A. J. Douglas and M. Bogyo, "Chemical proteomics and its application to drug discovery," *Curr. Opin. Biotechnol.*, vol. 14, pp. 87–95, 2003.

[23] U. Haedke, E. V Kütter, O. Vosyka, Y. Yang, and S. H. L. Verhelst, "Tuning probe selectivity for chemical proteomics applications," *Curr. Opin. Biotechnol.*, vol. 17, pp. 102–109, 2013.

[24] M. C. Hagenstein and N. Sewald, "Chemical tools for activity-based proteomics," *J. Biotechnol.*, vol. 124, pp. 56–73, 2006.

[25] H. Katayama and Y. Oda, "Chemical proteomics for drug discovery based on compound- immobilized affinity chromatography," *J. Chromatogr. B Anal. Technol. Biomed. Life Sci.*, vol. 855, pp. 21–27, 2007.

[26] M. Raida, "Drug target deconvolution by chemical proteomics," *Curr. Opin. Chem. Biol.*, vol. 15, no. 4, pp. 570–575, 2011.

[27] E. Weerapana, G. M. Simon, and B. F. Cravatt, "Disparate proteome reactivity profiles of carbon electrophiles," *Nat. Chem. Biol.*, vol. 4, no. 7, pp. 405–407, 2008.

[28] P. Ciborowski and J. Silberring, *Proteomic Profiling and Analytical Chemistry*, 2nd ed. 2016.

[29] A. Bodzon-Kulakowska *et al.*, "Methods for samples preparation in proteomic research,"*J. Chromatogr. B Anal. Technol. Biomed. Life Sci.*, vol. 849, no. 1–2, pp. 1–31, 2007.

[30] B. Y. H. Hoch, "Comparison of Electrophoretic Patterns of Human Sera obtained in Phosphate and in Diethylbarbiturate Buffer," *Biochem*, vol. 46, pp. 539–541, 1949.

[31] M. J. V. Shapiro A.L., Vinuela E., "Molecular wieght estimation of polypeptide chains by electrophoresis in SDS-polyacrilamide gels," *Biochem. Biophys. Res. Commun.*, vol. 28, no. 5, 1967.

[32] Laemmli U.K., "Cleavage of Structural Proteins during the Assembly of the Head of Bacteriophage T4," *Nature*, vol. 227, 1970.

[33] O. P.H., "High Resolution Two-Dimensional Electrophoresis of Proteins," *J. Biol. Chem.*, vol. 250, no. 10, pp. 4007–4021, 1975.

[34] A. Görg, W. Weiss, and M. J. Dunn, "Current two-dimensional electrophoresis technology for proteomics," *Proteomics*, vol. 4, pp. 3665–3685, 2004.

[35] H. Towbin, T. Staehelin, and J. Gordon, "Electrophoretic transfer of proteins from polyacrylamide gels to nitrocellulose sheets: procedure and some applications.," *Proc. Natl. Acad. Sci. U. S. A.*, vol. 76, no. 9, pp. 4350–4, 1979.

[36] W. N. Burnette, "'Western Blotting': Electrophoretic transfer of proteins from sodium dodecyl sulfate-polyacrylamide gels to unmodified nitrocellulose and radiographic detection with antibody and radioiodinated protein A," *Anal. Biochem.*, vol. 112, no. 2, pp. 195–203, 1981.

[37] D. J. Macphee, "Methodological considerations for improving Western blot analysis," *J. Pharmacol. Toxicol. Methods*, vol. 61, no. 2, pp. 171–177, 2010.

[38] R. Aebersold, A. L. Burlingame, and R. A. Bradshaw, "Western Blots versus Selected Reaction Monitoring Assays : Time to Turn the Tables ?," *Mol. Cell. Proteomics*, vol. 12, no. 9, pp. 2381–2382, 2013.

[39] R. Ekman, J. Silberring, A. M. Westman-Brinkmalm, and A. Kraj, *Mass spectrometry*. 2009.

[40] G.A. Howard and A.J.P. Martin, "The Separation of the C12-C18 Fatty Acids by Reversed-phase Partition Chromatography," *Biochem. J.*, vol. 46, no. 3, pp. 532–538, 1948.

[41] S. Fanali, P. R. Haddad, C. F. Poole, P. Schoenmakers, and D. Lloyd, *Liquid Chromatography*. 2013.

[42] I. Molnar and C. Horvath, "Reverse-Phase Chromatography of Polar Biological Substances : Separation of Catechol Compounds by High-Performance Liquid Chromatography," *Clin. Chem.*, vol. 1502, pp. 1479–1502, 1976.

[43] J. B. Fenn, M. Mann, C. K. A. I. Meng, S. F. Wong, and C. M. Whitehouse, "Electrospray Ionisation for Mass Spectrometry of Large Biomolecules," *Science (80-.).*, vol. 246, no. 6, pp. 64–71, 1989.

[44] M. Karas, D. Bachmann, U. Bahr, F. Hillenkamp, and U. Miinster, "Matrix-Assisted Ultaviolet Laser Desorption of Non-volatile compounds," *Int. J. Mass Spectrom. Ion Process.*, vol. 78, pp. 53–68, 1987.

[45] K. J. Lewis, J. Wei, and G. Siuzdak, "Matrix-Assisted Laser Desorption/Ionization Mass Spectrometry in Peptide and Protein Analysis," in *Encyclopedia of Analytical Chemistry*, 2006.

[46] L. H. Cazares, D. A. Troyer, B. Wang, R. R. Drake, and O. J. Semmes, "MALDI tissue imaging : from biomarker discovery to clinical applications," *Anal Bioanal Chem*, vol. 401, pp. 17–27, 2011.

[47] J. Kriegsmann, M. Kriegsmann, and R. Casadonte, "MALDI TOF imaging mass spectrometry in clinical pathology : a valuable tool for cancer diagnostics (Review)," *Int. J. Oncol.*, no. 22, pp. 893–906, 2015.

[48] R. Thomas, *Practical guide to ICP-MS a tutorial for beginners*. 2013.

[49] R. Lobinski, J. S. Becker, H. Haraguchi, and B. Sarkar, "Metallomics : Guidelines for terminology and critical evaluation of analytical chemistry approaches (IUPAC Technical Report)*," *IUPAC*, vol. 82, no. 2, pp. 493–504, 2010.

[50] J. Bettmer *et al.*, "The emerging role of ICP-MS in proteomic analysis," *J. Proteomics*, vol. 72, no. 6, pp. 989–1005, 2009.

[51] J. S. Becker, A. Matusch, and B. Wu, "Bioimaging mass spectrometry of trace

elements – recent advance and applications of LA-ICP-MS : A review," *Anal. Chim. Acta*, vol. 835, pp. 1–18, 2014.

[52] J. S. Becker *et al.*, "Bioimaging of metals by Laser Aablation Inductively Coupled Plasma Mass Spectrometry (LA-ICP-MS)," *Mass Spectrom. Rev.*, pp. 156–175, 2010.

[53] P. M-M, R. Weiskirchen, N. Gassler, A. K. Bosserhoff, and J. S. Becker, "Novel Bioimaging Techniques of Metals by Laser Ablation Inductively Coupled Plasma Mass Spectrometry for Diagnosis Of Fibrotic and Cirrhotic Liver Disorders," *PLoS One*, vol. 8, no. 3, pp. 1–12, 2013.

[54] U. Kubitscheck, *Fluorescence Microscopy*. Wiley, 2017.

[55] C. M. Brown, "Fluorescence microscopy – avoiding the pitfalls," *Cell Sci. a Glance*, vol.120, no. 10, pp. 1703–1705, 2007.

[56] J. W. Lichtman and J. Conchello, "Fluorescence microscopy," *Nature*, vol. 2, no. 12, pp. 910–919, 2005.

[57] N. G. Anderson *et al.*, "The Fluorescent Toolbox for Assessing Protein Location and Function," *Science.*, vol. 312, no. April, pp. 217–225, 2006.

[58] R. Aebersold and M. Mann, "Mass-spectrometric exploration of proteome structure and function," *Nature*, vol. 537, pp. 347–355, 2016.

[59] R. Aebersold and D. R. Goodlett, "Mass Spectrometry in Proteomics," *Chem. Rev*, vol. 101, pp. 269–295, 2001.

[60] A. Tholey and D. Schaumlo, "Metal labeling for quantitative protein and proteome analysis using inductively-coupled plasma mass spectrometry," *Trends Anal. Chem.*, vol. 29, no. 5, pp. 399–408, 2010.

[61] S. Ong and M. Mann, "Mass spectrometry – based proteomics turns quantitative," *Nat.Chem. Biol.*, vol. 1, no. 5, pp. 252–262, 2005.

[62] T. E. Angel *et al.*, "Mass spectrometry-based proteomics : existing capabilities and future directions," *Chem. Soc. Rev.*, vol. 41, pp. 3912–3928, 2012.

[63] M. H. Elliott, D. S. Smith, and E. Parker, "Special Feature : Tutorial Current trends in quantitative proteomics," *J. Mass Spectrom.*, vol. 44, no. December, pp. 1637–1660, 2009.

[64] M. Bantscheff and M. Schirle, "Quantitative mass spectrometry in proteomics : a critical review," *Anal. Bioanal. Chem.*, vol. 389, pp. 1017–1031, 2007.

[65] A. Prange and D. Pro, "Chemical labels and natural element tags for the quantitative analysis of bio-molecules ¨," *J. Anal. At. Spectrom.*, vol. 23, pp. 432–459, 2008.

[66] R. Beynon and J. Pratt, "Metabolic Labeling of Proteins for Proteomics," *Mol. Cell.Proteomics*, no. August 2005, pp. 857–872, 2005.

[67] Y. Oda, K. Huang, F. R. Cross, and D. Cowburn, "Accurate quantitation of protein expression and site-specific phosphorylation," *PNAS*, vol. 96, no. June, pp. 6591–6596, 1999.

[68] C. C. Wu, M. J. Maccoss, K. E. Howell, D. E. Matthews, and J. R. Yates, "Metabolic Labeling of Mammalian Organisms with Stable Isotopes for Quantitative Proteomic Analysis," *Anal. Chem.*, vol. 76, no. 17, pp. 4951–4959,

2004.

[69] S. Julka and F. Regnier, "Quantification in Proteomics through Stable Isotope Coding : A Review," *J. Proteome Res.*, vol. 3, pp. 350–363, 2004.

[70] M. Miyagi and K. C. S. Rao, "Proteolytic 18 O-labeling strategies for quantitative proteomics," *Mass Spectrom. Rev.*, vol. 26, pp. 121–136, 2007.

[71] M. B. Goshe and R. D. Smith, "Stable isotope-coded proteomic mass spectrometry," *Curr.Opin. Biotechnol.*, vol. 14, pp. 101–109, 2003.

[72] Y. Shiio and R. Aebersold, "Quantitative proteome analysis using isotope-coded affinity tags and mass spectrometry," *Nat. Protoc.*, vol. 1, no. 1, pp. 139–145, 2006.

[73] A. Schmidt, J. Kellermann, and F. Lottspeich, "A novel strategy for quantitative proteomics using isotope-coded protein labels," *Proteomics*, vol. 5, pp. 4–15, 2005.

[74] H. Liu *et al.*, "Method for Quantitative Proteomics Research by Using Metal Element Chelated Tags Coupled with Mass Spectrometry," *Anal. Chem.*, vol. 78, no. 18, pp. 6614– 6621, 2006.

[75] P. A. Whetstone, N. G. Butlin, T. M. Corneillie, and C. F. Meares, "Element-Coded Affinity Tags for Peptides and Proteins," *Bioconjug. Chem.*, vol. 15, pp. 3–6, 2004.

[76] T. J. Kerr and J. A. Mclean, "Peptide quantitation using primary amine selective metal chelation labels for mass spectrometry w," *Chem. Commun.*, vol. 46, pp. 5479–5481, 2010.

[77] L. Yang *et al.*, "Metallic Element Chelated Tag Labeling (MeCTL) for Quantitation of N‐Glycans in MALDI-MS," *Analyical Chem.*, no. 89, pp. 7470–7476, 2017.

[78] M. Wind and W. D. Lehmann, "Element and molecular mass spectrometry — an emerging analytical dream team in the life sciences," *J. Anal. At.Spectrom.*, vol. 19, pp. 20–25, 2004.

[79] G. Schwarz, L. Mueller, and M. W. Linscheid, "DOTA based metal labels for protein quantification : a review," *J. Anal. At. Spectrom.*, vol. 29, pp. 221–233, 2014.

[80] D. E. Kalume, H. Molina, and A. Pandey, "Tackling the phosphoproteome : tools and strategies," *Curr. Opin. Chem. Biol.*, vol. 7, pp. 64–69, 2003.

[81] A. Sanz-Medel, J. R. Encinar, and M. L. Ferna, "ICP-MS for absolute quantification of proteins for heteroatom-tagged , targeted proteomics," *Trends Anal. Chem.*, vol. 40, pp. 52–63, 2012.

[82] S. F. Boulyga, V. Loreti, J. Bettmer and K. G. Heumann, "Application of SEC-ICP-MS for comparative analyses of metal-containing species in cancerous and healthy human thyroid samples," *Anal. Bioanal. Chem.*, vol. 380, pp. 198–203, 2004.

[83] S. Bomke, T. Pfeifer, and B. Meermann, "Liquid chromatography with complementary electrospray and inductively coupled plasma mass spectrometric detection of ferrocene- labelled peptides and proteins," *Anal. Bioanal. Chem.*, vol. 397, pp. 3503–3513, 2010.

[84] R. Ahrends *et al.*, "A Metal-coded Affinity Tag Approach to Quantitative

Proteomics,"
Mol. Cell. Proteomics, vol. 6, no. 11, pp. 1907–1916, 2007.

[85] A. H. El-Khatib, D. Esteban-Fernández, and M. W. Linscheid, "Dual labeling of biomolecules using MeCAT and DOTA derivatives : application to quantitative proteomics," *Anal. Bioanal. Chem.*, vol. 403, pp. 2255–2267, 2012.

[86] R. Ahrends, S. Pieper, B. Neumann, C. Scheler, and M. W. Linscheid, "Metal-Coded Affinity Tag Labeling : A Demonstration of Analytical Robustness and Suitability for Biological Applications," *Anal. Chem.*, vol. 81, no. 6, pp. 2176–2184, 2009.

[87] G. Schwarz, S. Beck, M. G. Weller, and M. W. Linscheid, "MeCAT — new iodoacetamide reagents for metal labeling of proteins and peptides," *Anal. Bioanal. Chem.*, vol. 401, pp. 1203–1209, 2011.

[88] G. Schwarz, S. Beck, D. Benda, and M. W. Linscheid, "MeCAT - comparing relative quantification of alpha lactalbumin using both molecular and elemental mass spectrometry," *Analyst*, vol. 138, pp. 2449–2455, 2013.

[89] K. Brueckner, K. Schwarz, S. Beck, and M. W. Linscheid, "DNA Quantification via ICP- MS Using Lanthanide-Labeled Probes and Ligation-Mediated Ampli fi cation," *Analyical Chem.*, vol. 86, pp. 585–591, 2014.

[90] D. Esteban-Fernández, F. S. Bierkandt, and M. W. Linscheid, "MeCAT labeling for absolute quantification of intact proteins using label-specific isotope dilution ICP-MS," *J. Anal. At. Spectrom.*, vol. 27, no. 10, p. 1701, 2012.

[91] L. Waentig, N. Jakubowski, H. Simone, C. Scheler, P. P. Roos, and M. W. Linscheid, "Comparison of different chelates for lanthanide labeling of antibodies and application in a Western blot immunoassay combined with detection by laser," *J. Anal. At. Spectrom.*, vol. 27, pp. 1311–1320, 2012.

[92] S. Hoesl *et al.*, "Internal standardization of LA-ICP-MS immuno imaging via printing of universal metal spiked inks onto tissue sections," *J. Anal. At. Spectrom.*, vol. 31, no. 3, pp.801–808, 2016.

[93] A. H. El-Khatib, D. Esteban-Fernandez, and M. W. Linscheid, "Inductively Coupled Plasma Mass Spectrometry-Based Method for the Specific Quantification of Sulfenic Acid in Peptides and Proteins," *Anal. Chem.*, vol. 86, pp. 1943–1948, 2014.

[94] Y. He, D. Esteban-Fernández, and M. W. Linscheid, "Novel approach for labeling of biopolymers with DOTA complexes using in situ click chemistry for quantification," *Talanta*, vol. 134, pp. 468–475, 2015.

[95] Y. He, D. Esteban-Fernández, B. Neumann, U. Bergmann, F. Bierkandt, and M. W. Linscheid, "Application of MeCAT-Click labeling for protein abundance characterization of E . coli after heat shock experiments," *J. Proteomics*, vol. 136, pp. 68–76, 2016.

[96] E. Polo, M. Collado, B. Pelaz, and P. Pino, "Advances toward More Efficient Targeted Delivery of Nanoparticles in Vivo: Understanding Interactions between Nanoparticles and cells," *ACS Nano*, no. 11, pp. 2397–2402, 2017.

[97] D. Drescher, C. Giesen, H. Traub, U. Panne, J. Kneipp, and N. Jakubowski,

"Quantitative Imaging of Gold and Silver Nanoparticles in Single Eukaryotic Cells by Laser Ablation ICP-MS," *Anal. Chem.*, vol. 84, pp. 9684–9688, 2012.

[98] C. Zhang, Z. Zhang, B. Yu, J. Shi, and X. Zhang, "Application of the Biological Conjugate between Antibody and Colloid Au Nanoparticles as Analyte to Inductively Coupled Plasma Mass Spectrometry," *Anal. Chem.*, vol. 74, no. 1, pp. 96–99, 2002.

[99] S. D. Mueller, R. A. Diaz-Bone, J. Felix, and W. Goedecke, "Detection of specific proteins by laser ablation inductively coupled plasma mass spectrometry (LA-ICP-MS) using gold cluster labelled antibodies w," *J.Anal.At.Spectrom*, no. 20, pp. 907–911, 2005.

[100] X. Lou *et al.*, "Polymer-Based Elemental Tags for Sensitive Bioassays," *Angew Chem Int Ed.*, vol. 46, pp. 6111–6114, 2007.

[101] S. Pan *et al.*, "Mass Spectrometry Based Targeted Protein Quantification : Methods and Applications reviews," *J. Proteome Res.*, vol. 8, pp. 787–797, 2009.

[102] S. A. Gerber, J. Rush, O. Stemman, M. W. Kirschner, and S. P. Gygi, "Absolute quantification of proteins and phosphoproteins from cell lysates by tandem MS," *PNAS*, vol. 100, pp. 6940–6945, 2003.

[103] D. A. Megger, T. Bracht, H. E. Meyer, and B. Sitek, "Biochimica et Biophysica Acta Label-free quanti fi cation in clinical proteomics," *Biochim. Biophys. Acta*, vol. 1834, pp. 1581–1590, 2013.

[104] T. Lenz, J. J. Fischer, and M. Dreger, "Probing small molecule-protein interactions: A new perspective for functional proteomics," *J. Proteomics*, vol. 75, no. 1, pp. 100–115, 2011.

[105] A. Medvedev, A. Kopylov, O. Buneeva, V. Zgoda, and A. Archakov, "Affinity-based proteomic profiling : Problems and achievements," *Proteomics*, vol. 12, pp. 621–637, 2012.

[106] Y. Liu and M. Guo, "Chemical proteomic strategies for the discovery and development of anticancer drugs," *Proteomics*, vol. 14, pp. 399–411, 2014.

[107] S. Serim, U. Haedke, and S. H. L. Verhelst, "Activity-Based Probes for the Study of Proteases : Recent Advances and Developments," *ChemMedChem*, vol. 7, pp. 1146–1159, 2012.

[108] F. Kroll, M. Glinski, M. Dreger, E. Dülsner, and H. Köster, "CCMS: A new era in toxicoproteomics," *Innov. Pharm. Technol.*, no. 29, pp. 38–41, 2009.

[109] E. W. C. Dalhoff, M. Hüben, T. Lenz, P. Poot, E. Nordhoff, H. Köster, "Synthesis of S- adenosyl-L-homocysteine Capture Compounds for Selective Photoinduced Isolation of Methyltransferases," *ChemBioChem*, vol. 11, no. 1982, pp. 256–265, 2010.

[110] J. J. Fischer *et al.*, "Comprehensive identification of staurosporine-binding kinases in the hepatocyte cell line HepG2 using capture compound mass spectrometry (CCMS)," *J. Proteome Res.*, vol. 9, no. 2, pp. 806–817, 2010.

[111] J. J. Fischer *et al.*, "Dasatinib , imatinib and staurosporine capture compounds — Complementary tools for the profiling of kinases by Capture Compound Mass Spectrometry (CCMS)," *J. Proteomics*, vol. 75, no. 1, pp. 160–168, 2011.

[112] L. J. Brown *et al.*, "Using S-adenosyl-L-homocysteine capture compounds to characterize S-adenosyl-L-methionine and S-adenosyl-L-homocysteine binding proteins," *Anal. Biochem.*, vol. 467, pp. 14–21, 2014.

[113] T. Lenz, P. Poot, E. Weinhold, and M. Dreger, "Profiling of methyltransferases and other S-adenosyl-L-homocysteine-binding proteins by capture compound mass spectrometry," *Methods Mol. Biol.*, vol. 803, pp. 97–125, 2012.

[114] Y. Luo *et al.*, "GDP-Capture Compound — A novel tool for the profiling of GTPases in pro- and eukaryotes by capture compound mass spectrometry (CCMS)," *J. Proteomics*, vol. 73, no. 4, pp. 815–819, 2009.

[115] Y. Luo *et al.*, "The cAMP Capture Compound Mass Spectrometry as a Novel Tool for Targeting cAMP-binding Proteins," *Mol. Cell. Proteomics*, pp. 2843–2856, 2009.

[116] C. Blex *et al.*, "Targeting G-protein-coupled receptors by Capture Compound Mass Spectrometry (CCMS) - a case study with sertindole," *ChemBioChem*, 2017.

[117] E. M. Sletten and C. R. Bertozzi, "Bioorthogonal Chemistry : Fishing for Selectivity in a Sea of Functionality Angewandte," *Angew Chem Int Ed.*, vol. 48, pp. 6974–6998, 2009.

[118] J. C. Jewett and C. R. Bertozzi, "Cu-free click cycloaddition reactions in chemical biology," *Chem. Soc. Rev.*, vol. 39, no. 4, p. 1272, 2010.

[119] C. P. R. Hackenberger and D. Schwarzer, "Chemoselective Ligation and Modification Strategies for Peptides and Proteins Angewandte," *Angew Chem Int Ed.*, vol. 47, pp. 10030–10074, 2008.

[120] H. C. Kolb, M. G. Finn, and K. B. Sharpless, "Click Chemistry : Diverse Chemical Function from a Few Good Reactions," *Angew Chem Int Ed.*, vol. 40, pp. 2004–2021, 2001.

[121] M. D. Best, "Click Chemistry and Bioorthogonal Reactions : Unprecedented Selectivity in the Labeling of Biological Molecules," *Biochemistry*, vol. 48, pp. 6571–6584, 2009.

[122] S. K. Mamidyala and M. G. Finn, "In situ click chemistry: probing the binding landscapes of biological molecules," *Chem. Soc. Rev.*, vol. 39, no. 4, pp. 1252–1261, 2010.

[123] E. Saxon and C. R. Bertozzi, "Cell Surface Engineering by a Modified Staudinger Reaction," *Science*, vol. 287, no. March 2000, pp. 2007–2011, 2007.

[124] R. Huisgen, "Kinetics and reaction mechnisms: examples from the experience of forty years," *Pure Appl. Chem*, vol. 61, no. 4, pp. 613–628, 1989.

[125] V. V Rostovtsev, L. G. Green, V. V Fokin, and K. B. Sharpless, "A Stepwise Huisgen Cycloaddition Process : Copper (i) -Catalyzed Regioselective ™ Ligation of Azides and Terminal Alkynes," *Angew Chem Int Ed.*, vol. 41, no. 14, pp. 2596–2599, 2002.

[126] C. W. Tornøe, C. Christensen, and M. Meldal, "Peptidotriazoles on Solid Phase : [1, 2, 3]-Triazoles by Regiospecific Copper (I) -Catalyzed 1 , 3-Dipolar Cycloadditions of Terminal Alkynes to Azides," *J.Org.Chem*, vol. 67, no. I, pp. 3057–3064, 2002.

[127] H. C. Kolb and K. B. Sharpless, "The growing impact of click chemistry on drug discovery," *Res. Focus*, vol. 8, no. 24, 2003.

[128] B. T. Worrell, J. A. Malik, and V. . Fokin, "Direct Evidence of a Dinuclear Copper intermediate in Cu (I)-Catalyzed Azide-Alkyne Cycloadditions," *Science*, vol. 340, no. April, pp. 457–461, 2013.

[129] T. R. Chan, R. Hilgraf, K. B. Sharpless, and V. V Fokin, "Polytriazoles as Copper (I) - Stabilizing Ligands in Catalysis," *Org. Lett.*, vol. 41, no. I, pp. 2002–2004, 2004.

[130] V. Hong, N. F. Steinmetz, M. Manchester, and M. G. Finn, "Labeling Live Cells by Copper-Catalyzed Alkyne - Azide Click Chemistry," *Bioconjug. Chem.*, vol. 21, pp. 1912–1916, 2010.

[131] D. Soriano *et al.*, "Biocompatible Copper (I) Catalysts for in Vivo Imaging of Glycans,"
J.Am.Chem.Soc, vol. 132, no. I, pp. 16893–16899, 2010.

[132] V. Bevilacqua *et al.*, "Copper-chelating azides for efficient click conjugation reactions in complex media," *Angew. Chemie - Int. Ed.*, vol. 53, no. 23, pp. 5872–5876, 2014.

[133] N. J. Agard, J. A. Prescher, and C. R. Bertozzi, "A Strain-Promoted [3 + 2] Azide - Alkyne Cycloaddition for Covalent Modification of Biomolecules in Living Systems," *J.Am.Chem.Soc*, vol. 126, pp. 15046–15047, 2004.

[134] M. L. Blackman, M. Royzen, and J. M. Fox, "Tetrazine Ligation : Fast Bioconjugation Based on Inverse-Electron-Demand Diels - Alder Reactivity," *J.Am.Chem.Soc*, vol. 130, pp. 13518–13519, 2008.

[135] H. Köster *et al.*, "Capture Compound Mass Spectrometry: A Technology for the Investigation of Small Molecule Protein Interactions," *Assay Drug Dev. Technol.*, vol. 5, no. 3, pp. 381–390, 2007.

[136] J. J. Fischer, O. Graebner, M. Dreger, M. Glinski, S. Baumgart, and H. Koester, "Improvement of capture compound mass spectrometry technology (CCMS) for the profiling of human kinases by combination with 2D LC-MS/MS," *J. Biomed. Biotechnol.*, vol. 2011, 2011.

[137] J. Moreau, E. Guillon, J. C. Pierrard, J. Rimbault, M. Port, and M. Aplincourt, "Complexing mechanism of the lanthanide cations Eu3+, Gd 3+, and Tb3+ with 1,4,7,10-tetrakis (carboxymethyl)-1,4,7, 10-tetraazacyclododecane (dota) - characterization of three successive complexing phases: Study of the thermodynamic and structural properties," *Chem. - A Eur. J.*, vol. 10, no. 20, pp. 5218–5232, 2004.

[138] I. Hemmilä and V. Laitala, "Progress in lanthanides as luminescent probes," *J. Fluoresc.*, vol. 15, no. 4, pp. 529–542, 2005.

[139] J. Sabine Becker, "Imaging of metals in biological tissue by laser ablation inductively coupled plasma mass spectrometry (LA-ICP-MS): state of the art and future developments.," *J. Mass Spectrom.*, vol. 48, no. 2, pp. 255–268, 2013.

[140] T. Büchner *et al.*, "Relating surface-enhanced Raman scattering signals of cells to gold nanoparticle aggregation as determined by LA-ICP-MS micromapping," *Anal. Bioanal. Chem.*, vol. 406, no. 27, pp. 7003–7014, 2014.

[141] L. Mueller, A. J. Herrmann, S. Techritz, U. Panne, and N. Jakubowski,

"Quantitative characterization of single cells by use of immunocytochemistry combined with multiplex LA-ICP-MS," *Anal. Bioanal. Chem.*, pp. 1–10, 2017.

[142] J.-M. Beaulieu and R. R. Gainetdinov, "The Physiology, Signaling, and Pharmacology of Dopamine Receptors," *Pharmacol. Rev.*, vol. 63, no. 1, pp. 182–217, 2011.

[143] C. Missale *et al.*, "Dopamine Receptors : From Structure to Function," *Physiol. Rev.*, vol.
78, no. 1, pp. 189–225, 1998.

[144] A. Usiello, J. Baik, and Â. Dierich, "Distinct functions of the two isoforms of dopamine D2 receptors," *Lett. to Nat.*, vol. 408, no. November, pp. 199–203, 2000.

[145] N. M. Richtand, J. A. Welge, A. D. Logue, P. E. Keck, S. M. Strakowski, and R. K. McNamara, "Dopamine and Serotonin Receptor Binding and Antipsychotic Efficacy," *Neuropsychopharmacology*, vol. 32, no. 8, pp. 1715–1726, 2007.

[146] E. Lindström and S. Levander, "Sertindole: efficacy and safety in schizophrenia," *Expert Opin. Pharmacother.*, vol. 7, no. 13, pp. 1825–1834, 2006.

[147] D. Rampe, M. K. Murawsky, J. Grau, and E. W. Lewis, "The antipsychotic agent sertindole is a high affinity antagonist of the human cardiac potassium channel HERG.," *J. Pharmacol. Exp. Ther.*, vol. 286, no. 2, pp. 788–793, 1998.

[148] M. Corte-Rodríguez *et al.*, "Quantitative evaluation of cellular uptake, DNA incorporation and adduct formation in cisplatin sensitive and resistant cell lines: Comparison of different Pt-containing drugs," *Biochem. Pharmacol.*, vol. 98, no. 1, pp. 69–77, 2015.

[149] B. Holz, S. Klimasauskas, S. Serva, and E. Weinhold, "2-Aminopurine as a fluorescent probe for DNA base flipping by methyltransferases," *Nucleic Acids Res.*, vol. 26, no. 4, pp. 1076–1083, 1998.

[150] K. Goedecke, M. Pignot, R. S. Goody, a J. Scheidig, and E. Weinhold, "Structure of the N6-adenine DNA methyltransferase M.TaqI in complex with DNA and a cofactor analog.," *Nat. Struct. Biol.*, vol. 8, no. 2, pp. 121–125, 2001.

6. Abbreviations

2-DE	Two dimensional gel electrophoresis
ABPP	Activity-based protein profiling
CCs	Capture compounds
CCMS	Capture compound mass spectrometry
CuAAC	Copper-(I)-catalyzed azide-alkyne cycloaddition
DNA	Deoxyribonucleic acid
DMF	Dimethylformamide
DMSO	Dimethyl sulfoxide
DOTA	1,4,7,10-tetraazacyclododecane- N,N′,N″,N‴-tetraacetic acid
DRD2	Dopamine D2 receptor
DTPA	Diethylentriamine- N,N′,N″,N‴-pentaacetic acid
ECAT	Element Coded affinity Tag
ECL	Enhanced chemoluminescence
ESI	Electrospray ionization
GPCR	G-protein coupled receptors
HEK	Human embryonic kidney
HPLC	High performance liquid chromatography
ICAT	Isotope coded affinity tag
ICP	Inductively coupled plasma
IPCL	Isotope coded protein label
iTRAQ	Isobaric tag for relative and absolute quantification
LA	Laser Ablation
LC	Liquid chromatography
Ln	Lanthanide
LOD	Limit of detection
MALDI	Matrix Assisted Laser Desorption Ionization
MeCAT	Metal-coded affinity tag
MECT	Metal element chelate tag
MS	Mass spectrometry
MS/MS	Tandem mass spectrometry
MSI	Mass spectrometry imaging
M.TaqI	Adenine N6 methyltransferase
MW	Molecular weight
nanoLC	Nanoflow liquid chromatography
NHS	N-hydroxysuccinimide
PD	Parkinson’s disease
PFA	Paraformaldehyde
pI	Isoelectric point
PROTEIN-AQUA	Protein absolute quantification
PTM	Post-translational modification
RF	Radio frequency
RNA	Ribonucleic acid

Abbreviations

RP-HPLC	Reversed phase liquid chromatography
SAH	s-adenosyl-L-homocycteine
SAM	s-adenosyl-L-methionine
SDS-PAGE	Sodium dodecyl sulphate polyacrylamide gel electrophoresis
SILAC	Stable isotope labeling by amino acids in cell culture
TAMRA	Carboxytetramethylrhodamine
Tb	Terbium
TEA	Triethylamine
TCO	Trans-cyclooctene
UV	Ultra violet
WB	Western blotting